Feasibility and Geotechnical Design of Subsurface Dams in Dry Ephemeral Rivers for the Augmentation of Shallow Groundwater Supply

by

Daniell du Preez

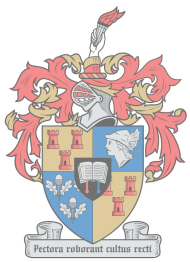

UNIVERSITEIT
iYUNIVESITHI
STELLENBOSCH
UNIVERSITY

Thesis presented in fulfilment of the requirements for the degree of Master of Engineering in Civil Engineering in the Faculty of Engineering at Stellenbosch University

Supervisor: Leon Croukamp
Co-supervisor: Nebo Jovanovic

March 2018

Declaration

By submitting this thesis electronically, I declare that the entirety of the work contained therein is my own, original work, that I am the sole author thereof (save to the extent explicitly otherwise stated), that reproduction and publication thereof by Stellenbosch University will not infringe any third party rights and that I have not previously in its entirety or in part submitted it for obtaining any qualification.

Date: March 2018

Signature: _____

Abstract

Recent droughts and projected climate changes in South Africa make it an essential priority to augment water availability, particularly in the most vulnerable rural communities. The Molototsi River, a torrential tributary of the Letaba River in the Limpopo Province was selected as case study. The research proposes new methods for determining the feasibility and design of subsurface dams in dry ephemeral rivers. The methods are predominantly based on the physical factors affecting the decision-making for constructing subsurface dams. This is typical geotechnical engineering approach which involves an applied evaluation of parameters obtained from site visits, field surveys, geological data, geophysical data, precipitation and runoff data, laboratory testing, desktop studies, numerical modelling, irrigation requirements, abstraction demand, and construction costs. The specific objectives of the project are: 1) to identify possible sites to construct subsurface dams; 2) to investigate the geological and geotechnical characteristics; 3) to undertake a hydrogeological and hydrological assessment; and 4) to design and determine the technical feasibility of subsurface dam. The results of the Molototsi River (quaternary catchment B81G and B81H) case study indicates that the assessment of these physical factors are critical prior to construction decision-making. The geological and geotechnical investigation, including GIS applications, proved effective for finding the most favourable subsurface dam sites. The hydrogeological assessments found satisfying yields and are evidently one of the most important aspects of the study as the reservoir yield is directly related to the specific yield and porosity of the riverbed sand. The hydrological modelling also confirms that subsurface dams can significantly increase water availability throughout the dry season. The geotechnical design of this study, according to the estimations made, were deemed adequate and safe against overturning. The cantilever retaining wall also proved to be the most robust and cost effective structure to build, therefore found feasible. It is envisaged that such technology, if feasible, could mitigate water shortages in the rural communities across South Africa, reduce evaporation losses, and contribute to the conservation of fresh water resources, influencing the livelihood of the population directly.

Table of Contents

Declaration ii
Abstract iii
1 Introduction 12
1.1 Study Area 12
1.2 Problem Statement 13
1.3 Aims and Objectives 15
1.4 Research Contribution 15
1.5 Outline of the Thesis 16
2 Literature Review 17
2.1 Subsurface Dams 17
2.1.1 What is a Subsurface Dam? 17
2.1.2 Global History of Sand Dams 17
2.1.3 Previous Studies 18
2.1.4 Advantages of Subsurface Dams 20
2.1.5 Types of Subsurface Dams 20
2.2 Geology 21
2.2.1 Regional Geology 21
2.2.2 Local Geology 23
2.2.3 Structural Geology 24
2.3 Hydrogeology 26
2.3.1 Aquifer Systems 27
2.3.2 Weathered-Fractured Rock Concept 28
3 Methodology 30
3.1 Site Identification 30
3.2 Geological Investigation 30
3.2.1 Structural Geology 30
3.2.2 Geophysical Survey 31
3.2.3 Borehole Drilling 33
3.2.4 Geological Model 34
3.3 Hydrogeological Assessment 34
3.3.1 Aquifer Parameters 34
3.3.2 Groundwater Recharge 36
3.3.3 Groundwater Quality 36
3.3.4 Evaporation Losses 37
3.3.5 Groundwater Monitoring 37
3.3.6 Groundwater Reserves 38
3.3.7 Groundwater Modelling 38
3.4 Hydrological Study 39
3.5 Geotechnical Investigation 42

3.5.1 Test Pits and Profiles 43
3.5.2 DCP 43
3.5.3 Soil Parameters 45
3.6 Subsurface Dam Design 47
3.6.1 Traditional Method 47
3.6.2 Limit State Approach 48
4 Results 49
4.1 Site Selection 49
4.2 Geological Investigation 51
4.2.1 Geology of the Site 51
4.2.2 Proposed Dam Wall Site 53
4.2.3 Geophysical Survey 54
4.2.4 Borehole Geology 55
4.2.5 Geological Cross Sections 60
4.2.6 Geological Model 61
4.3 Hydrogeological Assessment 62
4.3.1 Sand Aquifer Parameters 62
4.3.2 Groundwater Recharge 64
4.3.3 Groundwater Quality 65
4.3.4 Groundwater Discharge 68
4.3.5 Evaporation Losses 68
4.3.6 Groundwater Monitoring 68
4.3.7 Groundwater Reserves 71
4.3.8 Groundwater Modelling 72
4.4 Hydrological Study 77
4.4.1 Topography and Drainage 77
4.4.2 Catchment Yield 77
4.4.3 Rainfall 79
4.4.4 Flood Peak 83
4.4.5 Flood Model 83
4.4.6 Floodlines 85
4.4.7 Sediment Transportation 85
4.5 Geotechnical Investigation 87
4.5.1 Soil Profiles 87
4.5.2 DCP 91
4.5.3 Excavatability 93
4.5.4 Construction Material Investigation 93
4.5.5 Soil Erosion 94
4.5.6 Soil Parameters 95
4.6 Subsurface Dam Design 98
4.6.1 Geotechnical Design 98

4.6.2 Design Plans 103
5 Discussion 104
5.1 Sustainability of Subsurface Dams 104
5.2 Feasibility of Subsurface Dams 105
5.2.1 Cost 106
6 Conclusions and Recommendations 108
Acknowledgements 112
7 References 113
Appendices 117
Appendix A: Geophysical survey of targeted boreholes on the Duvadzi farm. 118
Appendix B: DCP Results 121
Appendix C: Hydrological Determinations 123
Appendix D: Sieve analysis 127

List of Tables

Table 2-1: The geological timeline in chronological order (after Kramers J. M., (2006)). 22
Table 2-2: The recommended drilling targets per structural domain (Holland, 2011).....27
Table 3-1: Return period factors (van Vuuren, van Dijk, and Smithers, 2013). 42
Table 4-1: Results of newly installed boreholes.....56
Table 4-2: Porosity determined for the riverbed sand of the Molototsi River.....62
Table 4-3: Specific yield determined for the riverbed sand of the Molototsi River.....63
Table 4-4: Hydraulic conductivity calculated for the riverbed sand of the Molototsi River.....63
Table 4-5: The flow rate within the Molototsi riverbed was determined in the lab using the constant-head method. 63
Table 4-6: Transmissivity of the Molototsi riverbed calculate for the summer and winter. 64
Table 4-7: Groundwater recharge estimates for the two aquifers (alluvial and crystalline) based on the CMB method. The average Cl_p concentration of 0.69 mg/ℓ for the Letaba Lowveld was obtained from Holland (2011) and the Cl_{gw} were obtained from the water quality tests (see Water Quality section 4.3.3).....64
Table 4-8: Groundwater quality of the Molototsi riverbed and BH2 (H14-1702).....67
Table 4-9: Evaporation loss experiment conducted on the original sand sample collected from the Molototsi River with a porosity (n) of 0.39.....68
Table 4-10: The groundwater depth of the three newly drilled boreholes on the Duvadzi research farm showing one datum as no to little groundwater fluctuation was observed.....69
Table 4-11: The shallow groundwater depth from riverbed level. 69
Table 4-12: The extractable groundwater reserves are calculated for the natural alluvium aquifer in the Molototsi River for each season.....71
Table 4-13: The extractable groundwater reserves are calculated for the artificial aquifer (which includes the subsurface dam wall) in the Molototsi River for each season.....72
Table 4-14: Details listing the area, hydraulic length, the slope of the entire Molototsi River and quaternary catchments. The site catchment details are the portion of the Molototsi catchment contributing to the subsurface dam site. The hydraulic length of the site is taken from below the Modjadji Dam in B81G to the subsurface dam site in B81H. 78
Table 4-15: Discharge for gauge station B8H069 in cubic meters per second (m^3/s) for every 10 cm rise in water level. The date recorded was 05-09-1997 which was during the dry season of the Molototsi catchment (Data was obtained from the Department of Water and Sanitation).....78
Table 4-16: Mean annual rainfall data of the six rainfall stations nearest to the subsurface dam site (data was obtained from the Daily Rainfall Extraction Utility programme by Lynch (2003)).....79
Table 4-17: Various storm rainfall depths for the subsurface dam site using the rainfall station, Eiland 0680280_W (data was obtained from the Design Rainfall programme by Smithers and Schulze (2002)).....80
Table 4-18: Time of concentration (T_c) results. 80
Table 4-19: Details and return periods of Leydsdorp taken from TR102 (Adamson, P.T, 1981). 81
Table 4-20: Modified Hershfield equation for calculating point precipitation using the 1 day return period values of Leydsdorp. 81
Table 4-21: Linear interpolation of the modified Hershfield point precipitation were then calculated due to T_c = 18.34 hours.....82
Table 4-22: Results of the area reduction factor. 82
Table 4-23: Rainfall intensity calculation results. 83
Table 4-24: Calibrated Runoff coefficient calculation used in the Standard Design Flood Method. 83

Table 4-25: Adopted flood peaks (Q) for various return periods of the project site with a contributing catchment area (A) of 855.02 km^2. 83
Table 4-26: Soil profile summary....87
Table 4-27: Water Content 95
Table 4-28: Specific gravity 95
Table 4-29: Dry Density....95
Table 4-30: Void Ratio....95
Table 4-31: Degree of saturation....95
Table 4-32: Porosity 96
Table 4-33: Air content 96
Table 4-34: Saturated density 96
Table 4-35: Buoyant unit weight....96
Table 4-36: Resulting forces that act on the retaining wall according to the traditional approach. 99
Table 4-37: Resulting forces that act on the retaining wall according to the limit state approach. 101
Table 5-1: Bill of quantities for constructing a subsurface dam wall. 107
Table 7-1: DCP results showing the consistency in mm/blow. 122
Table 7-2: Summary of the sieve analysis 128

List of Figures

Figure 1-1: Topography map of the Molototsi catchment (B81G and B81H). The red part shows the high lying areas towards the east and the Lowveld plains towards the west. The light blue line represents the Molototsi River and the dot in B81G is indicating the location of the Modjadji Dam. The coordinates of the site: latitude -23.568542°, Longitude 30.823947°. 12
Figure 1-2: A landcover map showing the dispersment of the villages in black and the cultivated areas in green in quaternary catchments B81G and B81H (Molototsi River, tributary of the Letaba River in Limpopo). Coordinates of the site: latitude -23.568542°, Longitude 30.823947°. 14
Figure 2-1: A typical section of a) subsurface dam and b) sand storage dam (Jamali, 2016). 17
Figure 2-2: Subsurface dam types from Nilsson (1988) presents a) clay dam, b) concrete dam, c) stone masonry, d) reinforced concrete dam, e) plastered wall, f) plastic sheet, g) steel sheet, and h) injected screen (Nilsson, 1988). 21
Figure 2-3: A geological map constructed from data received by the Council for Geoscience (1: 250 000 Tzaneen Sheet 2230), which show the regional geology. Coordinates of the site: latitude -23.568542°, Longitude 30.823947°. 22
Figure 2-4: A geological map constructed from data received by the Council for Geoscience (1: 250 000 Tzaneen Sheet 2230), which show the local geology and Molototsi River catchment. Coordinates: latitude -23.568542°, Longitude 30.823947°. 23
Figure 2-5: Aeromagnetic map of the north eastern parts of the Kaapvaal Craton and the LMB adapted from Stettler et al., (1989) which was subdivided into five domains (A to E) by Holland (2011) according to the prevailing aeromagnetic lineament pattern. 25
Figure 2-6: A geological map showing the extent of boreholes and the correlation with geological features. Coordinates: latitude -23.568542°, Longitude 30.823947°. 26
Figure 2-7: A conceptual understanding of the most significant features controlling groundwater occurrences of crystalline basement aquifers in the Letaba Lowveld with specific focus on the Molototsi River catchment. Photos were taken in the field and plotted along the conceptual model adopted from Holland (2011). The photos show the important characteristics of the catchment (alluvium, fractured rock (joint sets) and dykes). 28

Figure 2-8: Hydraulic conductivity and porosity in crystalline basement aquifers (Holland, 2011). 28

Figure 3-1: Magnetic and Electro-magnetic transects measured at the Duvadzi farm which is generated on a Google Earth map. Line 1 and 2 are traverses conducted on the Duvadzi research farm (outlined in red) and Line 3 within the Molototsi River. The three borehole (BH1, BH2 and BH3) sites can be seen as blue dots within the red Duvadzi farm outline and one well point within the riverbed. Coordinates: latitude -23.566213°, Longitude 30.820157°. 31

Figure 3-2: Standard Design Flood Basins obtained from the Drainage Manual (van Vuuren, van Dijk, and Smithers, 2013). 41

Figure 3-3: DCP locations are shown as red dots. DCP 1 to 4 was done across the riverbed and DCP 5 and 6 was conducted within the sand mining pit (yellow polygon) to reach the deeper profiles. The Duvadzi farm is outlined in red with the three newly drilled boreholes labelled in light blue and the well located within the riverbed. 44

Figure 3-4: A picture of the author using the DCP and an illustration of the DCP components which was obtained from (Jones, 2004). 44

Figure 4-1: A) Climate and topographical/elevation map. B) Geological map showing different lithologies. C) Hydrogeological map showing borehole depths and D) Social map including potential study sites. The solid red rectangle was the site studied in this thesis. 50

Figure 4-2: The photo is showing a fractured gneissic rock with numerous intersecting quartz veins seen in the Molototsi riverbed. Stereonet and rose diagrams derived from the strikes and dips of all joint planes (top) and dykes (bottom) measured. As illustrated above the main joint direction is towards the NW and the main dyke azimuth is in the ENE and NE direction. Coordinates of this outcrop: latitude -23.568531°, Longitude 30.825699°. 51

Figure 4-3: A) Slightly weathered dolerite with onion-like weathering and a joint in the ENE direction. B) Intact dolerite dyke in a NW direction intruding grey gneiss with occasional leucocratic bands. Joints are in an ENE direction. C) Dolerite dyke in an ENE direction which is in sharp contact with a leucocratic rock. 52

Figure 4-4: A geological map of the project site area, showing some of the major structural lines and outcrops observed. As seen on the map, rivers and streams tend to follow the structural lineaments. Coordinates: latitude -23.568542°, Longitude 30.823947°. 53

Figure 4-5: The top image shows a cross-section A-A' of the riverbed in the study area which represents the riverbed outline and the gradient. The bottom left image is a zoomed in area of the proposed subsurface dam site and the bottom right image shows a cross-section B-B' of the river valley at the particular area. 53

Figure 4-6: The geophysics of the Molototsi riverbed shows the magnetic and electro-magnetic results along with the corresponding resistivity data. The geophysics was taken in the riverbed of the Molototsi to distinguish the occurrence of geological structures and the extent of the sand aquifer. The red box shows the area of the proposed dam wall structure and the location of the resistivity results station 2 (620 m). Coordinates of the site: latitude -23.568542°, Longitude 30.823947°. 54

Figure 4-7: Results of the resistivity measurements taken in the Molototsi Riverbed at station 2 (620 m) are shown here. The graph of the left shows a weathered and a fractured zone containing shallow groundwater (blue line) up to 6 m (1.2 m to 11 m contains groundwater, however 6 m was chosen to be more conservative) below the riverbed aquifer. The graph on the right the same data on a scattered log-log graph. Each plot represents a layer with a different resistivity. 55

Figure 4-8: The three borehole location and a basic cross-section C-C' that crosscuts the river valley through BH3 and BH2. Coordinates of profile location: latitude -23.568097°, Longitude 30.819623°. 56

Figure 4-9: Borehole 1 description. 57

Figure 4-10: Borehole 2 description. 58

Figure 4-11: Borehole 3 description 59

Figure 4-12: A cross section of the site area (drawn in Excel), providing a better understanding of the geological layering of the Molototsi River. 60

Figure 4-13: A longitudinal section showing the average slope and layering of the Molototsi River. The proposed area of the subsurface dam location is shown in black. The water flow is from left to right (west to east). Note that the subsurface structure is situated on the weathered/fractured rock and not on scale. 61

Figure 4-14: Geological model created for the project site area with a satellite image overlaying it. The three boreholes were added as reference points. The blue represents granite gneiss base with the weathered and fractured rock layer above in light brown. The darker brown represent the soils and orange and yellow represents the different sand layers within the river bed. Orange being the clean coarse sands. The linear black structures seen represents the dykes in a NE-SW orientation. Coordinates: latitude -23.568542°, Longitude 30.823947°. 61

Figure 4-15: Mean annual recharge for the Molototsi catchment region in the Limpopo. The data was obtained from the Department of Water Affairs. Coordinates: latitude -23.568542°, Longitude 30.823947°. 65

Figure 4-16: Hourly groundwater levels (elevation) measured with Solinst loggers and manual dip meter readings at boreholes H14-1703 (top) and H14-1702 (middle), and daily rainfall data (bottom) at the Duvadzi farm. 70

Figure 4-17: Drawdown at the well point of the natural aquifer (without the subsurface dam structure). 73

Figure 4-18: Draw down map of the natural aquifer showing a minor cone of depression in dark blue around the well in the riverbed, pumping for 15 m^3/d every second day. Coordinates of the well: latitude -23.568148°, Longitude 30.819999°. 73

Figure 4-19: Drawdown at the well point of the artificial aquifer after implementing the subsurface dam structure. 74

Figure 4-20: Draw down map of the artificial aquifer showing a distinctive cone of depression in dark blue around the well, pumping at 40 m^3/d for every second day over a 71 day period. Coordinates of the well: latitude -23.568148°, Longitude 30.819999°. 75

Figure 4-21: Drawdown at the well point of the artificial aquifer after implementing the subsurface dam structure by pumping continuously. 76

Figure 4-22: A Google Earth map showing all the rainfall stations surrounding the site. The site is shown as a red square (and red dot is the proposed subsurface dam location). The rainfall stations ae shown in dark blue and the Molototsi River and Modjadji Dam in light blue. 79

Figure 4-23: Standard Design Flood Basins obtained from the Drainage Manual (van Vuuren, van Dijk, and Smithers, 2013). Drainage basin 5 indicated with a red boundary is representative of the project site. 81

Figure 4-24: Comparison of storm rainfall for the Leydsdorp and Eiland stations. 82

Figure 4-25: Flood modelling were done using ArcGIS and HecRAS where A) shows the 1:2 year return period peak flows and B) the 1:100 year peak flows . The results in B) clearly show bank overflows at the two tributary outlets. 84

Figure 4-26: The extent of the 1 in 100 and 1 in 2 year peak flow events for this reach of the Molototsi River. Coordinates of the wall structure: latitude -23.568542°, Longitude 30.823947°. 85

Figure 4-27: Cross section of the riverbed from the upper reaches (right) to the lower reaches (left). From the top is the 1:100 year peak flow line, second is the 1:50 peak flow, third is the 1:10 year and blue fill is the 1:2 year return period peak flow. The grey structure is the location of the subsurface dam wall; here sedimentation will occur behind the 1 m exposed wall. 86

Figure 4-28: Soil Profile 1 description. 88

Figure 4-29: Soil Profile 2 description. 89

Figure 4-30: Soil Profile 3 description. 90

Figure 4-31: DCP's done in the Molototsi River close to the Duvadzi Farm. DCP's 1 to 4 was done at riverbed level. DCP 5 was done at 1.20 m depth on the sand mining pit level. DCP 6 was done at 1.50 m depth within the test pit that was excavated. 92

Figure 4-32: Particle analysis of five samples which were all collected within the Molototsi River and plotted on a particle size distribution curve on a semi-logarithmic plot, the ordinate being the percentage by mass of particles smaller than the size given by the abscissa. The above

distribution curves are steep, therefore, indicating smaller particle size ranges which corresponds with the Unified Classification System workings. 94

Figure 4-33: Shear box test results conducted to determine the cohesion and shear resistance. 97

Figure 4-34: A cross sectional side view of the subsurface dam wall. All measurements are in meters (m) with a surcharge pressure of 10 kN/m^2 acting on the backfill behind the wall. F1-2 represents the horizontal overturning force and W1-4 are the vertical resisting force acting on the base. The saturated sand has a saturated unit weight of 21 kN/m^3 which was estimated in the Soil Parameters section above. 99

Figure 4-35: Minimum and maximum base pressure of the traditional approach calculation. 100

Figure 4-36: Minimum and maximum base pressure of the limit state approach. 102

Figure 4-37: Effect of the groundwater divide on the flow. 102

Figure 4-38: Cross sectional view looking downstream. 103

Figure 4-39: Plan view of the cantilever wall with counterforts or buttresses on the toe side. The downstream side is at the top of the illustration. Reno-mattresses are presented on the banks. 103

Figure 4-40: Visual layout of how the surface water (shown in blue) would dam up behind the 1 m exposed wall. Reno-mattress are shown in orange around the flanks. Coordinates: latitude -23.568542°, Longitude 30.823947°. 103

Figure 6-1: The potential artificial recharge areas of South Africa. The map was obtained from the artificial recharge website (Department of Water and Sanitation). 111

Figure 7-1: Results of the magnetic and electro-magnetic measurements for Duvadzi farm. The recommended drill positions for targeting groundwater are shown on the graphs as blue vertical dash lines. 119

Figure 7-2: Results of the resistivity measurements for Duvadzi farm are shown here. The top two are showing weathered and fractured zones (major anomalies) which were used as the recommended drilling positions. The bottom two graphs are representative of the top two plotted on a log-log graph. The left graphs represent the results of BH1 (H14-1701). The right graphs represent the results of BH2 (H14-1702) and BH3 (H14-1703) as it was drilled on the same profile. 120

Figure 7-3: Flood peak calculations done in excel using the Standard design Flood Method (van Vuuren, van Dijk, and Smithers, 2013). 124

Figure 7-4: Daily rainfall from TR102 obtained from the SANRAL Drainage manual (van Vuuren, van Dijk, and Smithers, 2013). 125

Figure 7-5: Regional catchment values obtained from the SANRAL Drainage Manual (van Vuuren, van Dijk, and Smithers, 2013). 126

List of Photos

Photo 3-1: The author taking structural readings and coordinates of the outcrops along the Molototsi River. Ponding of water can clearly be seen along the outcrops. 31

Photo 3-2: The G5 Proton Memory magnetometer used to conduct geophysical measurements. 32

Photo 3-3: The author assisting the Department of Water and Sanitation (DWS) with conducting geophysics by using the electromagnetic method. 32

Photo 3-4: The author assisting the DWS with conducting geophysics by using the resistivity method. 33

Photo 3-5: The 1.5 m deep well within the Molototsi River from which the Duvadzi farmer is pumping at a rate of 15 m^3/d (pumping every second day) to irrigate 0.175 ha crop plot. Coordinates of the well: latitude -23.568148°, Longitude 30.819999°. 37

Photo 3-6: Test pit (soil profile, SP1) excavated in the Molototsi River within the sand mining pit. Coordinates of this test pit: latitude -23.568068°, Longitude 30.818929°. 43

1 Introduction

1.1 Study Area

The study site is located in the Molototsi catchment, an ephemeral tributary of the Greater Letaba River, draining quaternary catchments B81G and B81H (see Figure 1-1). The Letaba catchment is a summer rainfall subtropical area. Rainfall occurs in a single rainy season during October to March. Rainfall is strongly influenced by the topography, with the mean annual precipitation (MAP) varying from less than 300 mm in the lowland plain (northern and eastern part of the catchment) to more than 1 000 mm in mountainous areas (recharge zone). The mean annual temperature ranges from about 18 °C in the mountainous areas to more than 28 °C in the northern and eastern region of the catchment. The average annual evaporation (as measured by a pan) ranges from 1 300 mm in the western mountainous region to 2 000 mm in the northern and eastern areas.

Most of the Letaba catchment is located in the mountainous Great Escarpment and it includes the northern parts of the Drakensberg, which extends in the South-North direction. The study area is at the interface between the granitic greenstone belt (GGB) of the Kaapvaal Craton and the metamorphic (predominantly gneiss) of the Southern Marginal zone of the Limpopo Mobile Belt (Holland, 2011). The mountainous areas in the western parts of the Letaba Lowveld are characterized by relatively impermeable bedrock (often fractured in the upper part) overlain by a layer of weathered regolith with variable thickness (less than 36 m). In these areas, composite aquifers usually occur. Deep fractured aquifers occur at the base of the escarpment in high-lying areas. Where the weathered layer is thin or absent, leucogranites are often exposed. Alluvial deposits can be found along the main rivers, where intergranular aquifers occur overlying weathered material (Holland, 2011). Both B81G and B81H are located predominantly in the Lowveld Plains, according to the Groundwater Resource Units (GRU) classification based on topography, surface-groundwater interactions and groundwater yield characteristics (DWA , 2014). Portions of B81G lie on the Escarpment (11%) and in Foothills and Valleys (26%), and portion of B81H (5%) in the Giyani GRU.

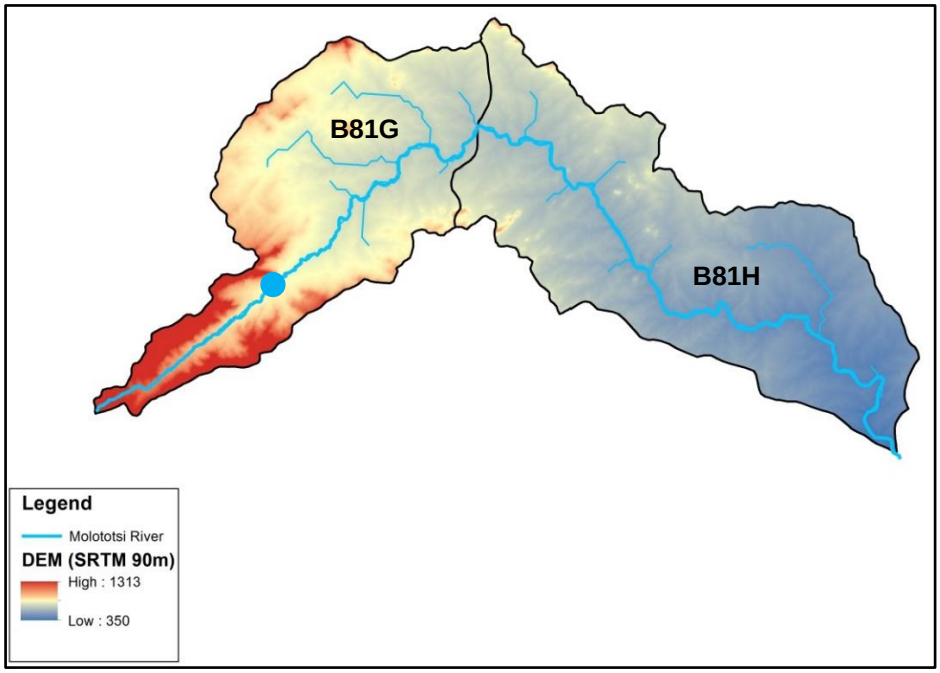

Figure 1-1: Topography map of the Molototsi catchment (B81G and B81H). The red part shows the high lying areas towards the east and the Lowveld plains towards the west. The light blue line represents the Molototsi River and the dot in B81G is indicating the location of the Modjadji Dam. The coordinates of the site: latitude -23.568542°, Longitude 30.823947°.

The Molototsi River has a minimal baseflow, being of torrential nature (mostly floods). According to DWA (2013), the Molototsi River falls under the Integrated Unit of Analysis IUA 6 (northern tributaries of the Letaba River). Quaternary catchments B81G and B81H fall into target Ecological Category D (largely modified). The Modjadji Dam (seen in Figure 1-1) in the upper reaches regulates the Molototsi River flow. The dam is used to supply water to the urban/domestic sector. Irrigation return flows have an impact on the water quality. The impacts/activities identified in B81G to runoff/effluent from urbanization are serious. They are large from agricultural land, erosion, urban areas, sedimentation, grazing/trampling and vegetation removal. The impacts/activities identified in B81H to runoff/effluent from urban areas are small. They are moderate in terms of agricultural land and exotic vegetation, and large impacts are identified at crossings of low water, and due to erosion, sedimentation and vegetation removal. Serious impacts occur from grazing/trampling. No critical impacts were identified and no important wetlands were indicated (DWA , 2013). The main economic activities are agriculture (citrus, mango and tomatoes), tomato processing (secondary sector) and eco-tourism (tertiary sector) (DWA , 2014). The land is almost entirely part of the former homeland with scattered villages and subsistence farming, and with considerable utilization of ecosystem goods and services.

According to the Resource Quality Objectives (RQO) of the Letaba catchment (DWA , 2014), groundwater is moderately utilized in B81G, and abstraction can be increased up to harvest potential with little or no impact on base flow. It is estimated that groundwater abstraction can be increased from 5.06 Mm^3/a to 6.78 Mm^3/a, with a 0.05 Mm^3/a reduction in baseflow. In B81H, groundwater use is low and it can be increased up to harvest potential with little or no impact on baseflow. Groundwater abstraction can be increased from 2.62 Mm^3/a to 7.97 Mm^3/a, with no reduction in baseflow. Limited groundwater development may therefore be feasible in the Molototsi catchment, given groundwater is abstracted below harvest potential, groundwater yields and quality are reasonable, and groundwater contributes little to baseflow. Given the knowledge on potential for groundwater utilization is limited and underexplored, this project aims to address this gap by investigating the extent and feasibility of subsurface groundwater storage and sustainable abstraction. The water quality in the catchment is generally high in nutrients, salts, algae growth and turbidity due to the presence of the GaKgapene wastewater treatment works, populated areas and agricultural activities. Quaternary catchments B81G and B81H fall therefore into moderate priority Resource Units (RU), with moderate ecological and socio-cultural importance. The upper reach B81G has low, whilst the lower reach B81H has high water resource use importance. The water quality within the sand riverbed is generally excellent and suitable for drinking according to the South African Water Quality Guidelines (DWAF, 1996) as it acts as a natural purifying filter.

1.2 Problem Statement

It is widely recognized that global warming has taken its effect on Earth, with consequences such as extreme climate variability and climate change in specific regions of the world. Over 40 percent of the Earth's land surface is classified as drylands; 35 percent of the human population lives in drylands (Neal, 2012), which sustain 80 percent of the world's poorest people. In Southern Africa, rural villages in the dry sub-humid and semi-arid to arid regions are among the most impoverished, inaccessible and poorly served communities. In such conditions, both physical access and water availability are the most important constraints of development. This is particularly relevant to South Africa given that climate predictions indicate a future increase in extreme weather events, such as droughts and floods, and corroborated by the current water stress situation caused by the occurrence of El Nino. Due to the variation and changes in climate across South Africa, Gbetibouo (2010) showed that the most vulnerable provinces were found to be areas of low socio-economic development, referring to small scale farmers that predominantly rely on rain fed agriculture. Pressure on water resources and competition between sectors (water supply to population, environmental flows, agriculture, industry, tourism and recreation) are particularly evident in the Limpopo Province.

Limpopo Province is South Africa's northern-most province. About 89% of the population lives in rural areas and over 88% of the area of the province is farmland. Water is generally obtained from surface and groundwater resources, but the current infrastructure is inadequate to supply water and sanitation to the entire rural population. The provision of services is difficult as most of the settlements are in the form of dispersed villages (see Figure 1-2). Agriculture is a key economic sector in the Limpopo Province. There are two distinct agricultural production systems in the Province: smallholder agriculture and large-scale commercial farming. Smallholder agriculture is located mostly in the former homeland areas and covers about 30% of the provincial agricultural land surface and is characterized by a low level of production technology with plots no larger than 1.5 ha. The smallholder sector production is predominantly for subsistence with small surpluses that are marketed. Although irrigated agriculture is of great importance to the Limpopo Province, shortages of water have major impacts on the sector. In order to enhance rural development in Limpopo, the South African Government established a number of irrigation schemes. However, over utilization of water upstream and droughts caused water shortages in the past decade, therefore, several irrigation schemes have been diverted to supply water to the population. Emerging farmers (livestock, vegetables, cash crop farming systems) therefore turned to alternative water supply sources, mainly pumping from adjacent streams and groundwater.

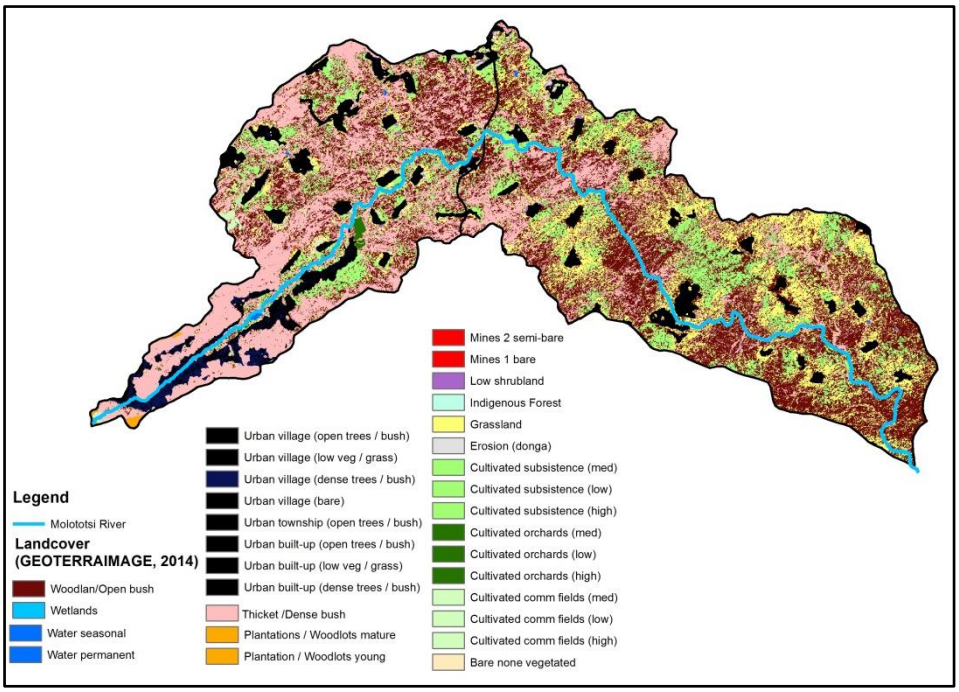

Figure 1-2: A landcover map showing the dispersment of the villages in black and the cultivated areas in green in quaternary catchments B81G and B81H (Molototsi River, tributary of the Letaba River in Limpopo). Coordinates of the site: latitude -23.568542°, Longitude 30.823947°.

Groundwater is currently under-utilized in the Limpopo Province. Recent estimates indicated that groundwater use was significant in the Klein Letaba catchment (the Luvuvhu/Letaba Water Management Area), but represented only 30% of the total water use (DWAF, 2004). There is therefore a need to explore new sustainable water sources, in particular the potential and sustainability of groundwater use in the Province. This project proposes to investigate the feasibility of augmenting water availability in rural areas of the Limpopo Province through the storage of groundwater in dry river beds for sustainable abstraction and water supply to the population and emerging farms. It is

envisaged that augmenting the water availability will benefit under-developed communities and emerging farms, and inform policy and decision-makers on the feasibility of such practice both at strategic and community scale levels. Both scientists and community will gain knowledge on how to effectively use groundwater resources for the sake of sustainable development. The main outcome of the research will support the decision-makers in strategic decisions on the potential of constructing subsurface dams in ephemeral rivers for the augmentation of water supply.

1.3 Aims and Objectives

The general aim of the project is to assess the technical feasibility of subsurface dams in dry ephemeral rivers of the Mopani District (Limpopo Province) for the augmentation of water availability. The specific objectives are:

1) To identify possible sites to construct subsurface dams;
2) To undertake a hydrogeological and hydrological assessment;
3) To investigate the geological and geotechnical characteristics;
4) To determine the design and feasibility of subsurface dams.

1.4 Research Contribution

The MEng is an original piece of research. A new perspective is taken on previously studied sand dam topics which mainly focuses on the hydrological functioning of these dams. The specific subject on subsurface dams has not been studied before, particularly not the feasibility and geotechnical design aspects. The study also involves the geological and hydrogeological characteristics of an ideal subsurface dam site. The author explores this new sustainable water resource utilization technology which is most certainly new to South Africa. No research or case study could be found on the topic. Given that the knowledge on shallow groundwater utilization of dry riverbeds in South Africa is limited and unexplored, this project aims to address this gap by investigating the abstraction volume and feasibility of subsurface dams.

The main research contributions this thesis adds to sand storage dam literature are:

- The geological and hydrogeological characteristics required for determining the ideal subsurface dam site. This study could be used as a guideline for locating subsurface dam sites in different regions across the world, especially in South Africa where similar dry ephemeral rivers occur;
- Groundwater modelling simulations are new to this field and could contribute tremendously to the numerical modelling research. The scenarios simulated in the thesis were only based on a two layered system and could consist of various different layers and scenarios. Since the measurements and scenarios show how subsurface dams would function, the results could contribute in planning and implementing the technology in other regions;
- A hydrological assessment which models the hydraulics of water flow through the natural river. The two-dimensional modelling method used determines the floodplain and how surface water flows would react if a wall structure is built within the river channel. From this, a floodline, a flood risk analysis, and structure damage probabilities can be determined which should be included in all dam investigations.
- The geotechnical design that consists of a reinforced concrete retaining wall which is determined as the most cost effective subsurface dam structure. This study designed for safety against overturning of the wall, safety against sliding between the base and the rock mass, and safety against ground bearing pressure on the supporting foundation;

- A feasibility study which takes into account all the above mentioned characteristics, design, and costs to determine whether the subsurface dam is viable;
- The feasibility study on subsurface dams will also support scientists, engineers and decision-makers at both strategic and community scale levels on the potential of constructing these dams in ephemeral rivers for the augmentation of water supply.

The research is therefore significant in the light of the current South African climate and the physical need for sustainable water resources. The MEng could also contribute greatly as a platform to future scholar topics in South Africa.

1.5 Outline of the Thesis

The thesis is structured in six main sections. In section 1, a general introduction of the study area was given and the problem of water availability in Limpopo Province was addressed. The need for more understanding of groundwater resources is outlined for the sake of sustainable abstraction and water supply or human consumption and emerging farms with the importance of using subsurface dams in potential areas. Section 2 starts with the literature review on subsurface dams along with the historical background and general advantages of subsurface dam interventions, a literature review on the regional and local geology is also presented along with a literature review on the hydrogeology of the study area. Section 3, presents the research methodology. In Section 4, the results are presented and discussed. Firstly, the result of site identification is presented followed by the geological survey, hydrogeological and hydrological interpretations, geotechnical investigation and design of the subsurface dam. Section 5 discusses the main outcome of the results and finally the technical feasibility study of subsurface dams. Section 6 summarizes the overall conclusions based on the results followed by recommendations, legal requirements and future study.

2 Literature Review

2.1 Subsurface Dams

The following section will discuss the literature published on subsurface and sand storage dams.

2.1.1 What is a Subsurface Dam?

Two types of groundwater or sand dams exist, namely a subsurface dam and a sand storage dam. Both refer to sand aquifers which retain water in the sediment pores. However, a subsurface dam (shown in Figure 2-1a) is constructed below riverbed level and arrests the flow in a natural aquifer. A sand storage dam (shown in Figure 2-1b) obstructs the river flow during flooding and stores water in sediments which accumulated behind the wall, enlarging the natural aquifer. Therefore, constructing these groundwater dams in ephemeral rivers will prevent a large volume of water to flow away and increase the availability of water all year around. The water can then be harvested using scoop holes or wells.

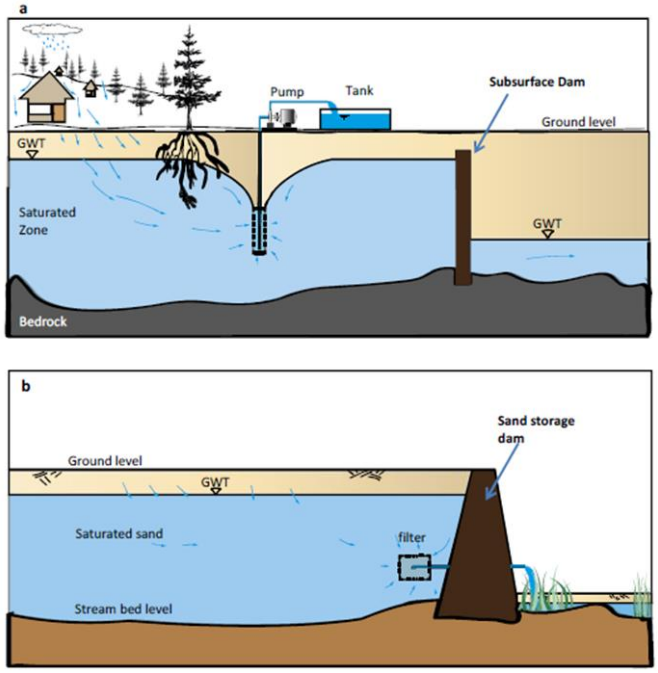

Figure 2-1: A typical section of a) subsurface dam and b) sand storage dam (Jamali, 2016).

2.1.2 Global History of Sand Dams

The use of shallow groundwater for conservation purposes is certainly not a new concept. Groundwater dams were constructed on Sardinia in Roman times and practiced by ancient civilizations in North Africa. More recently, various groundwater damming technologies have been developed and applied in many countries of the world, notably in Japan, Korea, China, India, Ethiopia, Burkina Faso, Brazil, Kenya and USA (Ishida S, 2011). In Africa, Kenya is actively promoting innovations of subsurface water harvesting in drylands. For instance in the Kitui District of Kenya, the Sahelian Solution Foundation began constructing sand storage dams in 1995 (RAIN, 2007). Since this period, over 500 sand dams have been constructed across Kenya. Other governments endorsing this technology in Africa include Benin, Egypt, Ghana, Guinea, Kenya, Mauritania, Rwanda, South Africa, Swaziland and Zimbabwe (PSD, 2005). Due to the growing interest in water harvesting, the RAIN (Rainwater Harvesting Implementation Network) Foundation was established in the Netherlands in

2004, motivated to address appeals for action to achieve effective water supply solutions. RAIN (2007) provides a practical guide to sand dam implementation by describing the success of two pilot case studies from Kenya and Ethiopia.

2.1.3 Previous Studies

This section provides a brief overview of previous studies conducted on sand dams in Africa.

Kenya

The large number of successful sand storage dams in the Kitui District of Kenya is based on the favourable hydrogeological conditions at the dam sites, particularly the sediment size (Ertsen and Hut, 2009). Numerous researchers conducted their studies in this part of Kenya as over 500 sand storage dams have been built. Lasage R. (2008) evaluated the effects of local water harvesting projects in Kenya concerning the construction of small-scale sand dams by communities. The results show increased availability of water, especially during dry periods, resulting in higher farm yields and providing over 100 000 people with water. The researchers also indicated the increase in average income by as much as 60 percent for farmers living close to these dams (Lasage R., 2008). Aerts et al. (2007) also did a study that shows the robustness of subsurface storage using sand dams under long-term climate change for the Kitui District in Kenya (Aerts, 2007).

A study on the hydrology of sand storage dam in the Kiindu catchment of Kenya was conducted by Borst & de Haas (2006). The study involved evaporation measurements, piezometer instalments, groundwater level measurements, and water quality measurements using electrical conductivity (EC) as an indicator. The results show that the response of the groundwater in the riverbed on rainfall and runoff was very rapid with a delayed rise of the groundwater levels in the riverbanks. Within a few weeks both the sediments of the riverbed and riverbanks were saturated. The effect that the sand storage dams have on the groundwater table in the riverbed is clear since a difference between the groundwater levels upstream and downstream can be observed. Results also showed that the salinity (EC) decrease significantly during the rainy season.

Researchers Quilis, Hoogmoed, Ertsen, and Foppen (2009) measured and modelled the hydrological processes of sand storage dams on different spatial scales by performing various scenarios. Measurements showed that the recession of groundwater levels during the dry season was more slow and more gradual at sand storage dam sites. Groundwater levels also increased quickly after precipitation. The dams have clear influence on groundwater levels, both on short and long terms. Based on these results, a groundwater model was developed by Quilis, Hoogmoed, Ertsen, and Foppen (2009). The model showed high sensitivity to hydraulic conductivity of the shallow aquifer on the riverbanks and thickness of the sand layer in the riverbed. A second model was performed for a series of dams. This indicated that the dam distance is an important parameter as the areas that did overlap caused a decrease in the stored volume (Quilis, Hoogmoed, Ertsen, & Foppen, 2009). Furthermore, it can be employed to estimate effects of different spacing scenarios of sand storage dams.

Ethiopia

Sand dam storage in semi-arid areas can help adapt to climate change, however, little is known on the downstream effects of local water storage. Lasage et al. (2013) employed a water balance model to perform a catchment scale assessment of local scale water storage in sand dams. Results indicated acceptable downstream impacts with local benefits of improved water supply (Lasage R. A., 2013). Sand dams appeared to be a viable way for supplying drinking water in semi-arid regions. Lasage and Andela (2011) tested whether sand dams improve water availability in dry seasons and how sustainable their introduction is to current and future circumstances. Their tests showed that lower river discharges under future climate scenarios will cause sand dams to consume a relatively larger

part of the river discharge (Lasage R. a., 2011). However, sand dams are a promising adaptation measure and development strategy for the semi-arid regions.

Namibia

Wipplinger (1953) did a study on the storage of water in sand dams where he investigated the properties of natural and artificial sand reservoirs and the methods of developing such reservoirs. The investigation was predominantly done on the Omaruru, Kuiseb and Swakop rivers. Wipplinger (1953) stated that due to the reduction of evaporation losses in sand storage dams, the water percentage used might be greater than in open storage dams. In addition, sand storage dams would have a regulating effect on runoff, increasing the period open water flows in the riverbed after a rainy season (Wipplinger, 1953). Thus, he concludes sand storage dams are worth encouraging where numerous small but dependable water supplies are required.

Zimbabwe

Groundwater use from alluvial aquafers of non-perennial rivers was also studied in the semi-arid region of Zimbabwe. De Hamera, D., Owend, Booija, and Hoekstra (2008) studied the potential water supply of a small reservoir. The research objective of the study was to calculate the potential water supply for the upper Mnyabezi catchment after implementing two storage dams. Three models were used to simulate the hydrological processes in the Mnyabezi catchment. The first was a rainfall-runoff model based on the SCS-method which was calibrated on only one rainfall event, this causes a large uncertainty in the amount of inflow into the reservoir model. The second was a spreadsheet-based model of the water balance of the reservoir where the calculated drying time was 2 - 3 months. The third was the finite difference groundwater model using MODFLOW to simulate the water balance of the alluvial aquifer (de Hamera, D., Owend, Booija, & Hoekstra, 2008). The results showed that the potential water supply in the Mnyabezi catchment ranges from 2,107 m^3 (5.7 months) in a dry year to 3,162 m^3 (8.7 months) in a wet year. The maximum period of water supply after implementation of the storage capacity measures in a dry year was 2,776 m^3 (8.4 months) and in a wet year the amount was 3,617 m^3 (10.8 months). This according to the authors, is a small storage capacity and can only be used as an additional water resource.

A case study on the groundwater and surface water interactions of small alluvial aquifers was researched by by Love, de Hamer, Owen, Booij, & Uhlenbrook (2007). In this study, three small alluvial aquifers in the Limpopo Basin of Zimbabwe were studied. In all three of these ephemeral rivers, the hydrogeological properties of the aquifer were studied. In each case the aquifer viability was determined. Results showed that the shallowness of the Bengu aquifer (0.3 m deep) means it has effectively no storage potential. The much higher storage of the Mushawe aquifer (0.9 m deep) showed that it can store water for slightly over two weeks. This time frame is in conjunction with the results or observations found by de Hamera, D., Owend, Booija, and Hoekstra (2008) which estimated drying time of the aquifer was 2 - 3 months. However, the Mushawe aquifer showed longer periods of storage after a flow event and has a depth of 2 m. The aquifer also has over half its depth below the evaporation line, suggesting no evaporation occurs below 1 m.

The evaluation of the groundwater potential of the Malala alluvial aquifer was conducted in the lower Mzingwane River of Zimbabwe by Masvopo (2008). The Mzingwane River is a 200 m wide river and covers a 1000 m stretch of the Malala aquifer. The alluvial sand has a porosity of 39 %, a hydraulic conductivity of 59.76 m/d, and a specific yield of 5.4 %. The results of the resistivity surveys showed that the alluviam has a thickness of 13.4 m. Observations from the installed piezometers showed that the water level dropped on by 0.75 m within 97 days. It was estimated that the alluvial aquifer system can store approximately 1 035 000 m^3 of water per 1000 m river stretch which is quite a large volume of readily available water.

South Africa

Sand dams are not commonly seen in South Africa. No government reports or academic research like the case studies of the above mentioned countries, can be found on groundwater or subsurface dams in South Africa. Although, a few sand storage dams have been built in rivers by local farmers on a small scale, minor research or information can be found about it. This indicates a large research gap in knowledge, particularly on subsurface dams in this country.

2.1.4 Advantages of Subsurface Dams

The use of surface reservoirs to store water in areas with dry climates has several serious disadvantages, such as pollution risks, reservoir siltation, and evaporation losses. Using subsurface dams to store ground water is one way of overcoming these problems. Compared to surface dams, a subsurface (groundwater) dam has the following advantages:

- A subsurface (groundwater) dam does not submerge land area, therefore, it does not damage the environment, nor does it cause social problems such as forced migration of the local people compared to a surface dam.
- Prevents the evaporation of reserved water because it is stored underground. This is crucial in the dry season especially in arid to semi-arid regions.
- The reserved water will be clean and of good quality for domestic use because the sand acts as a natural purifier. The water will also not be exposed to proliferate parasites, anopheles that transmits malaria, and germs.
- In general, a subsurface dam is more stable and secure than a surface dam from the viewpoint of dynamics because it is buried under ground. It also needs little maintenance when build to last. Even if it undergoes damage, it is not a safety hazard.
- Subsurface dams are a utilization of renewable resources because the shallow groundwater consumed from the subsurface dam system can be recharged by rainwater.

It is necessary to note that a subsurface dam also holds the following disadvantages: difficulties in site selection, low to moderate volumes of water storage, and it intercepts downstream groundwater flow. However, groundwater in the downstream area is not always recharged with groundwater from the dam site area. It is possible to design a dam with an appropriate dam structure that allows some of the reserved water to drain. Another disadvantage, is the cause of salinization in the reservoir area by evaporation of groundwater near the surface, this phenomenon can be avoided by building the highest level of the reserved groundwater (spillway of the dam) at a sufficient depth, preferably 1 m or more below the surface (riverbed level).

2.1.5 Types of Subsurface Dams

Understanding the concept of subsurface dams is relatively simple: a trench is excavated across the riverbed reaching down to bedrock, preferably an impermeable and solid layer, at a suitable location. In the trench, an impermeable wall or barrier is constructed that could be built with various materials such as clay, concrete, stone, reinforced concrete, brick, plastic, tarred-felt, sheets of steel, corrugated iron or PVC, and even by using an injected screen. The type of dam constructed will depend on several factors such as geological and hydrological conditions, technical efficiency and durability of the structure, availability and cost of material, and the need for skilled labour. The figure below presents the different types of subsurface dams that one could implement considering all the necessary factors.

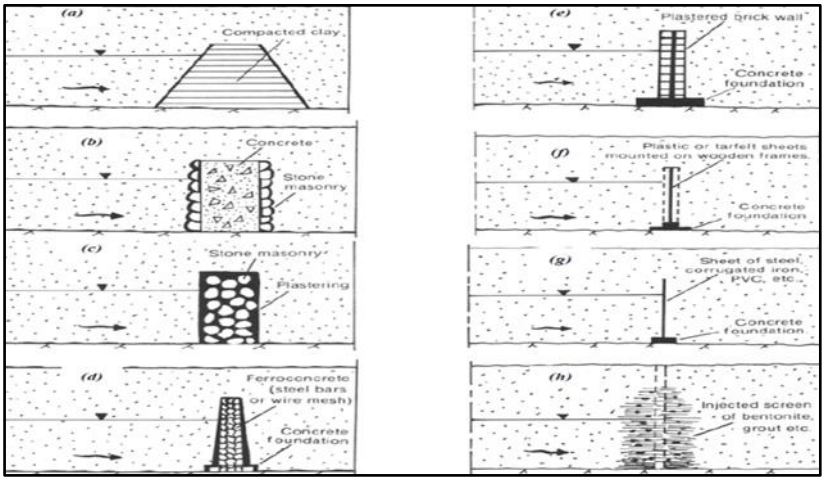

Figure 2-2: Subsurface dam types from Nilsson (1988) presents a) clay dam, b) concrete dam, c) stone masonry, d) reinforced concrete dam, e) plastered wall, f) plastic sheet, g) steel sheet, and h) injected screen (Nilsson, 1988).

2.2 Geology

Achieving a better understanding of the site and location to build the above mentioned retaining structure or subsurface dam, an in-depth geological and hydrogeological study needs to be undertaken which will be discussed in the results section. In this section the geological literature of the north eastern Kaapvaal Craton is discussed with more focus to the Molototsi River Catchment in the Letaba Lowveld. The main lithology found in the study area includes the Giyani Greenstone Belt, Goudplaats-Hout River Gneiss, Groot Letaba Gneiss, Duiwelskloof Leucogranite and Shimiriri Granite. A more detailed discussion of each outcrop follows.

2.2.1 Regional Geology

The north eastern Kaapvaal Craton is characterized by the abundance of granite-greenstone terranes belonging to the Archaean Eon (3600 – 2500 Ma) and the highly metamorphosed rocks of the Limpopo Belt. These Archaean rocks are generally referred to as the “crystalline basement rock” which shows a strongly developed E-W to ENE-WSW fabric (Du Toit, 1983). The Limpopo Mobile Belt (LMB) consists of three main geological zones, the Northern Marginal Zone, the Central Zone and the Southern Marginal Zone. These crustal zones lie parallel to one another in an ENE direction (Holland, 2011). The rocks of the Southern Marginal Zone consist of high-grade metamorphic equivalents of the adjacent granitoid-greenstone assemblage (Van Reenen, 1990). The study area is situated to the south of the Southern Marginal Zone on the Kaapvaal Craton where low-grade metamorphism is known. The distinct boundary between the Southern Marginal Zone and the Kaapvaal Craton is defined by the sharp drop in metamorphic grade and coincides with a thrust fault known as the Hout River Shear Zone (Kramers J. K., 2001).

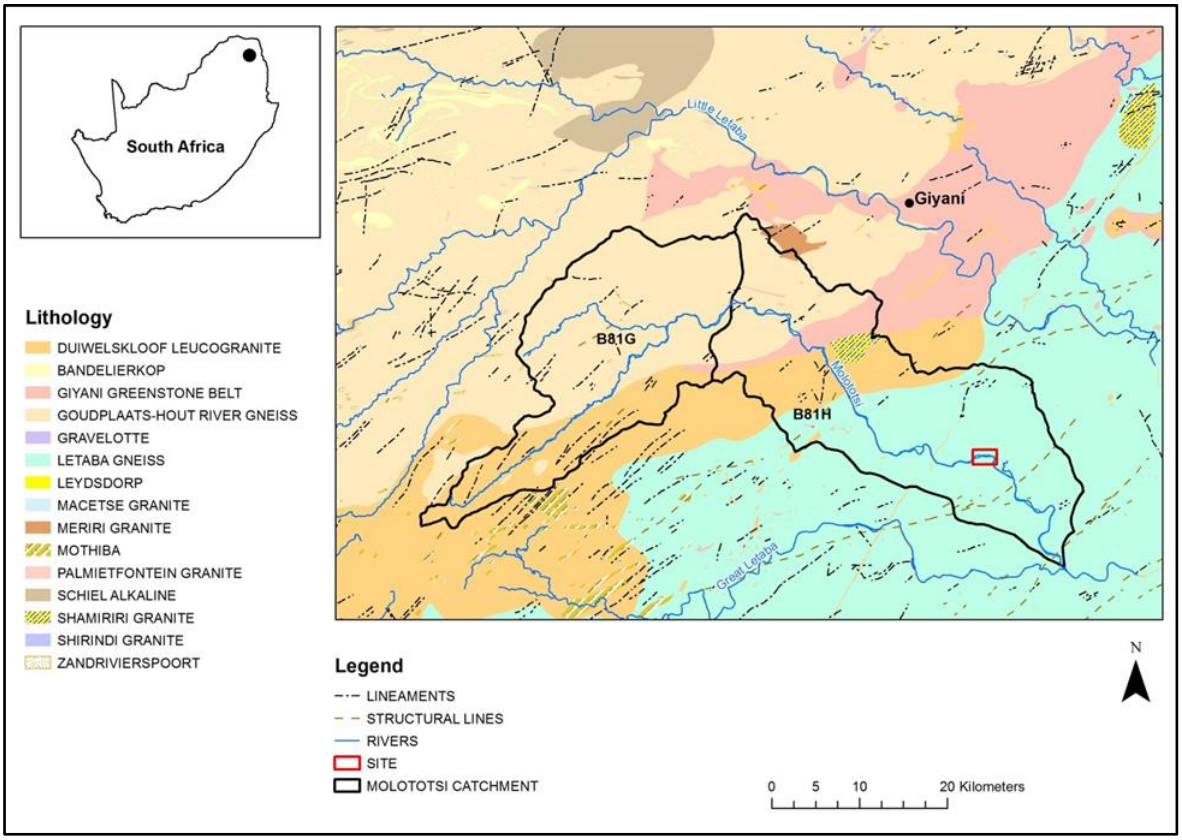

Figure 2-3: A geological map constructed from data received by the Council for Geoscience (1: 250 000 Tzaneen Sheet 2230), which show the regional geology. Coordinates of the site: latitude -23.568542°, Longitude 30.823947°.

The bounding shear zone comprises of strongly developed E-W striking, steeply north dipping thrust and reverse faults, along with several NE-SW striking faults (Smit and Van Reenen, 1997). This complex thrust system was developed over a width of approximately 4 km in certain areas and can be traced over 250 km in the Southern Marginal Zone in the LMB (Anhaeusser, 1992). Since the Archaean orogeny, the granite-greenstone rocks have been subjected to continuous erosional processes, which resulted in different morphological features that influence the later distributional deposits. The geological timeline summary of emplacement ages of each lithology (Kramers J. M., 2006) pertaining to the study area is listed below.

Table 2-1: The geological timeline in chronological order (after Kramers J. M., (2006)).

Geological Timeline	
3600 - 3 200 Ma	Palaeoarcheaen intrusions (Goudplaats-Hout River Gneiss Suite)
± 3 200 Ma	Greenstone Belts (Giyani, Pietersburg, Murchison Greenstone Belts)
3200 - 2 800 Ma	Mesoarcheaen intrusions (Groot Letaba Gneiss)
2 800 - 2 650 Ma	Neoarcheaen intrusions (Shimiriri Granite and Duiwelskloof Leucogranite)
2 700 Ma	Limpopo Belt (first event)
2 700 Ma	Ventersdorp mafic dykes
180 Ma	Karoo Dolerite Suite (dykes and sills)

2.2.2 Local Geology

The geology of the Molototsi catchment (Figure 2-4) predominantly consists of crystalline basement rocks (granite, gneiss and greenstone) which outcrop throughout the targeted catchment and is bordered by,

- the Duiwelskloof Leucogranite to the southwest, which is also the major surface water divide;
- the Goudplaats-Hout River Gneiss Suite to the northwest;
- the Giyani Greenstone Belt (GGB) to the northeast; and
- the Groot-Letaba Gneiss to the southeast.

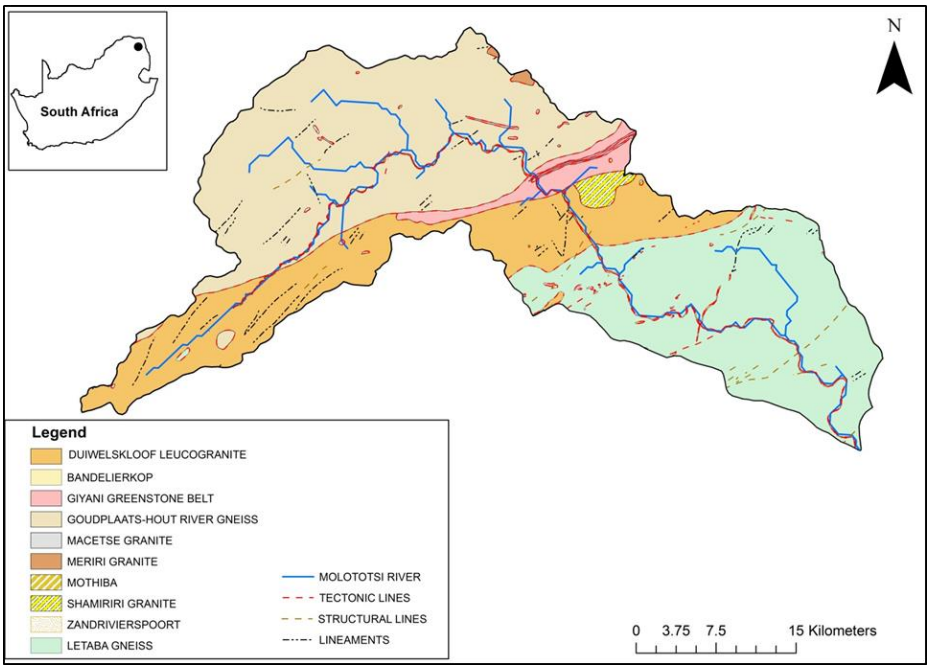

Figure 2-4: A geological map constructed from data received by the Council for Geoscience (1: 250 000 Tzaneen Sheet 2230), which show the local geology and Molototsi River catchment. Coordinates: latitude -23.568542°, Longitude 30.823947°.

Archaean Greenstone Belts

The Giyani Greenstone Belt (GGB) is situated at the north eastern edge of the Kaapvaal Craton and is regarded as a thin feature lying atop a southeast dipping thrust (De Wit et al., 1992b). The belt mainly consists of ultramafic to mafic rocks, iron formations, felsic schists and metasediments which have all been assigned to the Giyani Group (SACS, 1980). In general, the rocks of the GGB are poorly exposed, however, at a few localities the greenstones and gneisses are seen as tectonically interleaved (Kroner, 2000) with ages ranging between 3200 to 2800 Ma. On a regional scale the GGB is characterized by southwest to northeast prograde metamorphism and is almost completely enveloped by migmatitic gneisses (Vorster, 1979). This NE-trending feature extends towards the southern part of the South Marginal Zone of the LMB and is about 15 km wide and 70 km long. Towards the south-west the GGB splits into two arms, a northern Khavagari and a southern Lwaji arm (McCourt, 1992) of which the Lwaji arm occurs within the studied catchment. In the Lwaji arm, the metasediments are overlain by ultramafic schists. The structurally formed base consists of quartz-sericite schists, phyllites, chloritic schists and quartzites, which may grade laterally through ferruginous quartzite into magnetite-bearing iron-formation. The northern and southern margins of the GGB are locally

characterized by the late strike-slip shear zones, post-dating the intrusion of nearby undeformed granitoids (Brandl G. C., 2006).

Archaean Granitoid Intrusions

The geology of the targeted catchment is dominated by the occurrence of granitoid gneisses of various types and compositions. The Goudplaats-Hout River Gneiss Suite is composed of Palaeoarchaean intrusions (3600-3200 Ma) that range from homogeneous to strongly layered, leucocratic to dark-grey, and fine grained to pegmatoidal varieties (Anhaeusser, 1992). These gneissic bodies underlie terranes of the northern part of the Kaapvaal Craton, mainly to the north of the Pietersburg and Giyani Greenstone Belts (GGB) where they typically form flat ground with poor exposure. In the vicinity around the GGB the dominant phase comprises of a medium grained, whitish or, locally, pinkish leucocratic gneiss. Lesser amounts of light- to dark-grey, layered gneiss occur, with the leucosome bands locally transgressing the foliation (Robb, 2006). Ages of 3330-3230 Ma have been obtained from dark-grey tonalitic gneisses (Kroner, 2000). Since the dark-grey gneiss provides an age older than the surrounding greenstone belts, suggests it is either a basement to these successions or a separate crustal block adjacent to the greenstones.

The granitoid gneisses of Mesoarchaean (3200-2800 Ma) age which occurs between the Murchison and Pietersburg-Giyani greenstone belts have been grouped together with the term Groot-Letaba Gneiss (Holland, 2011). It comprises of various intermingled gneisses, including fine- to medium grained tonalite, coarse grained trondhjemite and minor banded and linear gneisses (Robb, 2006). At some localities the gneiss contains small fragments of mafic to ultramafic greenstones, indicating an intrusive relationship of the gneiss protolith with these greenstones. Gneiss ages of about 3170 Ma were reported south of the GGB (Brandl G. a., 1993).

The study area also experienced granitoid magmatic activity during early Neoarchaean times. Massive, unfoliated granites occurring as batholiths, plutons or stocks were emplaced around the Pietersburg and Giyani Greenstone Belts. In general, the granite intrusions form prominent topographic features with emplacement ages that range between 2800 and 2650 Ma. The Shamiriri Granite that is situated south and east of GGB forms two distinct intrusive stocks. The granite at both localities comprise of grey, medium grained rock, which can grade into a coarse to porphyritic phase composed of megacrysts of microcline-microperthite embedded in a groundmass of quartz, oligoclase, microcline and biotite.

In general, the Duiwelskloof Leucogranite has a massive appearance and varies in composition from a syenogranite to a monzogranite. The main constituents are sodic plagioclase, quartz, orthoclase, microperthitic microcline, biotite and muscovite. The leucogranite is also peraluminous in character and can be considered as S-type granite.

2.2.3 Structural Geology

The study area shows distinctive structural features, but the most differentiating features are the orientation and frequency of the dyke swarms. These features are useful paleo-stress indicators as they record fractures that result from regional stress regimes at the time (Holland, 2011).

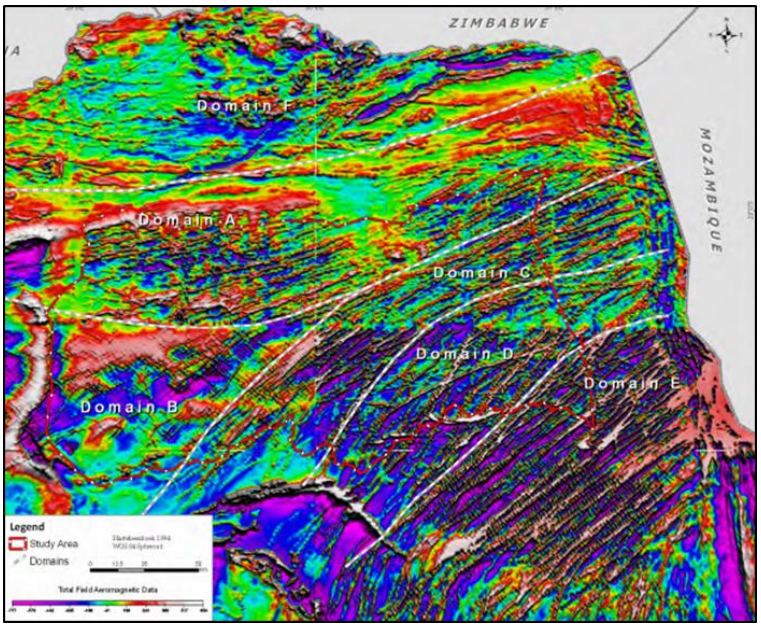

Figure 2-5: Aeromagnetic map of the north eastern parts of the Kaapvaal Craton and the LMB adapted from Stettler et al., (1989) which was subdivided into five domains (A to E) by Holland (2011) according to the prevailing aeromagnetic lineament pattern.

Interpreting these magnetic lineaments, the dominant ENE to NE trending dyke swarms and associated aeromagnetic lineaments correspond with the ages of the Ventersdorp (2700 Ma) and Karoo (180 Ma) dolerite dykes (Uken, 1997). Suggesting, the north eastern Kaapvaal Craton underwent NW-SE extension during these periods (dolerite intrusion) which is in contrast with the current NE-SW extensional regime. Although, according to Bird et al. (2006) southern Africa is not in a state of horizontal compression. The main ENE dyke swarm trend appears to be cut by NW trending dykes, suggesting that the latter intruded last.

Field observations by Petzer (2009) indicates that normal faults and open joints were also formed in a NW-SE orientation, being obliquely or even perpendicular to the main dyke orientation (Petzer, 2009); therefore showing poor correlation with regards to the dominant NE trending dyke orientations. This is evident that structures inherited from the Precambrian are most likely open to the regional neo-tectonic stress regime. Therefore, some of these joints could have formed due to dilatation. It is also believed that many of these joints are rather tectonically induced, suggesting that the study area was at one stage subjected to compression. For this reason it is favourable for the formation of open joints in the NE-SW orientation that were probably reactivated during successive tectonic events, closing many fractured structures that could have been favourable groundwater flow paths in the geological past (Holland, 2011). These NE-SW striking joints also lie parallel to one of the two preferred lineament orientations as identified by the main dyke azimuths (NE-SW and NNE-SSW).

Holland (2011) also subdivided the Letaba catchment into 4 structural domains on the basis of aeromagnetic lineament strike direction and frequency. Interpreting the study area from Holland (2011), the eastern domains of the Letaba catchment in the Limpopo Province are characterized by higher frequency dyke swarms and lineaments when comparing it to the western domains. The north-eastern and south-eastern structural domains also show a higher degree of preferred orientation with dykes trending predominantly ENE (63°) in the north eastern domain and cut obliquely across the GGB. Dykes in the south eastern domain, which forms part of this study area, have a strike orientation of 47° and are almost parallel to the elongated Duiwelskloof Leucogranite (Holland, 2011).

2.3 Hydrogeology

The hydrogeological characteristics of the north eastern Limpopo Province were discussed in depth by Holland (2011) where he split the basement aquifers according to the topography, surface drainage and geological domains. The western region is referred to as the Limpopo Plateau and the eastern region as the Letaba Lowveld with the latter being relevant to the study area. Adjacent to the escarpment to the west, the Letaba Lowveld is characterized by mountainous terrains, deep valleys, high rainfall and lush vegetation with numerous springs in the area. The Goudplaats Gneiss is highly weathered with a regolith thickness that rarely exceeds 30 m. The Duiwelskloof Leucogranite which underlays the higher lying areas including the footwalls east of the escarpment have a thin to absent weathering layer (Holland, 2011). These elongated granitoids intrusions occur as boulder outcrops with little soil cover. In the past, groundwater exploration has shown that targeting structural features and geological contacts provides more sufficient yields compared to the thin regolith. For this reason, the weathering layer has little influence on borehole productivity. While borehole analyses indicate that the lithology and rock type influences the borehole productivity, the factors involving the control of borehole yields, therefore, differs at each geological setting (Holland, 2011) which show distinct differences in groundwater potential. The following map shows the extent of the borehole in the Molototsi catchment.

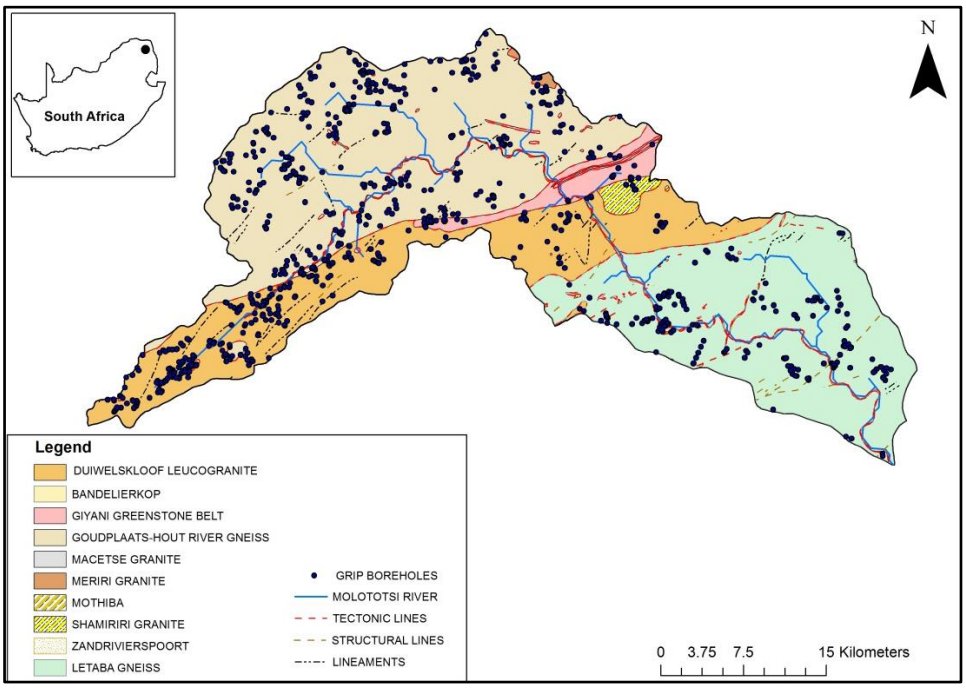

Figure 2-6: A geological map showing the extent of boreholes and the correlation with geological features. Coordinates: latitude -23.568542°, Longitude 30.823947°.

A survey conducted on the Letaba Lowveld groundwater region found that the success rate of boreholes is slightly lower compared to Limpopo Plateau groundwater region, with 39% of boreholes yielding between 0.1 L.s-1 and 3 L.s-1 (Holland, 2011). Holland also summarized that 60% of boreholes encountered water strikes before 30 meters, 34 % of boreholes exceeds 60 meters depth and only 8 % have water strikes below 50 meters in the Letaba Lowveld, suggesting a shallow base of weathering and fracturing which may explain the generally shallower drilling depths with a potentially higher risk of borehole failure during droughts.

In general, dykes are poor groundwater targets; however, drilling along these features in the study area may result in more successful yields, where these dykes may act as barriers to groundwater flow. If the strike direction of the dykes are not considered it may result in disappointing yields, especially in the Letaba Lowveld (Holland, 2011). The juxtaposition of the two lineament orientations generally provides different borehole yields with increased intensity of fracturing towards the lineaments. Although highly variable, it is expected that boreholes influenced by NW-SE striking lineaments should show higher yields than boreholes associated with lineaments striking NE-SW. However, according to Holland's results, higher borehole yields are associated with lineaments and dykes perpendicular to the current stress regime, especially lineaments in the ENE to E and WNW to W direction. This would suggest that the Letaba Lowveld could possibly be under N-S extension (Holland, 2011).

The geology has therefore been identified as the main influential factor on borehole yields while topography and the proximity to surface water drainages also have an influence on the groundwater potential. In many cases low topography settings such as valleys show higher borehole yields in fractured rocks (Holland, 2011). In most cases these higher borehole yields are associated with primary alluvial aquifers. These drainage channels generally follow zones of structural weakness such as lineaments and dykes, therefore, rocks in close proximity to rivers might be more intensely fractured, jointed and/or weathered (Holland, 2011). Major drainage channels consisting of alluvial deposits namely the Molototsi -, Groot Letaba- and Klein Letaba River are associated with composite aquifers. Suggesting that these rivers comprise of both primary and secondary aquifer components (i.e. the regolith or weathered granite is underlying a sand-filled river bed; weathered and fractured dolerite dykes are underlying alluvial deposits). A summary of the potential groundwater targets based on the knowledge obtained by Holland (2011) is listed in Table 2-2. The sections that follow give a general understanding and characterization of crystalline aquifers.

Table 2-2**:** The recommended drilling targets per structural domain (Holland, 2011).

Catchment	Letaba Lowveld
Region	SE Domain
Lineaments (proximity)	Minor influence on the borehole yields (within 150 m of lineament)
Lineaments (orientation)	ENE to E (60 to 90°) are associated with higher borehole yields compared to W to NW (270 to 315°) and NE (30 to 60°)
Neo-tectonics	High borehole yields observed oblique and perpendicular to current NW maximum horizontal stress regime

2.3.1 Aquifer Systems

A conceptual presentation of the Letaba Lowveld aquifer systems typically found in the targeted Molototsi catchment is shown in Figure 2-7 by Holland (2011). The catchment consists of

- Composite aquifers which consists of both primary (alluvial) and secondary (fractured rock) aquifer components, e.g. weathered granite or fractured dolerite dyke underlying a sand-filled riverbed (alluvial) aquifer;
- Deeper fractured aquifers within the granite gneiss basin which is localised along shearzones, faults, and dyke intrusions; and
- Alluvial aquifers which is situated within the riverbed sands and gravels.

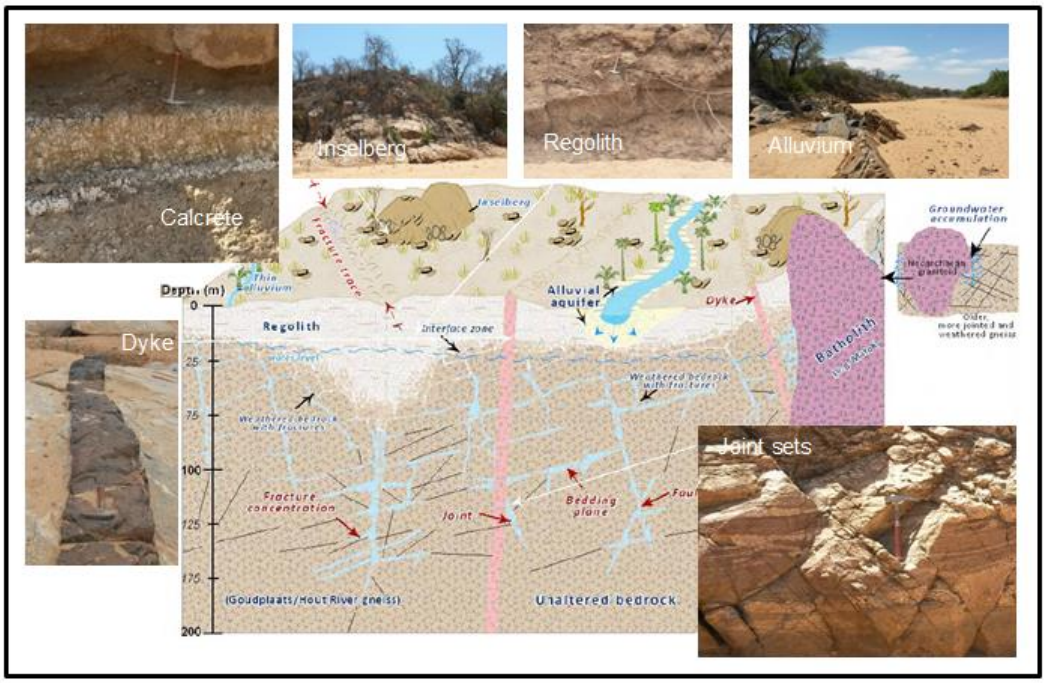

Figure 2-7: A conceptual understanding of the most significant features controlling groundwater occurrences of crystalline basement aquifers in the Letaba Lowveld with specific focus on the Molototsi River catchment. Photos were taken in the field and plotted along the conceptual model adopted from Holland (2011). The photos show the important characteristics of the catchment (alluvium, fractured rock (joint sets) and dykes).

2.3.2 Weathered-Fractured Rock Concept

Although more detailed literature is available on weathering profiles for crystalline basement rock, the classical weathered-fractured rock concept proposed by Jones, (1985), Acworth (1987), and Chilton and Foster (1995) still applies to most crystalline basement terrains, which is illustrated below.

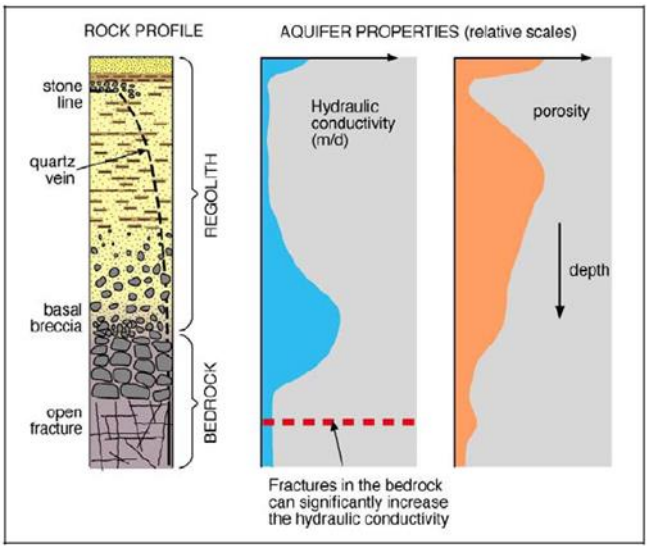

Figure 2-8: Hydraulic conductivity and porosity in crystalline basement aquifers (Holland, 2011).

The above crystalline basement aquifer model refers to the following layers, which shows specific hydraulic properties of each (Holland, 2011):

- An overlying residual layer (regolith) with varying thickness that could reach up to tens of meters.
- Weathering is more rapid in tropical regions compared to arid or higher lying areas.
- High porosity and a low permeability are normally expected within the regolith due to clay-rich material. If saturated, this layer can form part of the aquifer reservoir.
- The porosity of the weathered layers decreases with depth along the clay content, and increases along coarser material until fresh rock is reached.
- The hydraulic conductivity (permeability) however, decreases at the coarse material (gravel, cobbles, boulders) layer but increases in the fractured rock layer.
- The fractured layer between the fresh hard rock and the regolith frequently has a higher permeability, depending on the nature of the fracturing and the presence of clay in the fractures.
- This layer in crystalline basements is mainly assumed as the transmissive function in the aquifer and is pumped by most of the wells drilled.
- Fresh (un-weathered) basement rock is only locally permeable where deep tectonic fractures and contact are present.
- These structural features are extremely variable in nature with regard to interconnectivity.

Crystalline complexes from various regions may differ from weathering thicknesses, degree of saturation and the extent of fracturing. However, from a groundwater supply perspective, crystalline basement aquifers share a common viewpoint, that that long-term borehole yield relies on the weathered material overlying the fractured rock or an alternative source of recharge such as a river (Holland, 2011).

3 Methodology

This section discusses the theoretical analysis and methods applied to obtain the necessary results.

3.1 Site Identification

Site selection is the first and most important step in planning a subsurface sand dam. An appropriate site should be constructed on both physical and social grounds. Climate, topography, geology and hydrogeology are the four physical factors which govern the selection of suitable sites.

The Molototsi River catchment was selected as case study area, because it holds all the necessary characteristics for subsurface dam construction. From the physical perspective, it has a crystalline basement overlain by thick alluvial sands at a depth estimated between 2 and 10 m. From the social perspective, it is in the vicinity of rural communities that are in need of safe and secure water supply.

The site identification (of sand aquifers) was conducted by analysing large datasets of regional studies by using Geographical Information Systems (GIS). GIS together with spatial dimensions and associated attributes provides a rapid, integrated and cost effective tool for any site investigation. The use of detailed topographical and geological maps, existing core drilling data, electromagnetic and resistivity tomography surveys was also used to assist with the site investigation. With this approach it was possible to delineate surface and subsurface features such as geology, structures and rivers. In addition, two weekly field campaigns were envisaged in order to carry out field surveys to collect competent field data, as the accuracy of the site selection will determine the feasibility of the dam construction.

3.2 Geological Investigation

The geological investigation involves analysing the physical characteristics of the site, especially the sedimentary and rock structure. The study would involve identifying bedrock that is dense and non-porous, preferably crystalline rocks with overlaying coarse sand which will have a higher groundwater yield compared to volcanic rocks; areas with at least 2 to 3 meters of alluvial sand to secure a sufficiently thick sand aquifer; sites with solid bedrock (impermeable layer) preferably on both flanks of the river bed to prevent erosion of the flanks; areas where dykes (structural barriers) are visible which could impede normal lateral groundwater movement and could also act as groundwater feeders. However, these dykes do not have to be as continuous as other structural barriers such as faults and should be arranged perpendicular to the direction of the river and shallow groundwater flow. River catchment regions with a slope gradient between 0.2 and 4 percent are ideal sites for subsurface sand dams (Gezahenge, 1986) as they normally give the highest water storage; however, slopes of up to 16 percent can be considered.

Information on the geology (from the Council for Geoscience), topography maps (from the Council for Geoscience), digital elevation models (from Stellenbosch University), aerial photographs, satellite images and geophysical data (from the Department of Water and Sanitation) was sourced from Government departments. Borehole drilling and logging data of the Molototsi catchment was gathered from the Department of Water and Sanitation (DWS) and CSIR. The following instruments were used for each geological survey.

3.2.1 Structural Geology

The android application FieldMove Clino was used to determine the dip and strike (orientation) of numerous geological structures such as joints, dykes and fractures. Only the observed outcrops along the Molototsi River (see Figure 4-2, Figure 4-3, and Figure 4-4) were measured with FieldMove Clino. This is a data capturing app by Midland Valley, specifically developed for structural geologists which is a digital compass clinometer for measuring and capturing the orientation of these planar and linear

features in the field. A handheld Trimble GPS was also used to calibrate and compare the accuracy of the data by taking coordinate points and line features along dykes and outcrop. The FieldMove Clino orientation data obtained from the joint and dyke survey conducted on the outcrops in the Molototsi River was processed using Stereonet 9. Some of the line features taken with the Trimble GPS (dykes and lineaments) were imported to ArcGIS and Google Earth. These line features can be seen in Figure 4-4.

Photo 3-1: The author taking structural readings and coordinates of the outcrops along the Molototsi River. Ponding of water can clearly be seen along the outcrops.

3.2.2 Geophysical Survey

The geophysical survey conducted during April 2016 focussed specifically on the proposed CSIR research farm (Duvadzi research farm) and the Molototsi River. The objective of the survey was to investigate the subsurface geological structures and deep weathering zones and to optimize the selection of drilling sites. Three geophysical traverses were conducted which comprised of magnetic, electromagnetic and resistivity methods which will be discussed below.

Figure 3-1: Magnetic and Electro-magnetic transects measured at the Duvadzi farm which is generated on a Google Earth map. Line 1 and 2 are traverses conducted on the Duvadzi research farm (outlined in red) and Line 3 within the Molototsi River. The three borehole (BH1, BH2 and BH3) sites can be seen as blue dots within the red Duvadzi farm outline and one well point within the riverbed. Coordinates: latitude -23.566213°, Longitude 30.820157°.

Magnetic Method

The aim of the Model G5 Proton Memory magnetic method is to investigate the subsurface geology on the basis of anomalies in the earth's magnetic field resulting from the varying magnetic properties of underlying crystalline rocks. Different rock types have different magnetic susceptibilities, which may have remnant magnetism. The contrast in magnetic susceptibility and/or remnant magnetism gives rise to anomalies related to structures like intrusive dykes, faults, lithological contacts and weathered/fractured bedrock. Measurements were first taken at 10 m intervals along two traverses of approximately 220 m (line 2) and 280 m (line 1) as seen in white on Figure 3-1 above. The readings of the subsurface apparent conductivity were taken representative to depths of 60 m. Anomalies (inferred dolerite dyke and/or lineament) were identified which is shown as black lines in Figure 3-1.

Photo 3-2: The G5 Proton Memory magnetometer used to conduct geophysical measurements.

Electromagnetic Method

The Geonics EM-34 electromagnetic method was used for rapid measurements of the terrain's conductivity in milliSiemens/metre (mS/m) with a maximum effective penetration depth of approximately 15 meters. Vertical and horizontal coil orientation was used with a 20 m coil separation. The EM-34 is applied for its effectiveness to detect remnant and non-magnetic dykes and to determine the dip of dykes or geological structures. These measurements were conducted along the white lines seen on Figure 3-1 above.

Photo 3-3: The author assisting the Department of Water and Sanitation (DWS) with conducting geophysics by using the electromagnetic method.

Resistivity Method

The Resistivity was conducted with a metal probe (electrode) resistivity system. The most common mineral forming soils and rocks have very high resistivity in these dry condition of Limpopo. The resistivity of soils and rocks is therefore normally a function of the variations in water content and the concentration of dissolved ions in the groundwater. Resistivity investigation was thus used to identify zones with different electrical properties, which refer to different geological features. The electrode separation and survey protocol used, determined the depth of investigation. The measuring protocols used were Wenner Array (Horizontal Electrical Profiling) with an investigation depth of approximately 60 m, using 100 meter cables which consists of four electrodes in a line with equal spacing intervals as seen in the photo below. The geophysical traverses were surveyed at 10 m station intervals along the white lines (see in Figure 3-1), with all stations marked in the field during the survey. The combined results can be seen in Figure 4-6 (red line) with Figure 4-7 showing a detailed resistivity result at station 2 (620 m) where the proposed dam site is located.

Photo 3-4: The author assisting the DWS with conducting geophysics by using the resistivity method.

3.2.3 Borehole Drilling

After the geophysical survey the borehole drilling sites were established. Three preferable borehole locations were sited after which a drilling rig was made available by the Department of Water and Sanitation. The percussion drilling method was conducted which makes use of compressed air to help break up the hard crystalline rock formations. The compressed air operates an air hammer situated deep down the hole. The same air blown through the rods down the hole through the hammer eventually blow the crushed fragmented material up and out the hole. When the water strike or fracture area containing groundwater were hit the water blew out the hole. These water strikes were noted and the yields were measured. During drilling, the blown out chip material was sampled at one meter intervals, which was set aside in heaps for borehole logging (seen in Figure 4-9, 10 and 11). Samples of these heaps were collected at each depth where different lithology occurred and stored. After drilling the boreholes were cased with 177 mm steel pipes, slotted steel pipes were installed at water strikes which were gravel packed on the outsides. Finally, the boreholes were capped and marked. The three newly drilled boreholes (BH1, BH2 and BH3) locations can be seen in Figure 4-8 which were programmed into a text file and imported into the computer software dotPLOT (version dot7022) to create borehole logs seen in Figure 4-9, 10 and 11.

3.2.4 Geological Model

A basic geological model with a satellite image overlay was created for the site using computer software by Leapfrog Geo, which has dynamic and intuitive capabilities to create 3D surfaces. It is typically used to efficiently build simple to complex models from borehole, point and structural data. In this case, the data obtained from the geological survey which includes the major lithologies, mapped dykes, drilled boreholes and soil profiles were used to build the model. Logs of each borehole and soil profile (from test pits) lithology and dykes were listed in excel along with each layer's characteristics and orientation which were then imported into Leapfrog. The geological information from the test pits and boreholes have an associated geographical location as well an elevation.

The programme, through built-in complex statistical methodologies, extrapolates between all the data points, thereby creating contact surfaces between the different lithological units that have been identified. The general trend of the dykes was determined from observations on site, and this together with the actual mapped exposures were used to guide the construction and extrapolation of these structures.

Considering the fact that this was a conceptual model being built, and that there is an absence of comprehensive data, the model was refined to produce what can be seen in Figure 4-14. For the purpose of this study it is considered that the geological model together with the hydrogeological and geotechnical investigation knowledge provided a good conceptual understanding of the site which assisted with the groundwater model.

3.3 Hydrogeological Assessment

Hydrogeological information was obtained from the National Groundwater Archive of DWS and the GRIP database (Groundwater Resource Information Project) of the DWS Regional Office in the Limpopo Province (accessed on 9 November 2015). The data was used to determine the regional groundwater level and to identify areas of shallow water tables and high yields.

To ascertain the number of small-scale farmers that would benefit from the water storage, an approximate crop irrigation requirement of the Duvadzi farm and the water yield of the subsurface dam was calculated. The water yield of the selected location of the subsurface dam was derived from the dimensions of the storage obtained from the longitudinal and cross-sectional profiles and the water extraction ratio of the sand. It is worth mentioning that the riverbank might have to be included in the calculation of the water yield, if there is groundwater flow from the riverbanks to the riverbed, however, it was not included in this study.

The hydrogeological assessment also served to provide inputs to a groundwater flow model that was used to simulate groundwater flow in a porous aquifer and its behaviour as affected by the subsurface dam.

3.3.1 Aquifer Parameters

The aquifer parameter calculations used are described in this section. Three split samples (see Test Pits and Profiles section) were tested namely: the original sample (not sieved), medium grained sand sample (2 - 0.425 mm), and a course grained sand sample (< 0.425 mm). Each sand sample were saturated with water in a separate cylinder. The sand columns were first filled with water and then filled with small quantities of sand at a time to allow the samples to fully saturate. The bulk density of each were then determined by weighing the 1000 ml saturated sand.

The results of the original sample are the closest representative of the natural specific yield as it was in its original state and not sieved, therefore, the values obtained from this sample were predominantly used to determine other hydrogeological (Evaporation Losses and Groundwater Reserves) and geotechnical parameters (Soil Parameters).

On draining the water from the sand a compaction of about 1 % was observed in all three samples. After the sand was dried the dry density of the sand was then determined. A second yield test was done by again saturating the sand by means of a dripping tap over a prolonged period. The same degree of saturation as with the initial method of filling the sand into the water was not achieved. Even though the analysis were done on sand and not clay, saturating these sand deposits by surface application of water was by no means easy.

Porosity

Using the bulk and saturated densities, the porosity of these porous mediums (the three alluvium sand samples) were determined which describes the fraction of void spaces in the material. The void may consist of air or water which is defined by the ratio:

$$\mathrm{n} = \frac{V_V}{V_T}$$

where, V_V is the volume of voids and V_T is the total or bulk volume of material, including the solid and void components.

Specific Yield

Specific yield is defined as the volume of water released from storage by an unconfined aquifer. It is also called the effective porosity which is generally less than the total porosity of an unconfined aquifer. Bear (1979) relates specific yield and total porosity as follows:

$$n = S_y + S_r$$

where, n is the total porosity, S_y is the specific storage, and S_r is the specific retention which is the ratio of the volume of water retained by capillary forces against gravity drainage of an unconfined aquifer.

As mentioned above in the Aquifer Parameters introduction, sand samples of known volumes were fully saturated. Each column was slowly flooded and allowed to drain from the column by gravity. The ratio of the volume of water drained to the volume of the sand column is the specific yield.

Hydraulic Conductivity

Estimation from grain size: The empirical approach for calculating hydraulic conductivity using Hazen's equation, where, D_{10} is the diameter of the 10 percentile grain size or the effective size in mm.

$$\mathrm{K} = 10^{-2}(D_{10})^2$$

Inversed auger hole method: An experimental on site field method for approximating hydraulic conductivity can be estimated using the equation, where, K_s is the hydraulic conductivity, r is the radius of the well, h_0 water level at t_1 and h_1 the water level at t_2, and delta t is $t_2 - t_1$ which is time.

$$K_s = 1.15\, r\, (\log(h_0 + \frac{R}{2}) - \log(\frac{\left(h_1 + \frac{R}{2}\right)}{\mathrm{t}}))$$

Constant-head method: An experimental laboratory method for approximating flow rate, where, Q is the quantity of water measured, L is the length of the specimen, A is the cross-sectional area of the specimen, and h is the head.

$$\mathrm{K} = \frac{Q * L}{\mathrm{A} * \mathrm{h}}$$

Transmissivity

The hydraulic conductivity obtained from the experimental in-situ field test (auger hole) was used to measure the transmissivity and is given by the following:

$$T_i = K_i d_i$$

where, T_i is the transmissivity for horizontal flow of the $i - th$ soil layer, K_i horizontal hydraulic conductivity, d_i is the saturated thickness of the aquifer.

3.3.2 Groundwater Recharge

The groundwater recharge assessment is not intended to contribute to the literature but rather as an important method for determine recharge which will provide insight into recharge rates and connectivity between the two aquifers (crystalline and alluvial aquifers).

The average groundwater recharge of the two aquifers found on site, were determined using the Chloride Mass Balance (CMB) method which uses the Mean Annual Precipitation (MAP), Chloride (Cl) concentration of rainfall in the area, and the chloride concentration of the groundwater aquifers. For more detail on the theory behind the CMB method the reader is referred to the following publications: Wood (1999); Kinzelbach et al. (2002); Adams et al. (2004).

The CMB method have been used to estimate recharge of the saturated zone in basement aquifers throughout southern Africa to estimate recharge (Holland, 2011, Xu and Beekman, 2003; Adams et al., 2004). This method determines the recharge over an entire drainage area by integrating the ratio of average chloride content in rainfall (wet and dry deposition) to that of groundwater (Holland, 2011). The CMB method can be represented by the equation (Kinzelbach et al., 2002):

$$Rt = \frac{P * \ Cl_p + D}{Cl_{gw}}$$

where, Rt is the total recharge (mm/a), P is precipitation (mm/a), Cl_p is concentration of precipitation (mg/l), D is dry deposition (mg/m^2/a), Cl_{gw} is the concentration of recharging groundwater (mg/l).

The chloride of rainfall (Cl_p) was obtained from Holland (2011) which is an average used for the Letaba Lowveld, Limpopo. The chloride for the two groundwater aquifers (Cl_{gw}) were obtained from water quality test discussed later on in the hydrogeological assessment.

3.3.3 Groundwater Quality

Groundwater quality analysis was conducted for two samples. One sample from the newly installed borehole, BH2 (H14-1702), and the second sample from the Molototsi River. The water samples were sent to a SANAS accredited laboratory and analysed according to SANS 241 standards. The laboratory results were then compared to the Water Quality Guidelines (DWAF, 1996) to determine whether the water is fit for human consumption or irrigation.

3.3.4 Evaporation Losses

In the experiment to estimate evaporation losses of the Molototsi riverbed a 1000 ml cylinder was filled with sand. The experiment was only conducted on the original mixed sand sample. Before the sand column was saturated with water and placed in an exposed position in the sun, the dry and bulk unit weight was measured.

The amount of water evaporation in the sand at a constant time interval (shown in Table 4 9 below) was determined by weighing the cylinder and subtracting the known dry unit weight. These mass values were used to calculate the water content (see Soil Parameters in the Geotechnical Investigation methodology). The Saturated Depth (S_d) was visual measured from the 1000 ml cylinder and recorded every day. The Rate of Evaporation was determined by the following expression:

$$E_0 = \frac{S_d}{\mathrm{n}}$$

where, E_0 is the rate of evaporation (m/month), S_d is the saturated depth (water level in the sand column), and n is the porosity of the sand.

3.3.5 Groundwater Monitoring

Groundwater levels within the boreholes and the Molototsi riverbed was monitored quarterly with manual dip meters since the beginning of the project (see results in Table 4-10). The newly drilled boreholes H14-1702 and H14-1703 on the Duvadzi farm contain groundwater level loggers which were installed on 7 October 2016, just before the rainy season. Based on the geophysical survey, boreholes H14-1702 and H14-1703 were drilled on the same dolerite dyke assuming that they are penetrating the same aquifer.

The shallow groundwater of the Molototsi riverbed was also monitored (see Table 4-12) by taking measurements every season at a 1.5 meter deep well that was constructed in the riverbed by the Duvadzi farmer. Water was abstracted from this well for irrigation purposes from late September 2016 to early January 2017. During abstraction the pumping rate was recorded with a water meter, including the water level fluctuation in the well by measuring the drawdown and recovery over time pumped. From this, hydraulic tests and modelling were carried out (refer to the auger hole method in the Aquifer Parameters and Groundwater Modelling sections).

Photo 3-5: The 1.5 m deep well within the Molototsi River from which the Duvadzi farmer is pumping at a rate of 15 m^3/d (pumping every second day) to irrigate 0.175 ha crop plot. Coordinates of the well: latitude -23.568148°, Longitude 30.819999°.

3.3.6 Groundwater Reserves

In order to determine whether the subsurface dam would be a reliable and feasible water source, the potential extractable reserve needs to be estimated. The Aquifer Parameters (porosity and specific yield), Groundwater Monitoring, and information obtained from using GIS tools assisted with creating the following expressions:

$$R_p = \mathrm{L} * \mathrm{B} * S_d * \mathrm{n}$$

where, R_p is the potential groundwater reserve (m^3), L is the length of subsurface dam segment, B is the average width of the riverbed sand, S_d is the average depth of saturated sand aquifer, n is the porosity of the sand;

$$R_E = \mathrm{L} * \mathrm{B} * S_d * S_y$$

where, R_E is the potential groundwater reserve (m^3), L is the length of subsurface dam segment or river reach, B is the average width of the riverbed sand, S_d is the average depth of saturated sand aquifer, S_y is the specific yield of the sand.

The potential groundwater reserve and extractable reserve were calculated for each season due to the observed decline in the shallow groundwater level. These two estimation where calculated for both the natural river and the artificial subsurface dam using a river reach of 400 m. Knowing the volume of the extractable groundwater reserve, would be valuable information to the decision makers as it defines whether the natural river or subsurface dam supplies sufficient yields.

An approximate crop irrigation requirement was also estimated based on the current pumping schedule of the Duvadzi research farm. From the groundwater monitoring during site visits, it was estimated that the Duvadzi farmer abstracted approximately 15 m^3 (pumping from the Molototsi River) every second day to irrigate the crop. This was deemed sufficient to irrigate a crop plot of 0.175 ha and was therefore referred to as the sustainable irrigation volume, however, according to the DWA (2014), quaternary catchment B81H has an estimated riverbed baseflow of 10 000 m^3/a which corresponds to a pumping rate of 27.4 m^3/d. This is given by

$$Q_p = \frac{b_f}{a}$$

Where, $Q_p$is the pumping rate (m^3/d), b_f is the baseflow (m^3/a), a is the a constant of 365 days per year (d/a). The above calculated groundwater reserves and proposed pumping rates were determined in order to simulate various scenarios.

3.3.7 Groundwater Modelling

A hydrogeological model of the area of interest was built using the Visual MODFLOW computer software (GW Vista). The groundwater flow model was calibrated (parametrized) using data collected during the hydrogeological assessment. The aquifer parameters were used as inputs into the model e.g. hydraulic conductivity, transmissivity, porosity and specific yield (see Aquifer Parameters section

above). Modelling scenarios were performed in order to aid in the design of the subsurface dam as an impermeable barrier occurring in the riverbed (sand aquifer).

The first scenario was simulated to represent the natural conditions of the alluvial aquifer. After the realistic hydrogeological functioning of the riverbed sand was achieved, the pumping was activated which simulated the true abstraction rates. This was achieved by using a transient model approach. The objective was to simulate the realistic drawdown and decline in water levels over 71 days (2 September 2016 to 30 November 2016) of pumping (on average pumping 15m^3/d every second day).

For the second scenario, the objective was to see how much the extractable reserve would increase if a subsurface dam was constructed. The parameter of this scenario changed as a 3 m wall structure was included along with a 3 m sand aquifer thickness. The water level was kept at 0.5 m below the riverbed which corresponds to a saturated sand thickness of 2.5 m. The same pumping rate of 15 m^3/d over the same time period (pumping every second day) was used to compare the results with Scenario 1.

A third scenario, Scenario 3, was performed to determine how much water can be extracted before the artificial aquifer or subsurface dam runs dry. The pumping rate was increased to 30 m^3/d (pumping every second day) at the same time interval as Scenario 1 and 2. The same simulation was run for Scenario 4, however, pumping was increased to an even higher rate of 40 m^3/d. Note all the above scenarios were simulated to pump the actual days of irrigation which on average were every second day.

The artificial aquifer was also simulated to determine what would happen if pumping would occur continuously for 71 days (seen in Figure 4-21). This was determined using a conservative pumping rate of 15 m^3/d for Scenario 5, a potentially higher but sustainable pumping rate of 30 m^3/d for Scenario 6, and 40 m^3/d for Scenario 7.

3.4 Hydrological Study

The hydrogeological assessment will make use of climatic data (available from the South African Weather Services (SAWS), Agricultural Research Council, previous and current projects carried out in the area by CSIR), land cover/use maps (National Land Cover maps available at CSIR).

Rainfall and temperature patterns will be assessed using indices that represent a wide variety of rainfall and temperature characteristics for both the average regime and particularly the extreme behaviour of the rainfall events. The design rainfall depths were obtained from a grid estimated based on nearby rainfall stations using the program called ‘Design Rainfall Estimation of South (Smithers and Schulze 2002). In addition to the design rainfall data, the daily rainfall for the specific station was extracted from the Daily Rainfall Data Extraction Utility (Lynch, 2003). The utility assists users in extracting observed and infilled daily rainfall values from a database which was developed by Steven Lynch.

Hydrological variables reflecting important components of the hydrological regime will be analysed. These include the mean flows, maximum/minimum for given durations, dates of occurrences of the annual maximum/minimum flows and peak flow events. The flood frequency was considered which has important applications for sediment transport analysis and flood hydrology assessment in the Molototsi catchment. Flood peak determination will be based on the current state of the catchment using both the Rational and the Unit Hydrograph methods discussed below. The floodline modelling for the site will be done in HecRas (Hydrological Engineering Centre). The model employs standard backwater techniques to compute the high water level (HWL) for various steady flow conditions, taking into consideration road, railway and dam structures. The inputs for the HecRas model include the adopted flood peaks for various return periods and site information based on the site visits. In order to

use the HecRas model, the ArcGIS software was also used in the analysis by allowing digital cross-sections to be extracted for the watercourse using natural contours from the DEM obtained from National Geo-Spatial Information (NGI). The results obtained from the flood hydrology analysis will be assessed to determine the expected impacts on stream flows and therefore the design of the subsurface dam. The following methods was used to determine flood hydrology.

Rational Method

The Rational Method requires the catchment area, rainfall intensity and C-values (coefficient of runoff) which is a number comprising of soil permeability, vegetation and catchment slope to be selected for calculation of flood peaks for various return periods. It is one of the well-known methods to determine peak floods for small catchments of 15 km^2, however as the Molototsi is a large catchment the Standard Design Flood Methods (SDFM) will be used which is based on the Rational Method.

Standard Design Flood Method

The SDFM is a robust method that accommodates for the uncertainties in the current design estimations by using engineering factors of safety. The method is based on defined flood frequency relationships obtained from historical data. It is an empirical regional calibrated version of the Rational Method (van Vuuren, van Dijk, and Smithers, 2013). The catchment area, length of the river, slope of the main river and the drainage basin is the only data required.

Refer to Figure 7-3, Figure 7-4, and Figure 7-5 (in Appendix C) for the information required for calculating the flood magnitude using the SDFM . The second and third columns in Figure **7-5** are the SAWS station identification numbers from TR102. This publication provides the information required for determining the point rainfall for the specified return period and the calculated time of concentration in step 6 below.

Referring to Figure **7-3**, M is the average of the annual daily maximum rainfalls, and R is the average number of days per year on which thunder was heard. These two values are used in the modified Hershfield equation (step 6). C_2 and C_{100} are the run-off coefficients as used in the equation in Step 8. MAP is the mean annual precipitation and MAE is the mean annual Symons Pan evaporation. These two values are supplied for information only, and are not used in the analysis. They indicate the substantial role played by antecedent evaporation in the flood rainfall run-off process, and how annual evaporation varies inversely with annual rainfall (van Vuuren, van Dijk, and Smithers, 2013). The following steps were followed to determine the flood model:

Step 1: The drainage basin was Identified in which the site is located from the South African flood basin map seen in Figure 3-2 below.

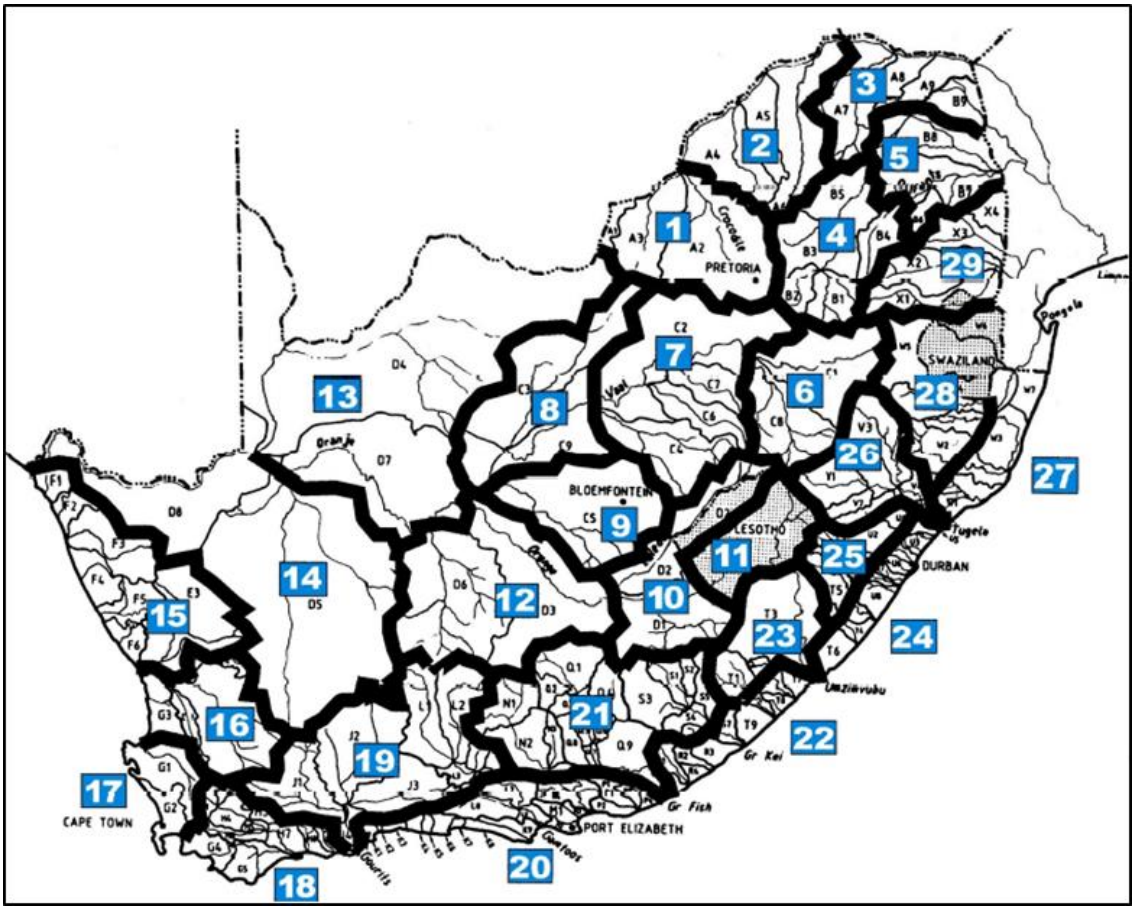

Figure 3-2: Standard Design Flood Basins obtained from the Drainage Manual (van Vuuren, van Dijk, and Smithers, 2013).

Step 2: Using ArcGIS computer software, the catchment boundary and area (A in km^2) was determined.

Step 3: The length (L in km) of the Molototsi River was determined using the measuring tool in ArcGIS.

Step 4: The elevation of the main river channel was determined in metres at two points located at 10% and 85% of the main channel length upstream of the site. The difference in elevation between these two points was divided by 75% of the main channel length. This is called the 1085-slope method which is given by S (m/km).

Step 5: The US Soil Conservation Service formula was applied to determine the time of concentration T_C (hours).

$$T_c = \left(\frac{0.87L^2}{1000\ S_{av}}\right)^{0.385}$$

where, T_c is the time of concentration (hours), L is the main river channel length (km), and S_{av} is the average slope (m/m).

Step 6: The T_c (hours) were converted to t (minutes). The point precipitation depth $P_{t,T}$ (mm) for the time of concentration t (min) and the return period T (years) was determined. Linear

interpolation, between the modified Hershfield and the TR102 values was used as the T_c was between 6 and 24 hours.

Step 7: The point precipitation depth $Pt_{,T}$ (mm) was multiplied by the area reduction factor ARF (%) to determine the average rainfall over the catchment for the required return period T (years). The corresponding rainfall intensity I_T (mm/h) is obtained by dividing this value by the time of concentration (T_c).

$$\mathrm{ARF} = (90000 - 12800\ln \mathrm{A} + 9830\ln t)^{0.4}$$

Step 8: The above steps constitute the standard procedure used in the conventional rational method. The SDFM uses calibrated run-off coefficients C_2 (2-year return period) and C_{100} (100-year return period) from Figure 7-5, instead of determining them from catchment characteristics. The run-off coefficients for the range of return periods T (years) were determined by applying the return period factors Y_T in Table 3-1, using the relationship in the equation below:

$$C_T = \frac{C_2}{100} + (\frac{Y_T}{2{,}33})(\frac{C_{100}}{100} - \frac{C_2}{100})$$

Table 3-1: Return period factors (van Vuuren, van Dijk, and Smithers, 2013).

T =	**2**	**5**	**10**	**20**	**50**	**100**	**200**
Y_T =	0	0.84	1.28	1.64	2.05	2,33	2.58

Step 9: Finally, the flood peak Q_T (m^3/s) for the required return period T is calculated which is the standard format used in the rational method. See the peak flow equation below:

$$\mathrm{Q} = \frac{C_T\ I_T\ \mathrm{A}}{3.6}$$

Step 10: The results from the sections above were used to model two scenarios in HecRas: One where the subsurface dam is below surface and not exposed at all, allowing the river to flow naturally. For the second scenario, flow peaks were modelled using a 1.0 m wall above riverbed level, disrupting the flow.

3.5 Geotechnical Investigation

Analysing the technical characteristics of the site involves the undertaking of geotechnical tests for the identification of the type, suitability and availability of construction material, and excavation conditions. The construction material locally available, such as sand, and rock outcrops will determine what type of subsurface dam to construct. For example, a concrete dam will be considered if sufficient stone aggregates are available in the area, otherwise a clay dam would be more suitable since transporting aggregates can be expensive. Geotechnical evaluation of the soil properties, founding conditions and design will be done. Below the necessary methods used will be discussed.

3.5.1 Test Pits and Profiles

Soil profiles were done on test pits (see soil profile, SP1 in Figure 4-28) dug within the Molototsi River, including suitable profiles of the banks (see SP2 in Figure 4-29) and a section near a failed dam (see SP3 in Figure 4-30). The soil profile where logged with a systematic description of each layer from the surface down. The important descriptors discussed for the soil classifications includes: moisture condition, colour, consistency, structure, soil type and origin (MCCSSO). The software used to create the soil profiles is dotPLOT, version dot7022. From the test pit near the centre of the Molototsi River which is excavated within the sand mining area (see sand mining area in Figure 3-3), one 3 kg sand sample were collected at 1 m depth (see Photo 3-6 below) for particle analysis at the Geotechnical Laboratories of Stellenbosch University. Two more profiles were done on the riverbed that showed very similar profiles and was not included. The analyses were conducted on split samples (discussed in Soil Parameters and Aquifer Parameters sections) to determine the various geotechnical properties associated with each soil and to classify each soil according to the Unified Soil Classification System. Shear Box tests (discussed in the Soil Parameters section) was also conducted on the split samples taken to determine the shear strength parameters.

Photo 3-6: Test pit (soil profile, SP1) excavated in the Molototsi River within the sand mining pit. Coordinates of this test pit: latitude -23.568068°, Longitude 30.818929°.

3.5.2 DCP

Six dynamic cone penetrometer (DCP) test was conducted which determined the consistency, stiffness and strength of the in-situ riverbed sand. Four DCP's were completed along the centre of proposed dam wall structure. Two were done within the sand mining (see yellow polygon in Figure 3-3). From these values the different density of the layers was determined which gave an indication of excavatability. Also, the approximate depth to bedrock was derived at areas where it was less than 2 m deep. The DCP's were conducted at the following locations shown below.

Figure 3-3: DCP locations are shown as red dots. DCP 1 to 4 was done across the riverbed and DCP 5 and 6 was conducted within the sand mining pit (yellow polygon) to reach the deeper profiles. The Duvadzi farm is outlined in red with the three newly drilled boreholes labelled in light blue and the well located within the riverbed.

The DCP has four parts: an 8 kg hammer, the upper rod, a ruler, a bottom rod and a 60° angle cone. The hammer is lifted and released which then falls a distance of 575 mm to account for one blow. With each blow the rod with the sharp cone penetrates the soil. Figure 3-4 shows an illustration of the components of the DCP in working. The penetration depth after 1 to 5 blows (the amount of blows depend on the compaction or stiffness of the sand), is captured and continues until a maximum depth of one meter or if solid rock is reached. It can be considered solid rock if after 15 blows the cone does not penetrate any further. The depth intervals of each blow will be logged and compiled to a graph.

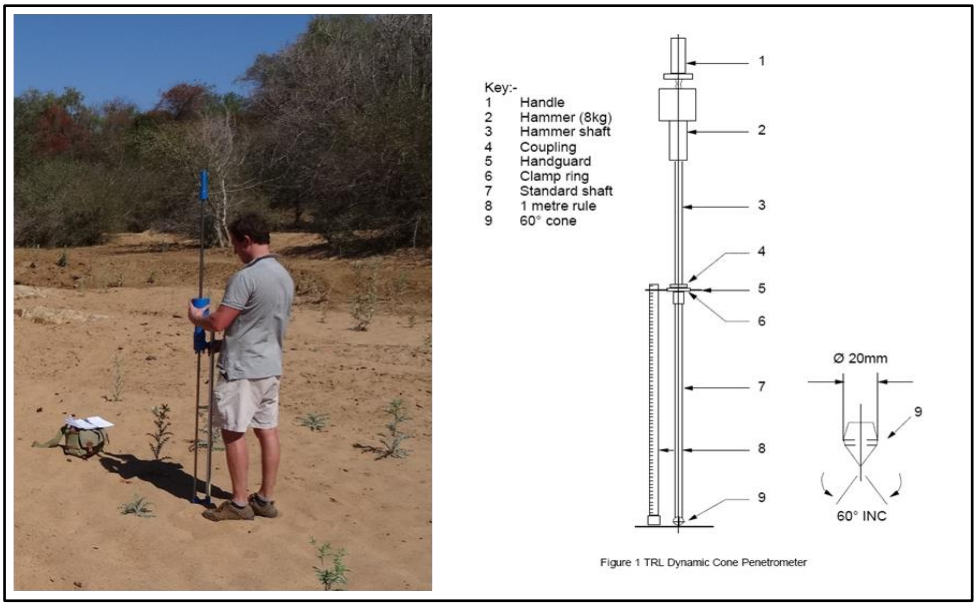

Figure 3-4: A picture of the author using the DCP and an illustration of the DCP components which was obtained from (Jones, 2004).

3.5.3 Soil Parameters

As mentioned in the Test Pits and Profiles section above, three split samples were tested that was taken from the tests pit excavated within the Molotostsi River. Similar sand column methods were used as discussed in the Aquifer Parameters section to determine the Soil Parameters. For this reason, the methodology will not be repeated. The following parameters were determined:

Water Content

The water content was determined by adding the sand sample to a 1000 ml cylinder. The cylinder was weighed to determine the dry mass. Water was added and left over night; thereafter it was weighed to calculate the water mass. The ratio consists of water mass over the mass of solids in the sand. The water content calculated gave similar results as the specific storage calculated in Aquifer Parameters section and was therefore used throughout the thesis.

$$\mathrm{W} = \frac{M_w - M_d}{M_d}$$

where, W is the water content (in %), M_w is the wet/saturated mass (g), and M_d is the dry mass (g).

Specific Gravity

The specific gravity of the soil particles is calculated by using the equation of dry mass and water density.

$$\mathrm{Gs} = \frac{M_d}{V_V - M_w}$$

where, M_d is the dry mass (g), V_V is the volume of the column/cylinder (ml), and M_w is the wet/saturated mass (g).

Dry Density

The dry density of the sand depends on the water content and the compaction. For completely dry sand, the dry density was calculated as follow.

$$P_d = \frac{1}{1 + \mathrm{W}}$$

where, P_d is the dry density (kg/m^3), and W is the water content (in %).

Void Ratio

Void density was determined using the equation between the specific gravity, water density and dry density.

$$P_d = \frac{G_s * P_W}{1 + \mathrm{e}}$$

Where, P_W is the density of water (1000 kg/m^3), and e is the void ratio.

Degree of Saturation

The degree of saturation is the equation of the water content and specific gravity over void ratio, which can range between the limits of 0 for completely dry sand and 1 for fully saturated sand.

$$S_r = \frac{\mathrm{W} * G_s}{\mathrm{e}}$$

Where, S_r is the degree of saturation

Porosity

The porosity in this section uses the equation of void spaces in the material.

$$n = \frac{\mathrm{e}}{1 + \mathrm{e}}$$

Air Content

Air content is the ratio of the air volume and the total volume of the sand; however, it was calculated using the equation of porosity and degree of saturation.

$$A = \mathrm{n}(1 - S_r)$$

Saturated Density

For a fully saturated sand, where Sr = 1, the following equation was used to calculate the saturated density.

$$P_{sat} = \frac{G_s + (S_r * e)}{1 + \mathrm{e}}$$

Buoyant Unit Weight

The buoyant unit weight of the sand is expressed as the saturated unit weight minus the unit weight of water.

$$Y_{sub} = \mathrm{Y}' = Y_{sat} - Y_W = (P_{sat} * g) - (P_W * g)$$

where, Y' is the buoyant unit weight (kN/m^3), and Y_W is 10 kN/m^3.

Shear Strength

The sample was collected at a depth of approximately 1.0 m. The sand of the Molototsi riverbed is homogeneous; therefore, only one 3 kg sample was needed. Two shear box tests were done on the split samples taken from the riverbed test pit to determine the shear angle of the sand. The split samples were tested three times under different loads of 50, 100 and 150 kPa.

3.6 Subsurface Dam Design

The design involves the determination of the stability of the subsurface dam, whether it will overturn under unfavourable conditions. Various geotechnical design calculations were estimated using the soil parameters determined from laboratory tests conducted at the University of Stellenbosch. The subsurface dam wall was designed according to different limit states which should be considered. The stability and satisfactory of the structure was determined by the traditional method (Craig, 2004) and the limit state approach of Eurocode 7 (EN 1997). The reinforcement required was estimated in this study. From all the above assessments and investigations, the feasibility of subsurface dams was determined.

There are different limit states which was considered in the design approach of retaining walls. The subsurface dam structure was designed for: 1) Safety against overturning of the wall; 2) Safety against sliding between the base and the rock mass; and 3) Safety against ground bearing pressure on the supporting foundation. To ensure that the base pressure remains compressive over the entire base width, the middle third rule was applied. Considerations are also given to the consequences of seepage effects.

The following two methods were used to determine the stability and satisfactory of the design:

3.6.1 Traditional Method

Firstly, each horizontal (H) and vertical (V) component of the resultant force (R) acting on the wall was determined by

Force (kN) x Arm (m) = Moment (kN m)

From this the sum of the horizontal forces (M_H) and vertical forces (M_V) was determined.

Secondly, the Rankine's K_a value was calculated by

$$K_a = \frac{1 - sin\emptyset}{1 + sin\emptyset}$$

Referring to the resultant forces calculated. The lever arm of base resultant was estimated by

$$\frac{\sum \mathrm{M}}{V} = \frac{100.88}{122.81} = 0.82$$

Thereafter, the eccentricity of the base reaction was calculated and is given by

$$e = Arm_{base} - \frac{\sum M}{V}$$

The eccentricity was check whether it exceed $\frac{1}{6}B$, where B is the base width. Finally, the following three steps were calculated:

1) The factor of safety against overturning of the wall which is given by

$$\text{Overturning FOS} = \frac{M_V}{M_H}$$

2) The factor of safety against sliding is given by

$$\text{Sliding FOS} = \frac{V\ tan\ \delta}{H}$$

Where, δ the friction angle between the base and foundation.

3) The maximum and minimum base pressures are given by

4)

$$\text{p} = \frac{V}{B}\left(1 \pm \frac{6\ e}{B}\right)$$

3.6.2 Limit State Approach

The limit state approach is similar to the traditional method, however, for each material, load, or force, a partial factor of safety is assigned individually depending on the case. Therefore, each element is more accurately assessed and allows the structure or material to utilize to its maximum strength during its lifespan. This suggest that the structure was designed according to more conservative values if satisfactory was reached.

4 Results

4.1 Site Selection

Site selection, as mentioned previously is the first and most important step in planning a subsurface sand dam. Climate, topography, geology, hydrogeological and social maps were used which are based on the physical and social factors that govern the selection of suitable sites.

In the first figure (Figure 4-1 A) we have the climate map of the Molototsi River catchment. The area, on average receives an annual rainfall between 200 – 500 millimetres per annum (mm/a) with the minor mountainous region receiving more than 1000 mm/a. However, it is important to note that the B81H area only received about 100 mm/a rain during 2015. Thus, suggesting that the Molototsi River catchment is water stressed, especially in the B81H section where access to water is more limited.

The topographical map (Figure 4-1 A) shows a quantitative representation of relief with the mountainous regions in the B81G and the Lowveld plains in the B81H quaternary catchment. This favours the selection of subsurface dams in the B81H quaternary catchment because it consists of a lower, more gradual slope, as the recommended slope for sand dams are between 1-5 %. Thus, suggesting that the B81H region of the Molototsi River catchment is an excellent starting block for locating sites to construct subsurface dams.

The second figure (Figure 4-1 B) is the geological map which shows lineaments, structural and tectonic lines that are predominantly orientated in a NE to ENE direction, suggesting that structural lines are parallel with the Molototsi River in the B81G quaternary catchment and only cross-cut the Molototsi River in the B81H quaternary catchment. This also supports site selection in B81H where dykes are cross-cutting the river in order to have hard rock to construct on. The dykes and lineaments are also good water indicators in the study area and may form a natural groundwater flow barrier.

The hydrogeological map shown in Figure 4-1 C displays the inverse distance interpolated groundwater levels where the dark blue show groundwater levels of 2-10 m which is of interest to the study. These shallow groundwater strike regions may possibly feed the subsurface dams during dry seasons, thus it could benefit from constructing subsurface dams in these regions. It is also important to note that the dark blue areas are also in close proximity of the structural line orientations, thus, supporting the theory that the fractured granitic rocks in close proximity of these dykes act as water conduits.

Next, a social map (Figure 4-1 D) is included which shows whether the selected dam sites would benefit the community and whether the localities make economically sense. Three of the localities seen on the map (red dashed lines) are either too remote with zero access roads to the river or too far from human settlements or farms. However, the second locality is close to a large village which could possibly cause an increase in contaminants and pollution of the water resource. Thus, the three mentioned localities were eliminated. The selected area (solid red line) for locating the subsurface dam site consists of all the necessary physical and social factors. The author also made use of existing core drilling data, electromagnetic and resistivity tomography surveys to delineate surface and geological features which supported the selection of the proposed dam site with the following coordinates: latitude -23.568542°, Longitude 30.823947°.

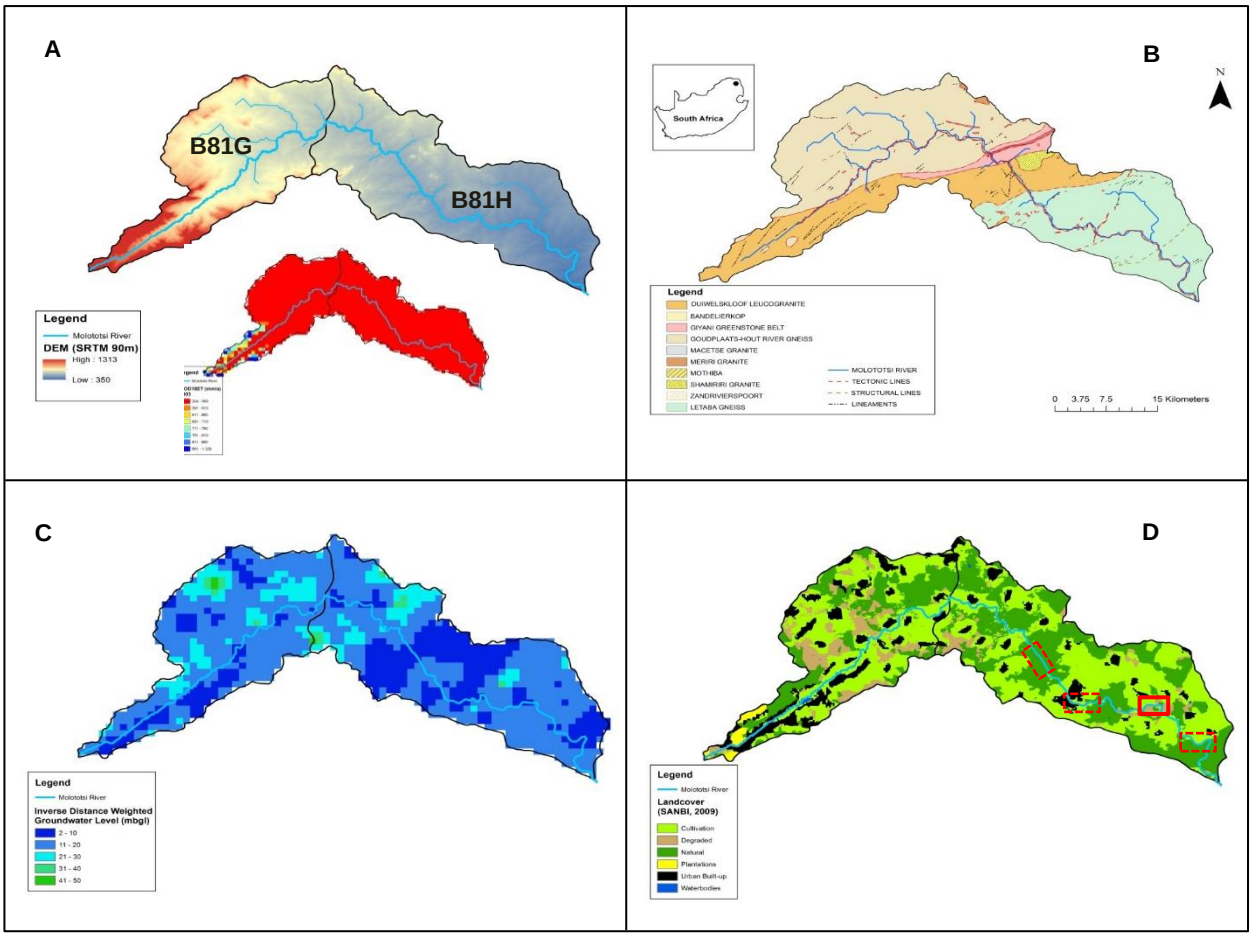

Figure 4-1: A) Climate and topographical/elevation map. B) Geological map showing different lithologies. C) Hydrogeological map showing borehole depths and D) Social map including potential study sites. The solid red rectangle was the site studied in this thesis.

4.2 Geological Investigation

The results of the geological investigation involve identifying the physical characteristics of the site with particular focus on the fractured rock formations, the alluvial sedimentary formations, and the general orientation of structures (dykes, lineaments, and joints) along the site.

4.2.1 Geology of the Site

The subsurface dam site area (see Figure 4-4 below) in the Molototsi River is underlain by crystalline basement rocks of the Groot Letaba Gneiss Suite which is of Mesoarchaean (3200-2800 Ma) age. The rock types found mainly consist of gneisses, such as granitoid gneisses, biotite gneisses and intermingled gneisses, including fine- to medium grained tonalite, coarse grained trondhjemite and minor banded and linear gneisses. The associated minerals consist of oligoclase, microcline, quartz and biotite. Sphene, epidote, apatite and opaque minerals occur as accessories. Although, most of the rocks in the selected study area are grouped under the term Groot Letaba Gneiss Suite the mineralogy of the rock outcrops differs significantly from east to west. The outcrops in the east consist mostly of intermingled leucocratic gneiss which possibly originated from a tonolitic protolith with minor quartz veining. To the middle of the selected study area, minor banded trondhjemite outcrops were observed. Towards the west, the leucocratic gneiss was highly fractured with numerous intersecting quartz veins. Among these leucocratic outcrops was a fine-grained pink granitic rock trending towards the NE. Also, more homogenous light grey, medium-grained gneiss with occasional distinct leucocratic bands occur to the far west of the study area which is possibly a result from local incipient anataxis. The structural trend of all these Archaean crystalline rocks found in the study area show strongly developed E-W to ENE fabric (between 45° and 75°). It was also observed that outcrops towards the river appears to be more highly fractured (see below) as well as outcrops in close proximity of massive dykes.

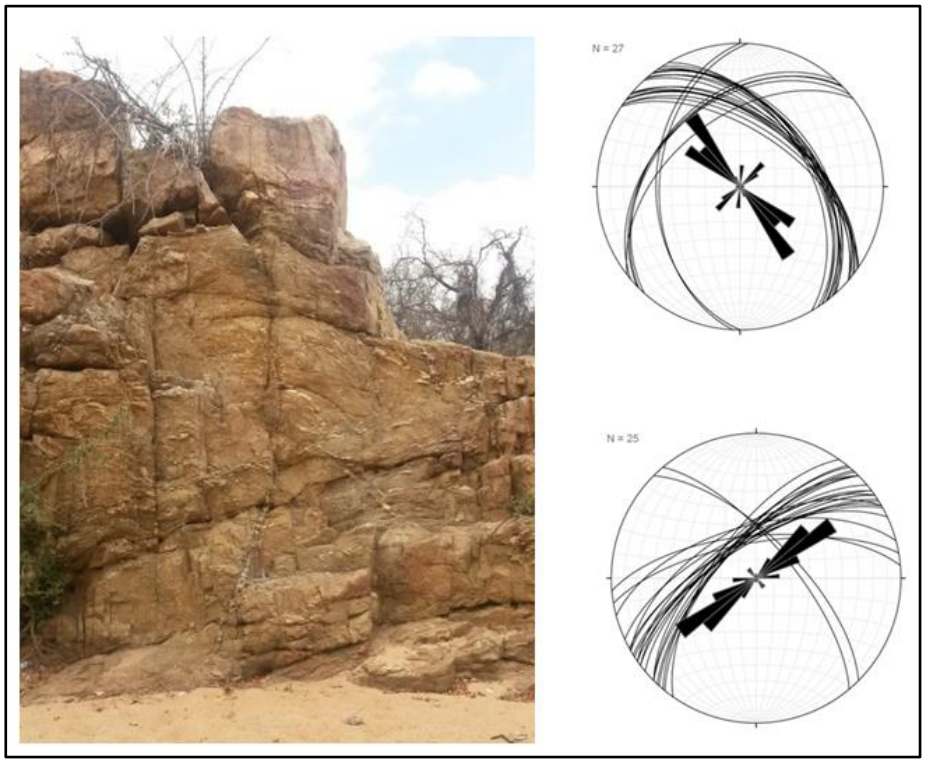

Figure 4-2: The photo is showing a fractured gneissic rock with numerous intersecting quartz veins seen in the Molototsi riverbed. Stereonet and rose diagrams derived from the strikes and dips of all joint planes (top) and dykes (bottom) measured. As illustrated above the main joint direction is towards the NW and the main dyke azimuth is in the ENE and NE direction. Coordinates of this outcrop: latitude -23.568531°, Longitude 30.825699°.

These Post-Karoo dolerite deposits are extensive and occur along the first 1 kilometer of the river in an ENE direction. However, numerous dykes crosscut the river in an ENE direction and at some locations the dykes and granitoids also seem intact. Here, the unweathered dolerite is a dark grey, hard, hypabyssal igneous rock which is a sought after hard rock aggregate. Some dolerite outcrops show onion-like weathering with joints predominantly in the NE-SW direction which act as favourable groundwater conduits. However, joints in the NW-SE orientation were observed, being obliquely or even perpendicular to the main dyke trends, suggesting the study area underwent successive tectonic events. Some dolerite outcrops show onion-like weathering with joints predominantly in the NE-SW direction which act as favourable groundwater conduits. However, joints in the NW-SE orientation were observed, being obliquely or even perpendicular to the main dyke trends. Suggesting the study area underwent successive tectonic events.

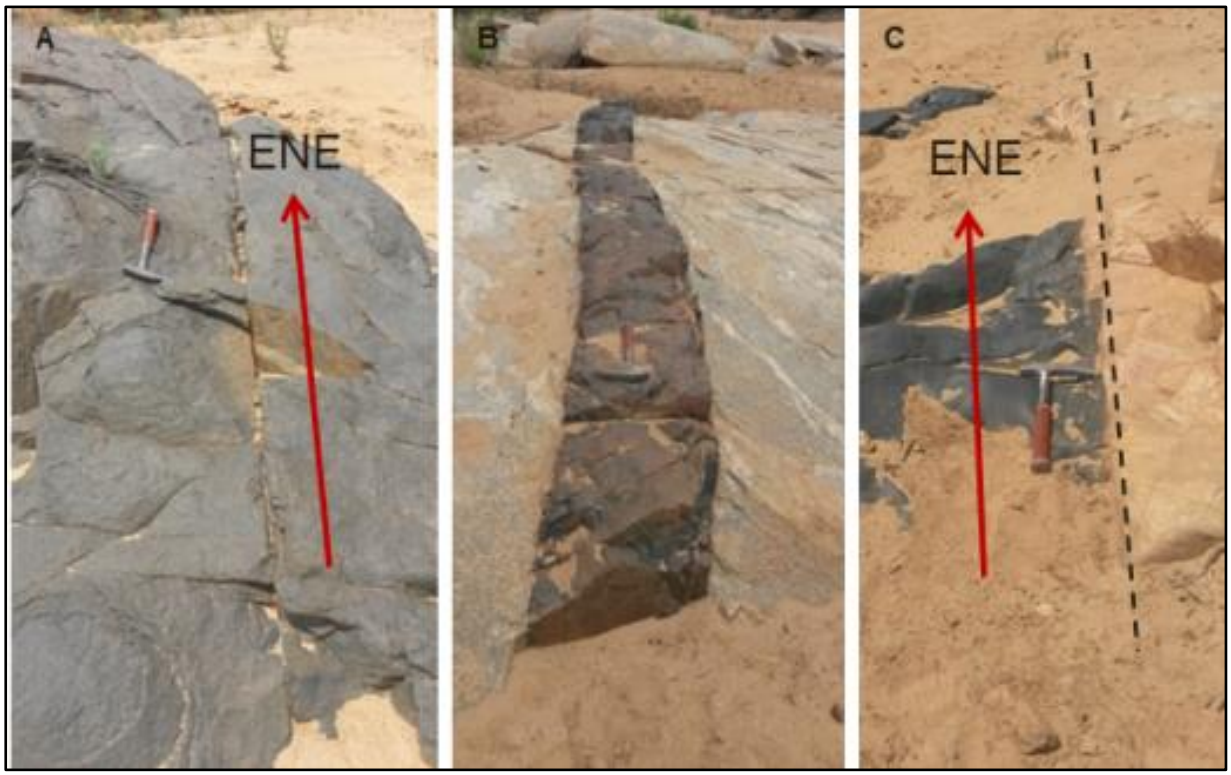

Figure 4-3: A) Slightly weathered dolerite with onion-like weathering and a joint in the ENE direction. B) Intact dolerite dyke in a NW direction intruding grey gneiss with occasional leucocratic bands. Joints are in an ENE direction. C) Dolerite dyke in an ENE direction which is in sharp contact with a leucocratic rock.

Rock outcrops as mentioned previously are highly fractured within the Molototsi River channel compared to outcrops some distance away from drainage channels (the outcrops along the project site can be seen in the geological map Figure 4-4). In addition, rivers or drainage channels tend to follow zones of structural weakness such as lineaments, faults, dykes and tectonic lines. Therefore, rocks in close proximity to the studied river are assumed to be more intensely fractured, jointed and/or weathered. The irregular valley floors are overlain by alluvial sands and minor colluvial soils which vary in depth and type as determined by factors such as geological parentage; distance from source; river gradient, and deposition period. The sand in the selected study area displays trough cross-bedding and cross-lamination which corresponds with the direction of the river flow during flash floods. The crest height of the crossbedding reaches up to 15 cm which indicate a high intensity of water flow. The riverbed is poorly sorted and consists of predominantly angular, coarse sand grains (2 – 0.425 mm), which is an erosional product of the local lithology, mainly gneisses and in close proximity of its source. The crystalline basement is fairly shallow and forms a phreatic aquifer that vary from 2 to 30

m in depth. Particle analysis (discussed in more detail in Geotechnical Investigation, section 4.5.4) show that the alluvial deposits at the dam site are mostly clean quartzitic or arenaceous sediments with minor clay content.

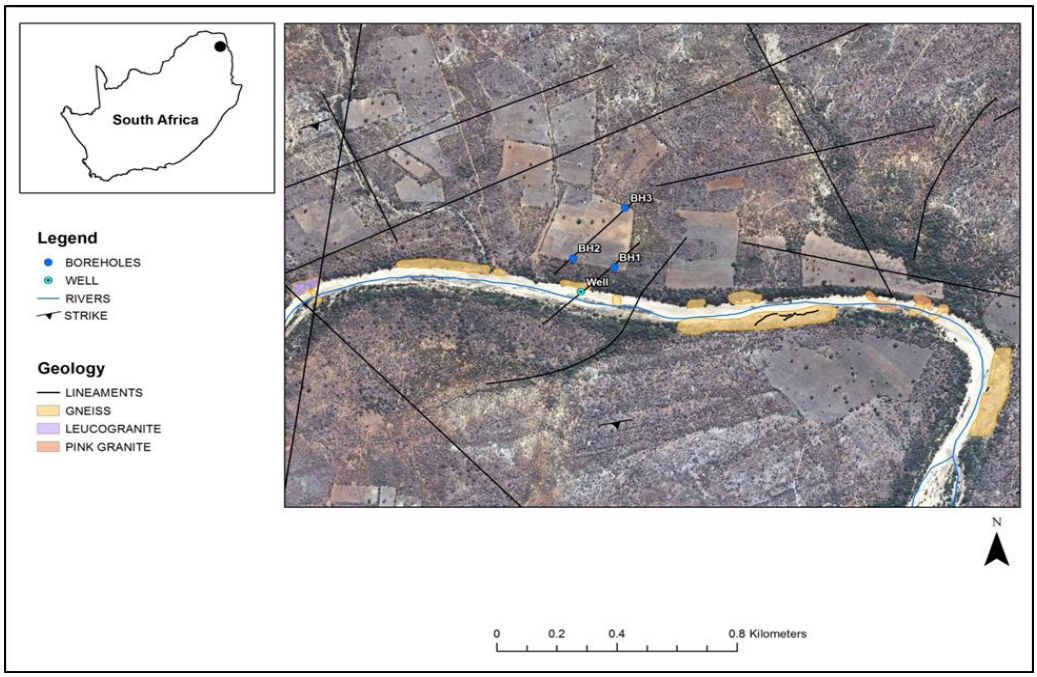

Figure 4-4: A geological map of the project site area, showing some of the major structural lines and outcrops observed. As seen on the map, rivers and streams tend to follow the structural lineaments. Coordinates: latitude -23.568542°, Longitude 30.823947°.

4.2.2 Proposed Dam Wall Site

The river valley cross-section which is seen below shows the lowest elevation section of the studied area. Just downstream from this location, the elevation increases significantly up to 2 m, assuming that the sandy valley bottom is roughly parallel with the underlying bedrock. This elevation boundary or gradient change would be a prominent subsurface dam location. The locality has no known obstacles or outcrops across the river. Hard rock can be observed on the southern slope and not too deep into the high elevated northern slope. Water from all three tributaries (seen in Figure 4-5) upstream would also contribute to the water accumulation behind the subsurface dam.

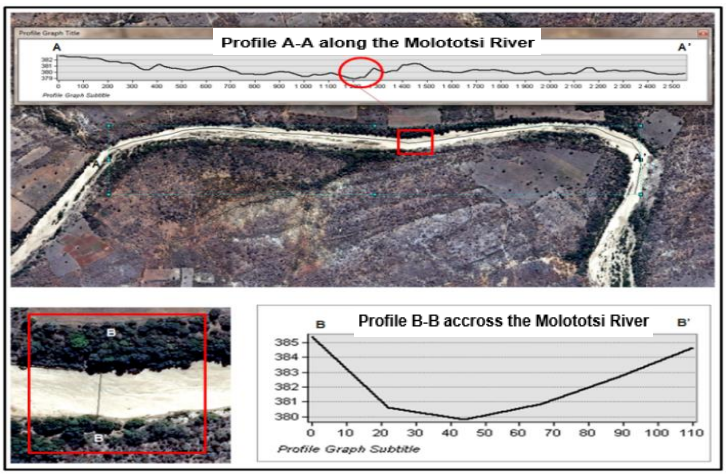

Figure 4-5: The top image shows a cross-section A-A' of the riverbed in the study area which represents the riverbed outline and the gradient. The bottom left image is a zoomed in area of the proposed subsurface dam site and the bottom right image shows a cross-section B-B' of the river valley at the particular area.

4.2.3 Geophysical Survey

Due to the absence of distinctive geological structures or aquicludes (i.e. dolerite sills and dykes) outcropping the study area, geophysical data needed to be considered to provide a reasonable understanding of the geology and hydrogeology. As mentioned in the methodology, anomalies (inferred dolerite dyke and/or lineament) were identified from which three provisional drilling sites were determined on the farm (seen in Figure 4-6). The geophysics conducted in the riverbed was used to determine the extent of the unconfined sand aquifer. Although the Molototsi River results remain the prime target in this study, it was useful to compare the results obtained on the Duvadzi farm.

Magnetic and Electro-Magnetics

Magnetometer measurements identified two prominent subsurface anomalies that strike in a NE direction across the farm which is similar to the structural trend and corresponds to the dykes shown on the geological map (Figure 4-4). The survey of the magnetic and electromagnetic (EM) measurements for the Molototsi riverbed is shown in Figure 4-6 below, which was conducted for a 1.3 km profile along the river to provide a more conclusive understanding of what is beneath the sand.

The results of the borehole targets of the Duvadzi research farm are shown in Appendix A (Figure 7-1). The targeted drilling sites are shown in blue dash lines. The graphs delineate the magnetic readings on the Y – primary axis (red dashed line) and the EM readings on the Y – secondary axis (EM horizontal shown as yellow solid line and EM vertical shown as grey solid line).

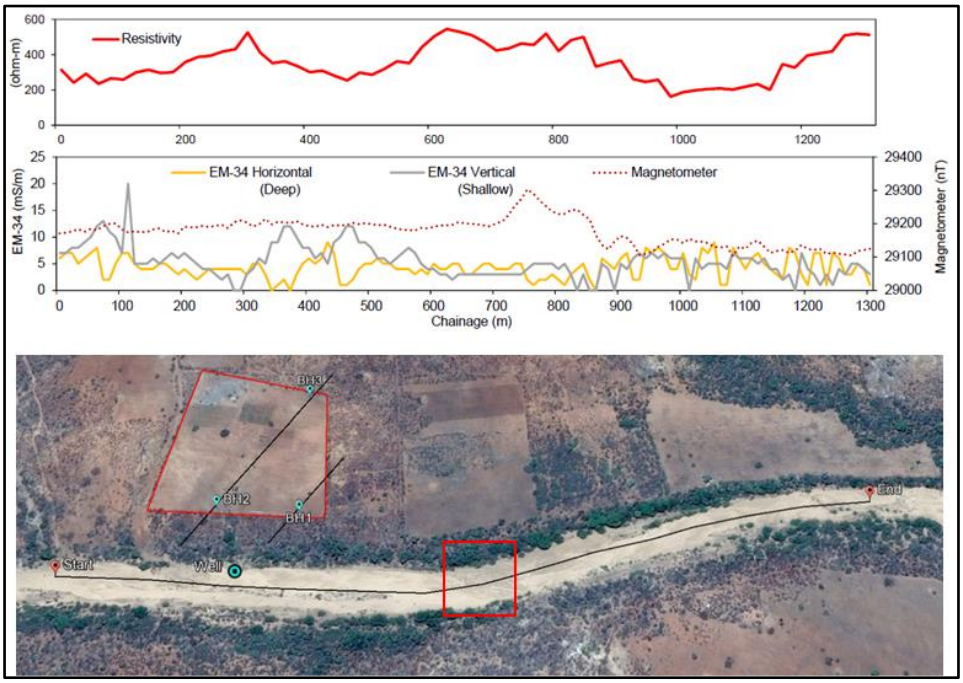

Figure 4-6: The geophysics of the Molototsi riverbed shows the magnetic and electro-magnetic results along with the corresponding resistivity data. The geophysics was taken in the riverbed of the Molototsi to distinguish the occurrence of geological structures and the extent of the sand aquifer. The red box shows the area of the proposed dam wall structure and the location of the resistivity results station 2 (620 m). Coordinates of the site: latitude -23.568542°, Longitude 30.823947°.

Resistivity

The main emphasis of the geophysical survey was to determine the nature of the underlying crystalline bedrock, the presence of faults, dykes and traces of water bearing zones. Using the magnetic and EM methods discussed above, the major anomalies such as dyke and lineament localities were identified.

However, the resistivity profiling method was used to trace lateral variation in resistivity to locate fractured and faulted features which are possible water bearing zones. The following results were obtained for the Molototsi riverbed, shown in Figure 4-6 above and Figure 4-7 below.

The geophysical measurements of the Molototsi riverbed suggest that the sand aquifer is overlying a weathered and fractured rock layer possibly containing shallow groundwater down to approximately 9 m. The results for the potential water strikes within the fractured crystalline rocks beneath the Duvadzi Research farm is shown in Appendix A (Figure 7-2). According to the geophysics the crystalline rock is highly weathered and fractured down to 17 meters below ground surface. Closer towards the river, fracturing increases down to 36 m. On average the weathering depth of these drilling targets according to the resistivity results is mainly shallow weathering with deep fracture zones.

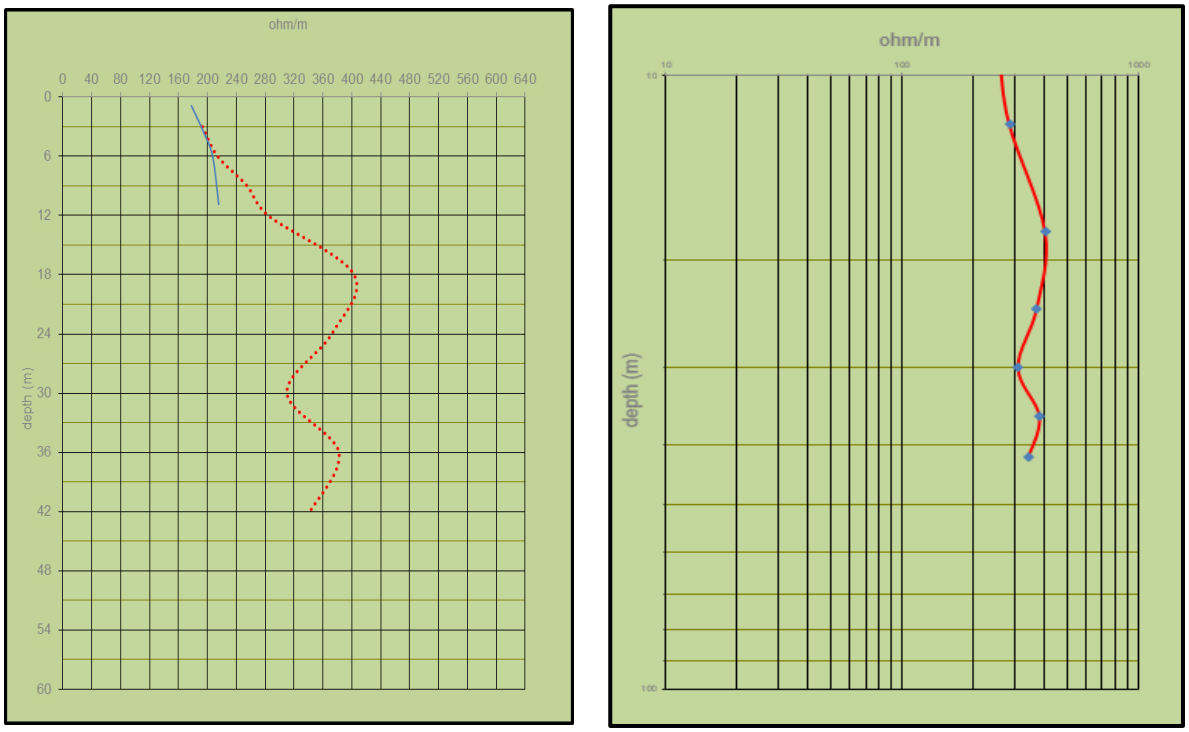

Figure 4-7: Results of the resistivity measurements taken in the Molototsi Riverbed at station 2 (620 m) are shown here. The graph of the left shows a weathered and a fractured zone containing shallow groundwater (blue line) up to 6 m (1.2 m to 11 m contains groundwater, however 6 m was chosen to be more conservative) below the riverbed aquifer. The graph on the right the same data on a scattered log-log graph. Each plot represents a layer with a different resistivity.

4.2.4 Borehole Geology

Three boreholes were installed at the drilling targets BH1, BH2, BH3 identified during the geophysical investigation. The success of the borehole installation, along with the favourable geological and hydrogeological data obtained reveal considerable groundwater potential around the study area.

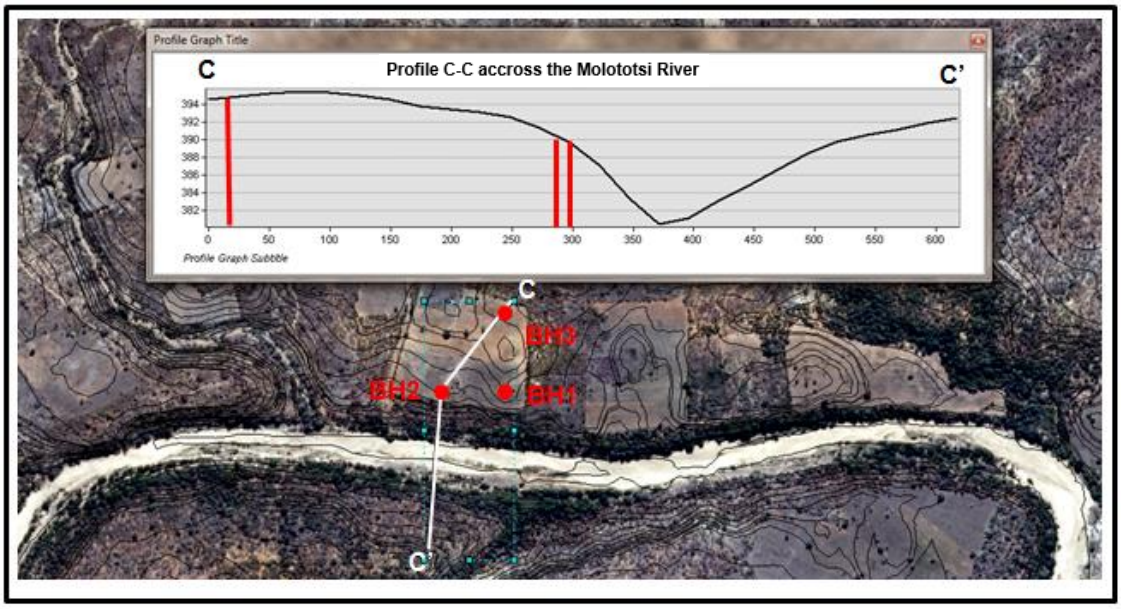

Figure 4-8: The three borehole location and a basic cross-section C-C' that crosscuts the river valley through BH3 and BH2. Coordinates of profile location: latitude -23.568097°, Longitude 30.819623°.

Due to the weathered and fractured formations prevalent in these areas, the boreholes were installed using a combination of percussion drilling methods. The construction of all three boreholes was completed by installing a steel slotted casing to depth, as well as a gravel pack to ensure its long term stability. All three boreholes intercepted water at depth with BH2 having three water strikes where it was cased with slotted pipes around which gravel was packed. Both boreholes BH1 and BH3 were drilled to a completion depth of 120 m and BH3 to 102 m. During drilling, material was sampled every meter and set aside in heaps for borehole logging (see Figure 4-9,

Figure **4-10**, and Figure 4-11). Selective samples of the heaped material were collected for observation. The results of the newly drilled boreholes are summarized in Table 4-1 below, while the detailed borehole geology follows.

Table 4-1: Results of newly installed boreholes.

Farm	Drilling targets on figure	Borehole name	Coordinates	BH depth (m)	Water strike depth (m)	Groundwater depth (m)	Final blow yield (L/s)
Duvadzi	BH1	H14-1701	23.56729 S 30.82098 E	120	22	13.62	3
Duvadzi	BH2	H14-1702	23.56712 S 30.81966 E	120	31, 47, 77	13.67	3
Duvadzi	BH3	H14-1703	23.56536 S 30.82118 E	102	27	18.25	1

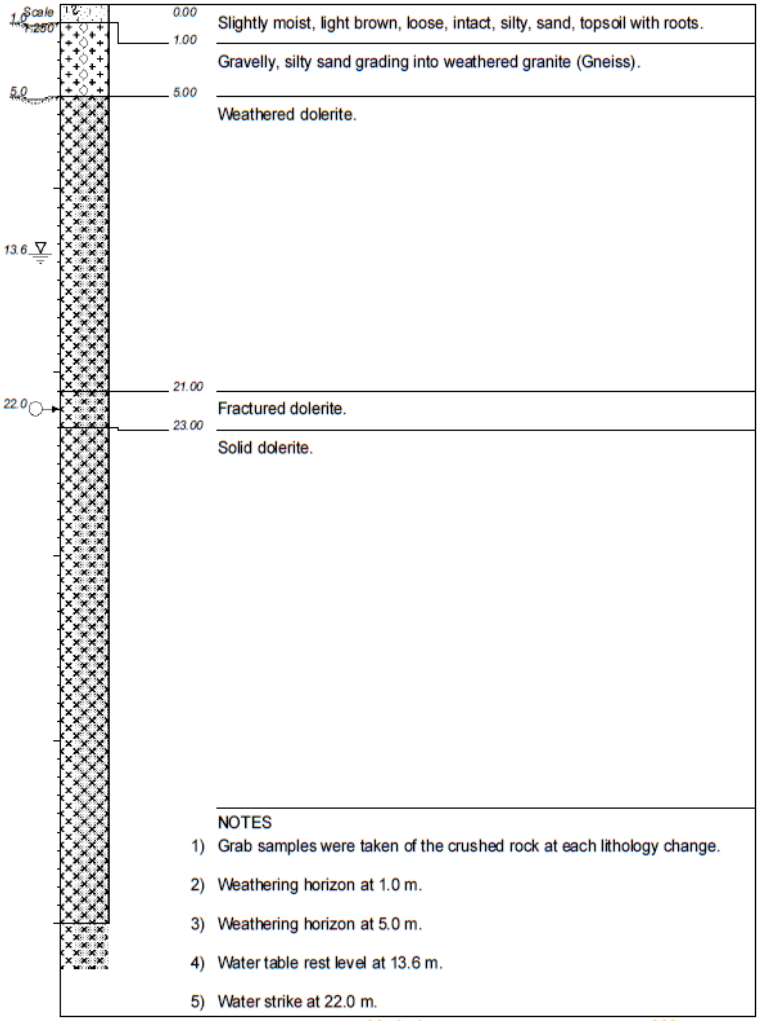

BH1 was drilled up to 120 m on Line 1 at 40 m. One water strike was found at 22 m depth and has a groundwater level of 13.62 m.

BH 1

Borehole 1 (H14 - 1701) was constructed on line 1 (see Figure 3-1) about 40 m from the eastern border of the Duvadzi farm. This hole was drilled to a completion depth of 120 m bgl using a percussion drilling method. One water strike was encountered at 22 m below ground level (bgl) and the borehole had a final blow yield of 3 L/s. The log shows a 1.0 m transported topsoil layer grading into a gravelly, silty sand residual layer. Highly weathered Goudplaats gneiss exists up to 5 m followed by a moderately weathered dolerite layer down to 21 m. A fractured dolerite probably of Karoo age occurs at 21 to 23 m where the water strike was encountered. Below 23 m down to 120 m only solid dolerite dyke was found.

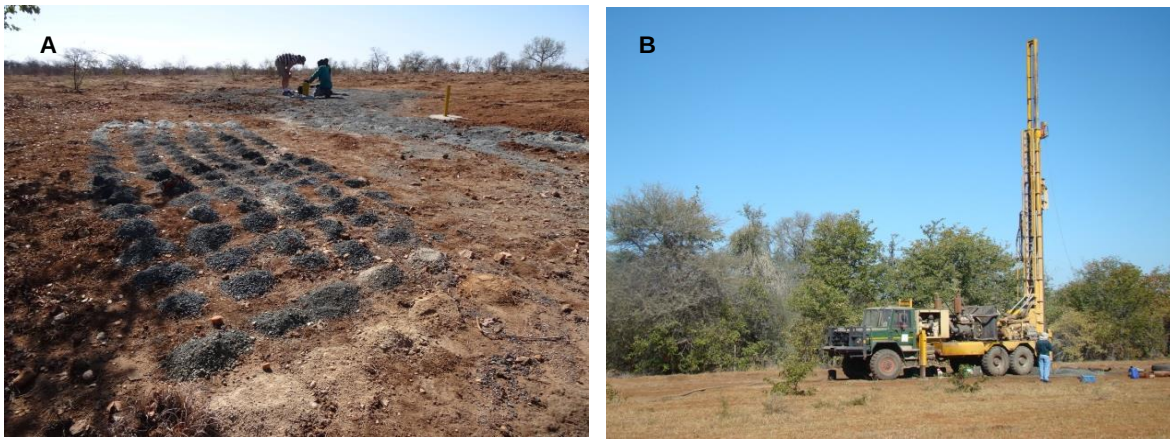

A) Rock chip heaps collected at regular intervals during the percussion drilling method. At the bottom of the figure the topsoil and weathered gneiss can be observed. B) The percussion drilling rig which is a destructive process involving breakup of rock and soil using a button bit.

Figure 4-9: Borehole 1 description.

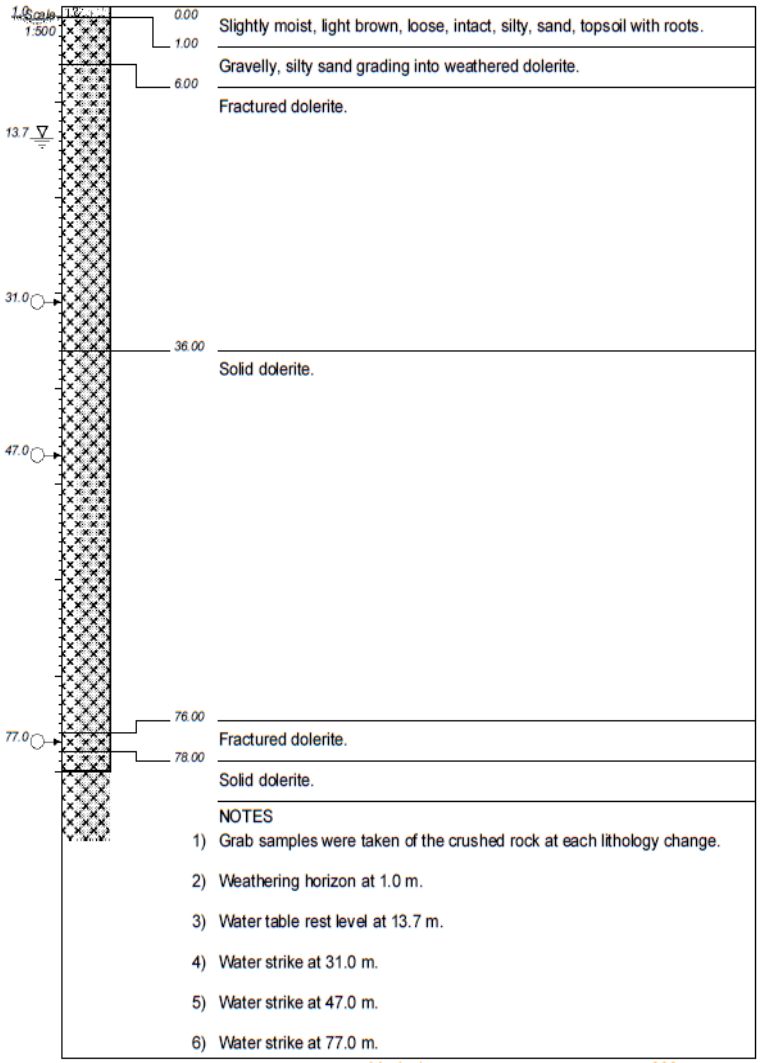

BH2 was drilled up to 120 m on Line 1 at 170 m. Three water strikes were found at 31, 47 and 77 m depth and have a groundwater level of 13.67 m.

BH 2

Borehole 2 (H14 - 1702) was constructed in line with BH1 (see Figure 3-1) about 170 m from the eastern border of the Duvadzi farm. It was also drilled to a completion depth of 120 m bgl using a percussion drilling method. Although these to borehole were drilled on the same line and in close proximity of one another, they penetrate two separate dyke anomalies which are both in a NE orientation. Three water strikes were encountered at 13.7, 31 and 47 m bgl. The borehole had a final blow yield of 3 L/s. The log shows a 1.0 m transported topsoil layer grading into a gravelly, silty sand residual layer. Highly weathered dolerite exists up to 6 m followed by a moderately weathered and fractured dolerite layer down to 36 m. The first water strike was found the fractured dolerite at about 31 m. Solid dolerite of Karoo age occurs down to 76 m. The second water strike was found at 47 m in the solid dolerite which was probably a contact or joint one. A 2 m fractured dolerite layer was encountered where the third water strike was found. Below 78 m down to 120 m only solid dolerite occurs.

A) Installed borehole capped with a steel casing. B) Rock chip heaps consisting of dolerite with topsoil and weathered dolerite seen at the top of the figure which was collected at regular intervals during the percussion drilling method.

Figure 4-10: Borehole 2 description.

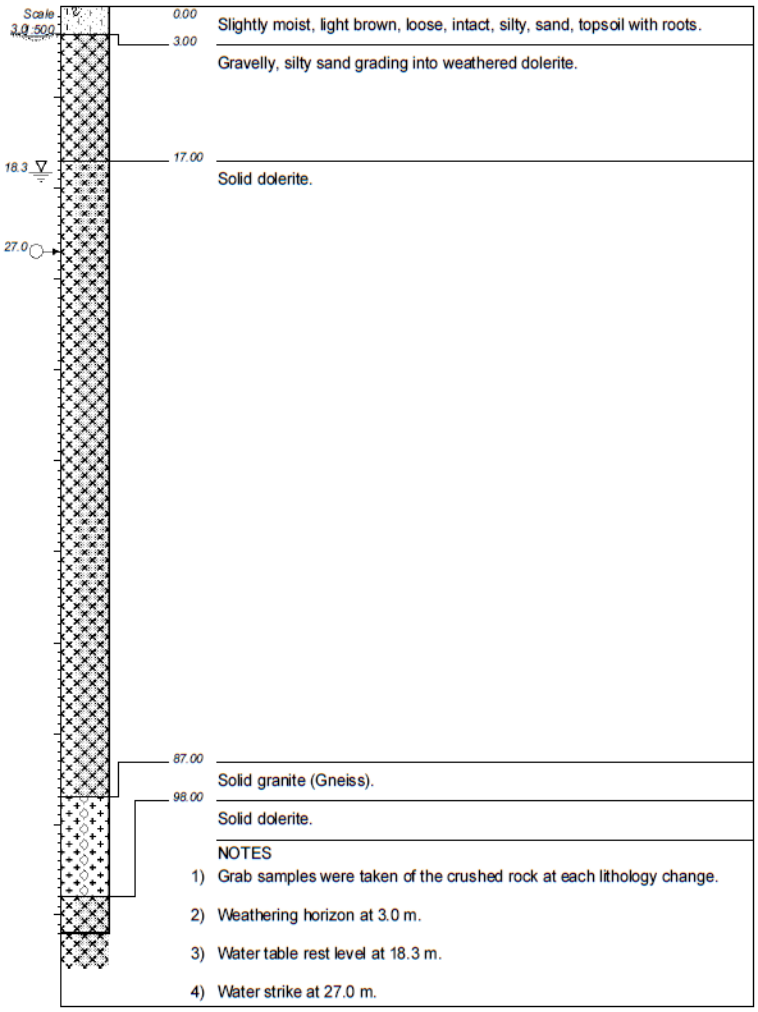

BH3 was drilled up to 102 m on Line 2 at 40 m. One water strike was found at 27 m depth and has a groundwater level of 18.25 m.

BH 3

Borehole 3 (H14 - 1703) was constructed on line 2 (see Figure 3-1) about 40 m from the eastern border of the Duvadzi farm. It was drilled to a shallower completion depth of 102 m bgl using a percussion drilling method. Boreholes 1 and 3 were drilled into the same dyke about 250 m apart which trend in a NE orientation. One water strike was encountered at 27 m bgl. The borehole had a final blow yield of 1 L/s. The log shows a 3.0 m topsoil layer of Quaternary period which grades into a gravelly, silty sand residual layer. Highly weathered in the upper region to slightly weathered dolerite down to 17 m. Solid dolerite of Karoo age exists down to 87 m where the only water strike was found at 27 m. Solid Goudplaats Gneiss of Archean age occurs down to 98 m followed by solid dolerite down to 102 m.

A) Dipmeter test at the installed borehole 3. B) Rock chip heaps consisting of dolerite collected at regular intervals during the percussion drilling method. The lighter grey heaps are leached zones and indicate water strikes.

Figure 4-11: Borehole 3 description

4.2.5 Geological Cross Sections

The general understanding of the geological layering obtained from the above information is shown in the cross sectional profile (see Figure 4-12 below) at the site and a longitudinal section (see Figure 4-13 below) of the Molototsi River along the geophysical survey line. In the cross section, the ground level is illustrated in brown which show the banks have an elevation of > 10 m above the riverbed level. The weathered gneiss layer varies from about 3 m on the banks to 9 m below the riverbed level. The sand has an average depth of approximately 2 m with an average shallow groundwater level of 0.5 m. In the dry winter months, the water level drop to about 1 m, but it is not yet known if the water of the sand aquifer is interconnected to the regional groundwater table or only to the highly weathered and fractured layer. This will be discussed in the Hydrogeological section. The Molototsi is a torrential river and only flows for a couple of days during the rainy season in the summer. The surface water can reach 1 to 2 m above the riverbed during a 1 in 2 year flash flood (refer to the Hydrological Study section for details on peak flow).

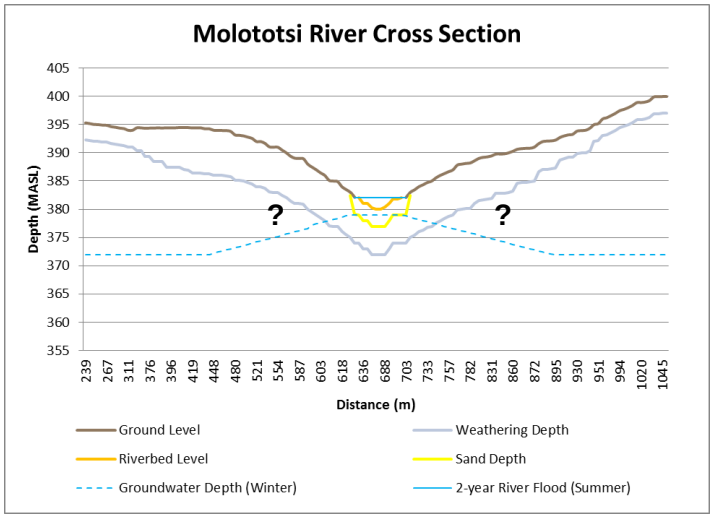

Figure 4-12: A cross section of the site area (drawn in Excel), providing a better understanding of the geological layering of the Molototsi River.

The distance of the longitudinal section is about 800 m along the geophysical profile in the Molototsi riverbed. It provides the average depths of the formations and layers found in the field. The average slope of the riverbed upstream of the site was 1:450, which is less than 1 %. The natural storing ability of the sand could clearly be seen at some localities in the Molototsi River where moist sand and ponds were found. These areas were predominantly found at outcrops in the riverbed (see Photo 3-1 in the Methodology section) and where distinctive gradient steps occurred. The locations where the deepest sand occurs are potential shallow groundwater reserves, therefore, including them within the dammed area would increase yields. Dykes and granite outcrops occur towards the middle of the geophysical surveyed line, resulting in shallower sand depths. The proposed location of the subsurface dam structure is at the gradient change (shown in black below).

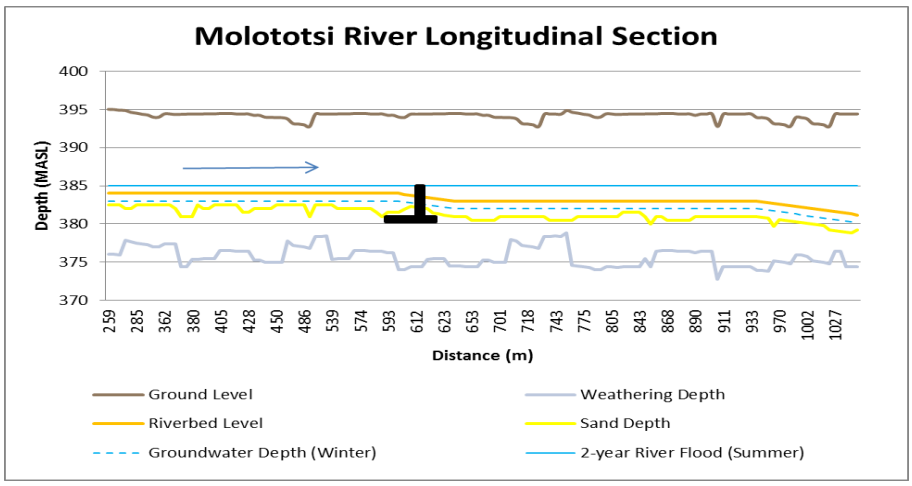

Figure 4-13: A longitudinal section showing the average slope and layering of the Molototsi River. The proposed area of the subsurface dam location is shown in black. The water flow is from left to right (west to east). Note that the subsurface structure is situated on the weathered/fractured rock and not on scale.

4.2.6 Geological Model

Based on the fields visits and data collected, a geological model of the site was developed. The model represents the conceptual model of the Molototsi River catchment with specific focus on the project site at the Duvadzi research farm.

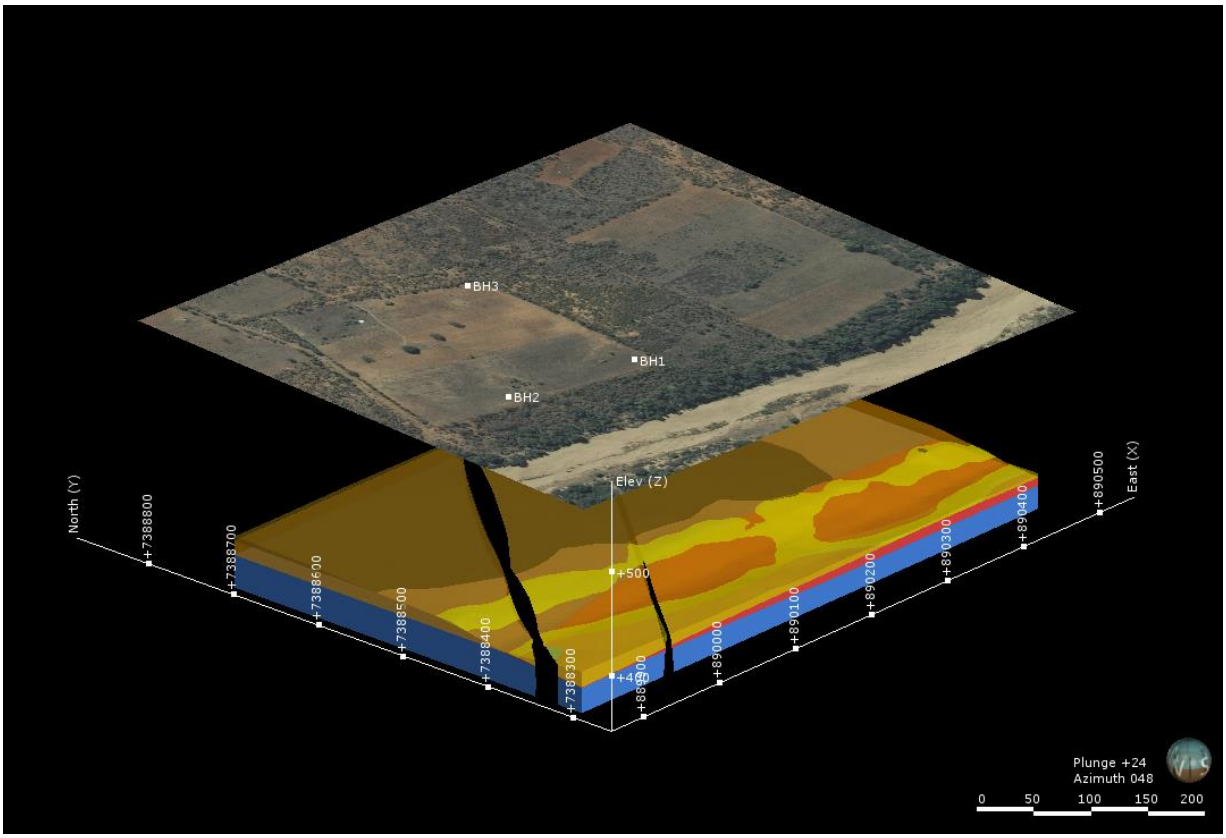

Figure 4-14: Geological model created for the project site area with a satellite image overlaying it. The three boreholes were added as reference points. The blue represents granite gneiss base with the weathered and fractured rock layer above in light brown. The darker brown represents the soils and orange and yellow represents the different sand layers within the river bed. Orange being the clean coarse sands. The linear black structures seen represents the dykes in a NE-SW orientation. Coordinates: latitude -23.568542°, Longitude 30.823947°.

4.3 Hydrogeological Assessment

Based on the available data from the drilled boreholes and the geophysical survey of the previously discussed geological units, the groundwater occurs in different types of lithologies and is present under confined or unconfined conditions. The Molototsi catchment consists of deeper crystalline aquifers in the weathered and fractured rock formations. The groundwater use of these crystalline aquifers is 30 to 40 % of the aquifer recharge and is within the harvest potential of both quaternary catchments (DWA , 2014). Groundwater in the B81H catchment is underutilized and abstraction could be increased from 2.62 Mm^3/a to 7.97 Mm^3/a (DWA , 2014), without impacting the baseflow of the Molototsi River. Shallow unconfined aquifers (< 20 m) also exist within the alluvial deposits of the Molototsi which contains sufficient amounts of water. The occurrence of the shallow groundwater is uncertain and remains the prime target for groundwater investigation in this study. The following sections will discuss the characteristics of the primary riverbed aquifers and the relation to the deep seated crystalline aquifers to determine the sustainability and extent of shallow groundwater abstraction.

4.3.1 Sand Aquifer Parameters

The Molototsi River consists of shallow sand aquifers with the following aquifer parameters.

Porosity

The porosity depends largely on particle size and shape, uniformity of the particles and compaction. Freshly deposited sands may have a very high porosity compared to older and more rounded alluvial deposits which become more consolidated over time due to the weight of the overlying material. The coarse grained sand has more porosity typically resulting in a higher hydraulic conductivity. The table below shows the porosity calculated and the equation used for the three split samples collected from the Molototsi River test pit.

Table 4-2: Porosity determined for the riverbed sand of the Molototsi River.

Porosity			
Equation		$n = V_V/V_T$	
Sample	Description	Porosity (n)	n (%)
1	Original sand sample (not sieved)	0.39	39
2	Course grained sand sample (2 – 0.425 mm)	0.44	44
3	Medium to fine grained (< 0.425 mm)	0.42	42

The porosity of the original sample was found to be 0.387 with complete saturation of the deposit. As mentioned in the literature the coarse sediments increase storage volumes because of the higher porosity (Quilis, Hoogmoed, Ertsen, & Foppen, 2009). The medium to fine grained sand was found to have a lower porosity than the course grained sample but higher than the original sample. This could be due to the smaller grains that fill the void spaces of the larger grains resulting in lower porosity.

Note: The sieve analysis of the sand from the Molototsi River is tabulated (see Appendix D) and discussed in the Geotechnical Investigation (section 4.5.4). The particle size analysis was used to calculate and discuss a number of aquifer parameters.

Specific Yield

The results of the original sample will be the closest representative of the natural specific yield thus the values obtained from this sample was predominantly used to determine other aquifer parameters. The table below shows the specific yield calculated and equation used for three samples collected from the Molototsi River.

Table 4-3: Specific yield determined for the riverbed sand of the Molototsi River.

Specific Yield			
Equation		$n = S_y + S_r$ (Total Porosity)	
Sample	Description	Specific Yield (S_y)	S_y (%)
1	Original sand sample (not sieved)	0.23	23
2	Course grained sand sample (2 – 0.425 mm)	0.28	28
3	Medium to fine grained (< 0.425 mm)	0.27	27

The Molototsi sand aquifer has a specific yield (also known as effective porosity) of approximately 23 % (extractable volume) which is less than the total porosity of 39 % (volume of water). This indicates that only 59 % of the water volume can be extracted, the remaining percentage of water is retained by bounding to sand particles through capillary forces. In order for a subsurface dam to be successful, the specific yield of the retaining material should be sufficient.

The conclusions drawn from these tests are that the maximum S_y occurs in the medium to coarse grain size range. These values are similar to the specific yield values found by other literatures and corresponds to the values listed by Borst (2006) who conducted similar hydrogeological studies on sand dams in the Kiindu catchment, Kenya. The aquifer parameters estimated up until this point are evidently one of the most important aspects of the study as the reservoir yield would directly be related to the specific yield and porosity of the riverbed sand.

Hydraulic Conductivity

The coefficient of hydraulic conductivity of the sand samples taken from the Molototsi riverbed varied from $K = 1.44 \times 10^{-4}$ m/s for the original mixed sample to $K = 4 \times 10^{-4}$ m/s for the coarse sand sample. The Molototsi River consists predominantly of coarse grained material (0.425 to 2 mm), however, the riverbed is often interbedded with fine grained sandy silt lenses which were deposited during the flood periods. The average hydraulic conductivity of the subsurface dam would therefore be similar to that of the original mixed sample with higher hydraulic conductivity in the coarse grained layers. The table below summarizes the methods used to calculate the average hydraulic conductivity.

Table 4-4: Hydraulic conductivity calculated for the riverbed sand of the Molototsi River.

Hydraulic Conductivity				
Method		Equation	K (m/s)	K (m/d)
1	Grain size (by Hazen)	$K = 10^{-2} (D_{10})^2$, D_{10} = 0.12 mm and 0.2 mm	4×10^{-4}	34.56
2	Inversed Auger Hole	$K_s = 1.15r (\log(h_0 + r/2) - \log(h_1 + r/2)) / t$	2.04×10^{-5}	1.76

The auger hole method shows K = 1.76 m/d, which is a field method for calculating hydraulic conductivity. The calculated value is, however, considerably smaller than the grain size method and is within the values recommended for fractured igneous and metamorphic rock aquifers. The permeability or flow rate of water through the sand was calculated using the constant-head method which showed a flow rate of 24.69 m^3/d.

Table 4-5: The flow rate within the Molototsi riverbed was determined in the lab using the constant-head method.

Flow Rate			
	Method	Equation	Q (m^3/d)
1	Constant-head	K = QL/Ah, Q (l/s converted to m^3/d)	24.69

Transmissivity

The transmissivity or horizontal flow direction of water through this sand aquifer must also be adequate enough to permit the water being extracted at the desired rate. The calculated transmissivity in a

homogeneous and isotropic unconfined aquifer varies with saturated thickness during various seasons. Where, d_{max} corresponds to the depth after a long recharge period, while d_{min} corresponds to the dry season where the saturation thickness declines and transmissivity decreases.

Table 4-6: Transmissivity of the Molototsi riverbed calculate for the summer and winter.

Transmissivity			
	Time	Equation	T (m^2/d)
1	Summer	$T = K.d_{max}$, d_{max} = 2 m	69.12
2	Winter	$T = K.d_{min}$, d_{min} = 1 m	34.56

Borehole analysis and geophysical measurements suggest that the rocks are weathered down to 6 m and highly fractured down to 20 m below ground level, which is roughly about 10 ± 3 meters below the riverbed. Below this the rocks are moderately fractured down to 30 ± 7 meters along the Molototsi River. However, it is determined during groundwater monitoring that the boreholes in the deep crystalline aquifers showed negligible response to rainfall. This suggests that the two aquifers are not directly connected and that the hydraulically active part is only located in the shallow weathered and densely fractured zones of the crystalline basement. It is also evident in the geophysical sounding curve seen in Figure 4-7.

4.3.2 Groundwater Recharge

The Molototsi River is strongly characterized by high flash floods (discussed in Flood Hydrology, section 4.4.4) during the summer months with peak flows of up to 113 m^3/s once every two years (discussed in more detail in Hydrology section). More conservative flows to expect for recharging the riverbed is 0.063 Mm^3/a, which corresponds to a flow rate of approximately 0.05 m^3/s. As a result, the floodwaters infiltrate freely into the sandy riverbed. While recharge over the clayey and loamy topsoil plains will be relatively low, the total volume of regional recharge from the permeable sands may still be considerable. This is the main recharge mechanism for replenishing the shallow groundwater aquifers. The average rate of recharge for the site is calculated using an average concentration of groundwater (chloride concentration factor), shown in table below.

Table 4-7: Groundwater recharge estimates for the two aquifers (alluvial and crystalline) based on the CMB method. The average Cl_p concentration of 0.69 mg/ℓ for the Letaba Lowveld was obtained from Holland (2011) and the Cl_{gw} were obtained from the water quality tests (see Water Quality section 4.3.3).

Average Groundwater Recharge					
Method		Equation			
Chloride Mass Balance (CMB)		$R_t = P \times Cl_p / Cl_{gw}$			
Aquifer	MAP (mm/a)	Cl_p (mg/l)	Cl_{gw} (mg/l)	Average Recharge (mm/a)	Average Recharge (% of MAP)
Shallow Sand Aquifer	477	0.69	9.2	35.78	7.50
Deep Crystalline Aquifer	477	0.69	235	1.4	0.29

Based on the results, rainwater infiltrates directly into the riverbeds, recharging the shallow sand aquifer with approximately 35 mm/a, however, according to the Department of Water Affairs (DWA), the average annual recharge for this region of the Molototsi River is between 10 and 15 mm/a (see Figure 4-15). The chloride concentrations could be site specific and may vary from time to time, depending on the sampling period (for instance sampling in the rainy or dry season). The shallow groundwater consists of 7.5 % recharge of the MAP, while the deep crystalline groundwater only consists of 0.29 % of MAP, therefore indicating minor direct rainfall recharge or shallow groundwater contribution from the shallow alluvial aquifer at the site. Through interflow the shallow groundwater

slowly feeds into faults, fractures, joints, and contact zones by gravity, recharging deeper secondary aquifers. However, the weathered near-surface and deep-seated aquifers in the fresh crystalline bedrock will only be recharged through infiltrating shallow groundwater where hydraulic continuity exists. This may vary significantly at a local, intermediate and regional scale as the loggers within the boreholes that penetrate the crystalline aquifer on site, did not respond to rainfall (discussed in Groundwater Monitoring, section 4.3.6). This indicates that the deep seated crystalline aquifer underlying the site and possibly the entire B81H quaternary catchment is not directly recharged by rainfall. The result of this could mean that the crystalline aquifer has intercalations of fine silts in the highly weathered zone, which may form a thin impermeable layer that obstruct recharge during rainy periods.

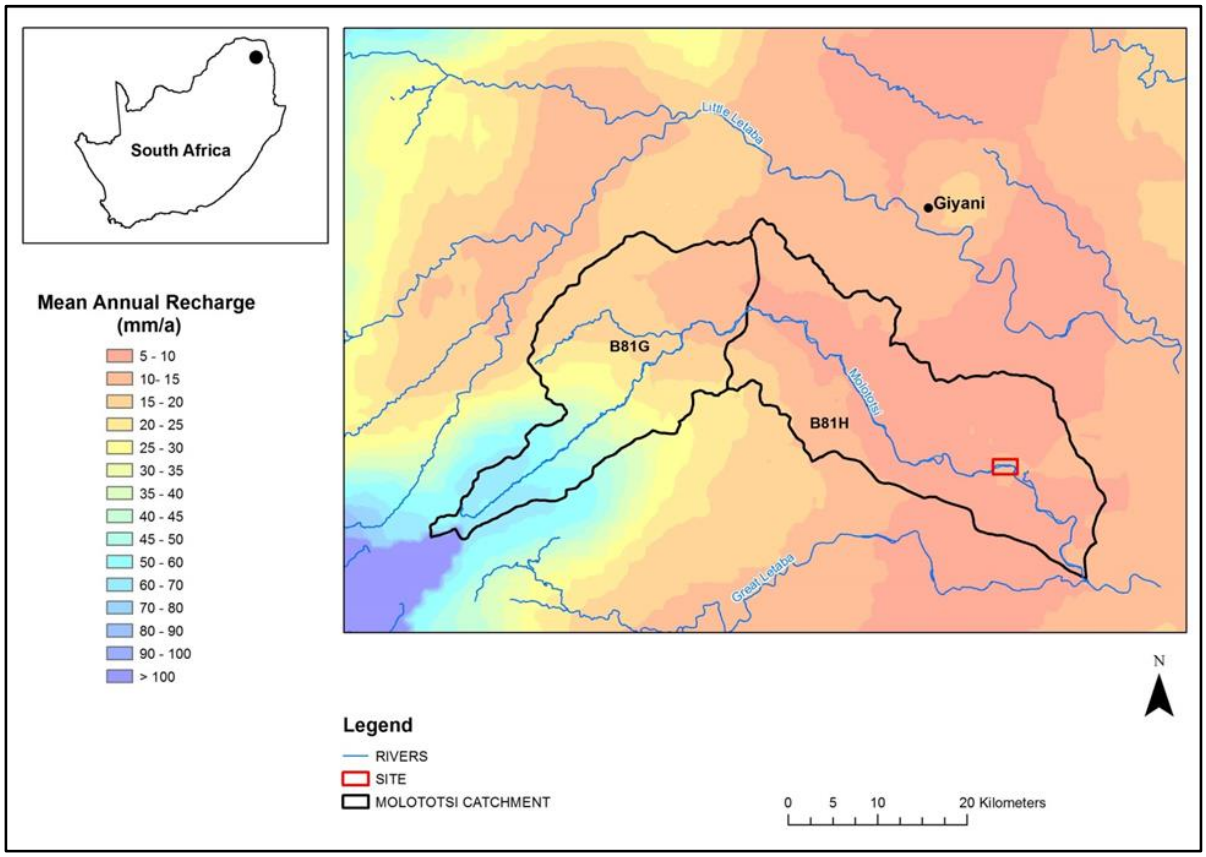

Figure 4-15: Mean annual recharge for the Molototsi catchment region in the Limpopo. The data was obtained from the Department of Water Affairs. Coordinates: latitude -23.568542°, Longitude 30.823947°.

4.3.3 Groundwater Quality

Water quality analysis was conducted for two samples, one from BH2 (H14-1702) and one from the Molototsi River. The tested borehole at the Duvadzi farm show higher peak concentrations of sodium, calcium, magnesium and especially chloride ions compared with the water quality analysis from the Molototsi River. The alkalinity of the borehole is also of higher concentration due to greater amounts of bicarbonate. The slightly lower pH could be explained by the high concentration of sodium. Fluoride concentration of these samples are between 0 - 1 mg/l which meets the requirements for healthy tooth structure according to the Water Quality Guidelines. The electrical conductivity taken in wells along the river did not show much variation, however, a significant increase was observed within the borehole sample.

The hypothesis of shallow groundwater in the Molototsi River would be more saline due to the low flow rate and the high evapotranspiration from sunlight and plants, and the direct exposure to pollution, however, this is not the case. The groundwater of the crystalline aquifer is evidently more saline and prone to pollution. This phenomenon can be explained by the low to absent groundwater flow within the crystalline aquifer which does not allow the water to filter through sand as with the shallow alluvial aquifers. The dissolvent of the host rock dissolvent could also result in high salinity, however, this would vary according the local geology (structures such as faults and dykes and the degree of weathering) and climate. Water quality could be significantly elevated if situated within saline rock with low recharge for prolonged periods, until chemical equilibrium is reached. This could be the case in the deep crystalline aquifers. Also, the process of evapotranspiration could increase the precipitation of salts in the unsaturated soil zone. The salt concentration of groundwater will increase where interconnectivity exist as this is the preferred flow path, particularly within the thin regolith and fractured zones. Since groundwater movement in crystalline aquifers is along fractures and joints, the fractured rock matrix provides minor retardation of contaminants compared to sand aquifers. While, the riverbed sand of this primary aquifer acts as a natural purifier which reduces the concentration of impurities.

The contamination by human activity should also be considered as agriculture and waste water is possibly the two major contributors to the high TDS concentration. The high TDS concentration in the borehole will result in a salty taste. Nonetheless, according to the drinking water standards the groundwater qualities of these samples are fit for drinking and agricultural use with no likely negative human health effect (DWAF, 1996). However, it is advised that water samples of the Molototsi River and especially the boreholes of the deeper crystalline aquifers be submitted for regular chemical and microbial analysis.

Table 4-8: Groundwater quality of the Molototsi riverbed and BH2 (H14-1702).

Analysis	Units	Samples	
		Molototsi River	H14-1702
Potassium as K as dissolved	mg/l	3.3	7.9
Sodium as Na dissolved	Mg/l	13	147
Calcium as Ca dissolved	mg/l	13	57
Magnesium as Mg dissolved	mg/l	4.8	46
Ammonia as NH_3 dissolved	mg/l	0.08	0.08
Sulphate as SO_4 dissolved	mg/l	4.2	30
Chloride as Cl dissolved	mg/l	9.2	235
Alkalinity as $CaCO_3$ dissolved	mg/l	61	303
Nitrate + Nitrite as NO_3 or NO_2 dissolved	mg/l	0.3	<0.1
Ortho-Phosphate as P dissolved	mg/l	0.06	<0.05
Fluoride as F dissolved	mg/l	0.2	1
Dissolved Organic Carbon	mg/l	3.9	0.9
Electrical Conductivity (EC) (25˚C)	mS/m	17	130
pH (20˚C)		7.9	7.7
Saturated pH (20˚C)		8.7	7.4
Total Dissolved Solids (TDS)	mg/l	109	832
Sodium Absorption Ratio (SAR)		0.8	3.5

After comparing the two water samples, there is clear evidence from the chemical analysis that these water bodies are not from the same source, as the sand aquifer is considerably less saline and of much better quality compared to the groundwater in the boreholes. Better quality of water is generally associated with unconsolidated sands that receive sufficient amounts of recharge due to high infiltration, suggesting that the water from the Molototsi River is not directly recharged by the deep crystalline aquifer but rather from surface runoff and precipitation. The chloride concentrations and water quality analysis, therefore, confirms that the two water bodies are not directly connect, as the sand aquifer is considerably less saline and of much better quality compared to the groundwater in the boreholes.

4.3.4 Groundwater Discharge

Discharge was not measured during the field visit as it was not one of the main objective, however measurements of the water table was carried out and discussed in the Groundwater Monitoring section. Discharge from aquifers in the Molototsi catchment is either by natural processes (baseflow) or by artificial processes (abstraction). According to DWA (2014), the baseflow of the shallow sand aquifers in quaternary catchments B81G and B81H is 5.87 Mm^3/a and 0.01Mm^3/a respectively. It is evident that the baseflow in B81H is considerably lower compared to upper B81G quaternary catchment. The assumption can be made that shallow groundwater from B81G to B81H is lost through infiltration to deeper aquifers and evapotranspiration (see a full discussion in Evaporation section 4.3.5 below) in the upper reaches. For this reason, the Molototsi can be classified as a losing river.

4.3.5 Evaporation Losses

The current climate conditions such as the El Nino of 2016, was the main contributor to the severe drought South Africa experienced. The drought was responsible for extreme evaporation rates and is therefore important to study these losses.

Determining the extent of evaporation losses in shallow sand aquifers contributes to the understanding and functioning of these subsurface dams. Permeability parameters such as hydraulic conductivity, transmissivity and capillarity evidently affected the rate of evaporation. The shallow groundwater in the sand aquifer at a constant time interval, evaporated between 12 mm/d and 8 mm/d for the first 10 days which dropped to 5 mm/d to 3 mm/d after the saturated water level decreased to 0.226 m. This suggests a clear water level reduction of approximately 0.10 m after 10 days, depending on the weather or climate condition. The weighing experiment, therefore, predicts a decrease in water level at an initial evaporation rate of 0.79 m/month. After about a month, when the water level was lowered to such an extent that the sand near the surface contains about 14.9 % of moisture, the rate of the declining water level was 0.31 m/month. It is important to note that this is only a potential evaporation rate as it may not be a true representative of the natural conditions of the sand aquifer.

Table 4-9: Evaporation loss experiment conducted on the original sand sample collected from the Molototsi River with a porosity (n) of 0.39.

Evaporation Loss			
Time (days)	Water Volume (%)	Saturation Depth (S_d) (m)	Evaporation Rate (S_d/n) (m/month)
0	38.6	0.310	0.79
0.5	36.8	0.298	0.76
1.5	35.6	0.288	0.74
2.5	34.3	0.278	0.71
3.5	33.3	0.270	0.69
4.5	32.2	0.261	0.67
5.5	31.3	0.253	0.65
10.5	27.9	0.226	0.58
30.5	14.9	0.120	0.31

4.3.6 Groundwater Monitoring

Interpreting the data of the newly installed loggers in boreholes H14-1702 and H14-1703, none of the boreholes responded to the high rainfall events of November 2016 to January 2017, indicating that the deep crystalline aquifer is not directly recharged by rainfall (See Figure 4-16).

Table 4-10: The groundwater depth of the three newly drilled boreholes on the Duvadzi research farm showing one datum as no to little groundwater fluctuation was observed.

Crystalline Groundwater Depth			
Borehole	BH1 : H14 - 1701	BH2: H14 - 1702	BH3: H14 - 1702
Depth (m)	13.62	13.67	18.25

The shallow groundwater monitoring results of the Molototsi riverbed can be seen in Table 4-11 which show the decline of water levels over a one year period in the 1.5 m deep well. The Duvadzi farmer abstracted water from this well for irrigation purposes from late September 2016 to early January 2017. The water level in the well significantly decreased after 2 to 3 months of pumping, decreasing to such an extent, which made it impossible to abstract water continuously after 30 November 2016.

Table 4-11: The shallow groundwater depth from riverbed level.

Alluvial Groundwater Depth		
Season	Months	Depth (m)
Summer	Dec-Feb	0
Autumn	Mar-May	0.3
Winter	Jun-Aug	0.7
Spring	Sept-Nov	1 -1.2

Abstraction was therefore interrupted and irrigation was put on hold. The drought was followed by a period of heavy rains during December 2016 and January 2017 which resulted in full recovery of the riverbed aquifer. On average, the farmer abstracted approximately 15 m^3/d (irrigating every second day) based on the water meter readings. In total, 507 m^3 of water was withdrawn from the riverbed aquifer to the Duvadzi farm during the first season which corresponds to 71 days (20 September 2016 to 30 November 2016) and 571 m^3 during the second season (30 November 2016 to 1 January 2017). The 571 m^3 was extracted for a crop growth plot of 0.175 ha (1750 m^3) in size, which corresponds to approximately 3263 m^3/ha. This is below the water irrigation requirements of 4000 m^3/ha. The pumping rate measured at the diesel pump outlet was 1.59 l/s and the delivery rate to the irrigated block measured by the water meter was 1 l/s.

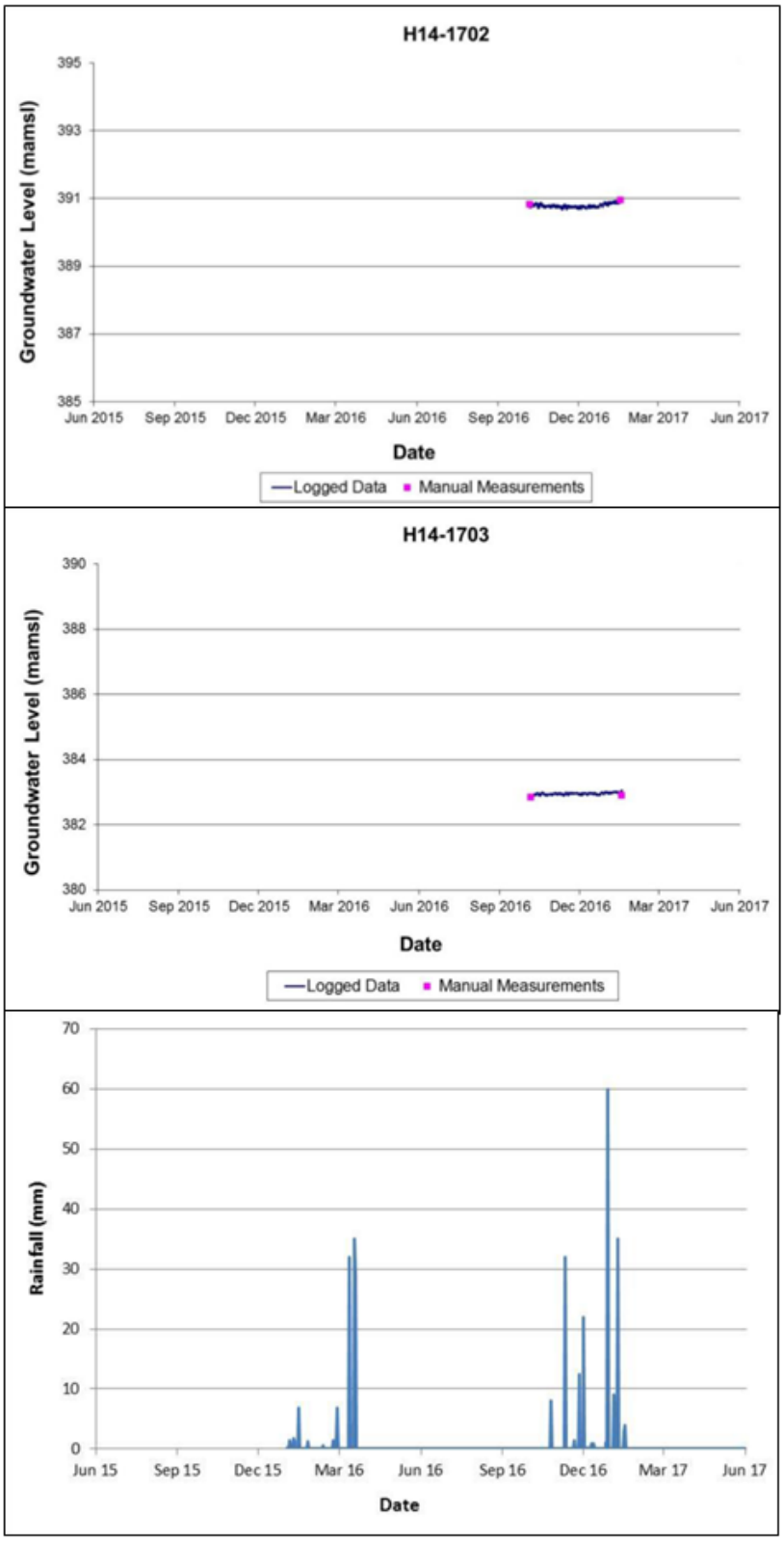

Figure 4-16: Hourly groundwater levels (elevation) measured with Solinst loggers and manual dip meter readings at boreholes H14-1703 (top) and H14-1702 (middle), and daily rainfall data (bottom) at the Duvadzi farm.

4.3.7 Groundwater Reserves

The groundwater volume in the shallow alluvium aquifers is currently unknown; therefore, the need to explore the potential extractable reserves is essential. An estimate has been made for the extractable groundwater reserve in the sand of the Molototsi riverbed, based on results and information from previous sections. The sand depth of the alluvium aquifer is irregular, varying between 1.5 m and 3 m with numerous rock outcrops in the riverbed. In addition, the average depth used for calculating the groundwater reserve in the sand aquifer is 2 m. The natural slope of the riverbed at the site is 1:450; therefore, a stretch of 450 m for determining the volume of each subsurface dam is sufficient. Upstream and downstream of this reach, a distinct change in elevation exists with outcrops cross cutting the riverbed. The average width of the riverbed section at the located site is approximately 70 m. The average saturation depth is 1.5 m as the riverbed rarely drops below 1 m (except in extreme drought conditions) and is at a depth above 0.5 m for about 6 month of the year. The porosity of the saturated medium is 39 %, meaning 1 m^3 of sand yields 0.39 m^3 of water. However, the extractable reserve would be equal to the specific yield (effective porosity) of 23 %. The average amount of extractable shallow groundwater for a 450 m river stretch is estimated to be 10 867.5 m^3. The volume of 10 867.5 m^3 would be sufficient to irrigate 2.72 ha of crops for one season without recharge, according to the irrigation requirements of 4000 m^3/ha. This is however, not sustainable as the estimated baseflow to recharge this river (not taking runoff or rainfall into account) at a given point in quaternary catchment B81H is 10 000 m^3/a (DWA , 2014). The maximum allowable abstraction per annum is therefore 10 000m^3/a. A more conservative abstraction volume would correspond to a river reach of approximately 400 m, which has a sustainable extractable reserve of 9 660 m^3/a (400 m x 70 m x 1.5 m x 0.23). The extractable groundwater reserves are calculated for the various sand aquifer depths for each season in Table 4-12 below.

Table 4-12: The extractable groundwater reserves are calculated for the natural alluvium aquifer in the Molototsi River for each season.

Natural Shallow Groundwater Reserves						
Season	Months	Sand Saturated Depth (S_d) (m)	River Reach (L) (m)	Riverbed Width (B) (m)	Potential Reserve (n = 39%) (m^3)	Extractable Reserve (S_y = 23%) (m^3)
Summer	Dec-Feb	2	400	70	21 840	12 880
Autumn	Mar-May	1.7	400	70	18 564	10 948
Winter	Jun-Aug	1.3	400	70	14 196	8 372
Spring	Sept-Nov	1	400	70	10 920	6 440

Based on the calculations above, the farmer abstracting from the Molototsi River at the Duvadzi research farm, is pumping well below the extractable potential. A baseflow of 10 000 m^3/a corresponds to a pumping potential of 27.4 m^3/d, which is double the current pumping rate of 15 m^3/d.

In order to increase the extractable reserve a subsurface retaining wall can be constructed in the riverbed. The Molototsi has an average sand aquifer depth of 2 m; therefore, implementing a 3 m wall could substantially increase the reserve. The exposed 1 m section would accumulate sediments behind the wall and eventually increase the aquifer thickness to 3 m. The increased aquifer would raise the shallow groundwater table behind the wall to an average height of 2.5 m. This artificial reserve would store 27 300 m^3 (400 m x 70 m x 2.5 m x 0.39) shallow groundwater with an average extractable reserve of 16 100 m^3 for a river reach of 400 m. This is 6 440 m^3 more than the extractable amount of the natural sand aquifer and corresponds to a pumping rate of 44.11 m^3/d which is three times more than the current 15 m^3/d. The farmer could therefore according to these calculations, irrigate 0.525 ha (3 x 0.175 ha) every day. The extractable groundwater reserves are calculated for the various artificial sand aquifer depths for each season (see Table 4-13 below).

Table 4-13: The extractable groundwater reserves are calculated for the artificial aquifer (which includes the subsurface dam wall) in the Molototsi River for each season.

Artificial Shallow Groundwater Reserves						
Season	Months	Sand Saturated Depth (S_d) (m)	River Reach (L) (m)	Riverbed Width (B) (m)	Potential Reserve (n = 39%) (m^3)	Extractable Reserve (S_y = 23%) (m^3)
Summer	Dec-Feb	3	400	70	32 760	19 320
Autumn	Mar-May	2.7	400	70	29 484	17 388
Winter	Jun-Aug	2.3	400	70	25 116	14 812
Spring	Sept-Nov	2	400	70	21 840	12 880

The fact that the Molototsi River is fully recharged after every rainy season in the summer, the constructed subsurface dam wall would store the recharged water without allowing it to flow away as baseflow. For this reason, the mentioned maximum allowable abstraction of 10 000 m^3/a for extracting sustainably from the natural sand aquifer would be very conservative as the minimum extractable reserve during the driest season is estimated to be 12 880 m^3. The designed subsurface dam would therefore be able to store groundwater for long periods and is thus not reliant on baseflow during the dry winter months. Surface runoff would be the main contributor for recharging this artificial aquifer. To test the above calculated scenarios groundwater modelling was undertaken.

4.3.8 Groundwater Modelling

The proposed modelling was conducted to determine how much water can be abstracted for irrigation from the Molototsi riverbed before it runs dry. The plan view of the targeted unconfined sand aquifer is shown in Figure 4-17 which consists of an 800 m river stretch. All the geological and hydrogeological information was used to simulate the model as accurate and realistic as possible. The model was consisting of one layer as the unconfined sand aquifer was the main target. It overlays a highly weathered and fractured crystalline base which is not necessarily connected, as fine silt intercalations possibly exist at the contact. The depth of the sand layer was set to be 2 m. The average shallow groundwater depth at the site is at 0.5 m below the riverbed, therefore the upstream and downstream boundary was set at constant head of 0.5 m. The topography and banks outside of the riverbed layer was given no flow cells as the lack of interconnectivity exists. This simplified the model considerably which allowed the author to determine functioning of the sand aquifer more accurately. The porosity of 0.4 calculated in the Aquifer Parameters section was used and the specific yield of 0.3 was deemed more sufficient in the model compared to the calculated specific yield of 0.23 (see Aquifer Parameters section). The model was very sensitive to fluctuations of specific yield. In the literature, a groundwater model was performed by Quilis, Hoogmoed, Ertsen, and Foppen (2009) which showed high sensitivity to hydraulic conductivity of the shallow aquifer on the riverbanks and thickness of the sand layer in the riverbed. However, the hydraulic conductivity of the model performed in this thesis was not as sensitive. Although, it is necessary to note that a hydraulic conductivity of 14 m/d presented more realistic results when simulating the scenarios compared to the calculated 34 m/d (see Aquifer Parameters section). The baseflow of 10 000 m^3/a for the B81H quaternary catchment was used along with a specific storage of 0.00001. Using MODFLOW computer software, simulations were run for various transient flow conditions for a time period of active pumping.

Natural Aquifer

Firstly, Scenario 1 was simulated and ran as a base-case to represent the natural conditions. Pumping was activated, simulating the actual rates with a transient model. During monitoring it was observed

that the 1.5 m deep well could no longer be pumped as water levels declined extensively, in other words the well ran dry by 30 November 2016. This was simulated for and is represented below.

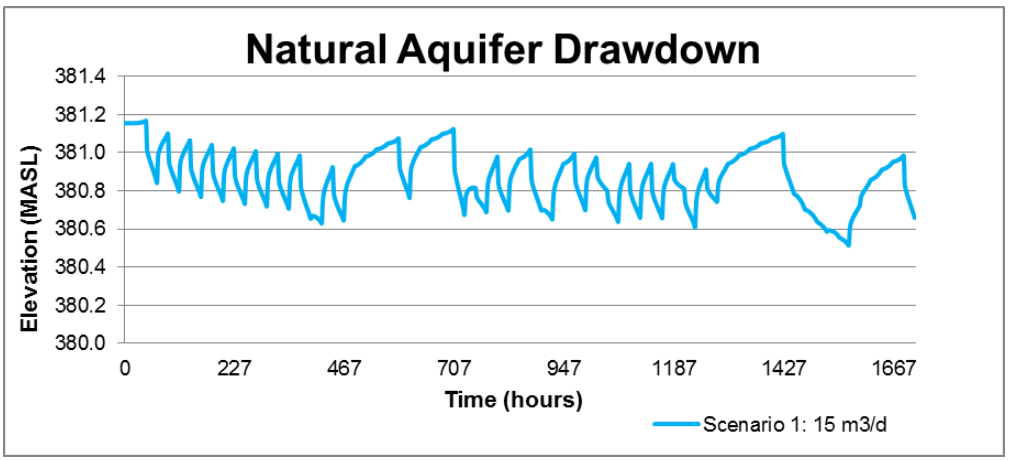

Figure 4-17: Drawdown at the well point of the natural aquifer (without the subsurface dam structure).

It is also important to mention that the simulation was run without recharge to allow for extreme circumstances. In reality some rainfall would have occurred by this time in November. The results of the groundwater heads show that the water level started declining to 0.7 m (381.2 m to 380.5 m) below riverbed level on day 64 (1549 hours) due to evaporation, baseflow, and pumping. Similar results were observed on site during monitoring and with the evaporation experiment conducted on the sand column which showed 0.31 m decline within 30 days. This made it difficult to pump towards the last week in November 2016. In the figure below the drawdown can be seen with a darker blue cone of depression around the well.

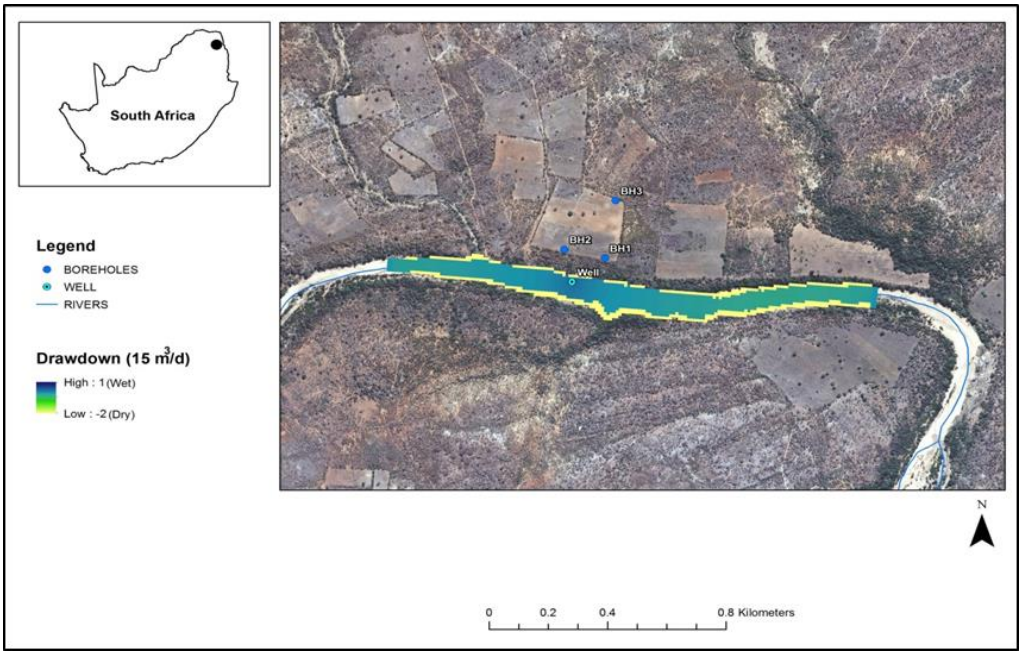

Figure 4-18: Draw down map of the natural aquifer showing a minor cone of depression in dark blue around the well in the riverbed, pumping for 15 m^3/d every second day. Coordinates of the well: latitude -23.568148°, Longitude 30.819999°.

Artificial Aquifer

The second scenario, Scenario 2, represents an artificial aquifer which shows and increase in water level due to the 1 m exposed subsurface dam wall that was included (see elevations to 381.7 m in Figure 4-19). This elevated water level would increase the extractable groundwater reserve significantly. The pumping of 15 m^3/d (pumping every second day) for 71 days did not have a major effect on the water levels of this artificial aquifer, therefore, pumping is sustainable.

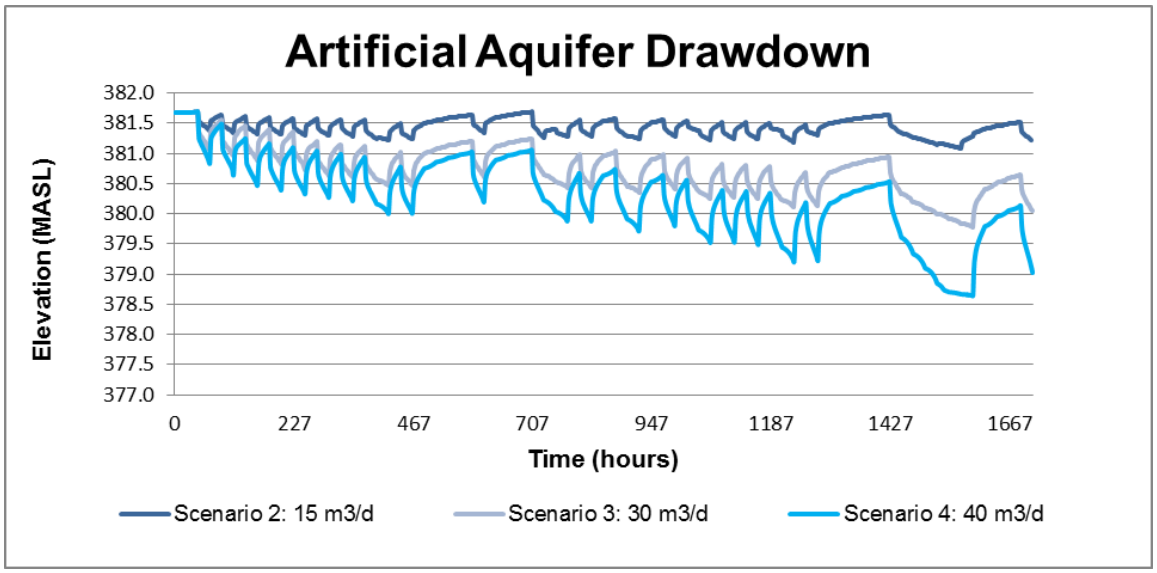

Figure 4-19: Drawdown at the well point of the artificial aquifer after implementing the subsurface dam structure.

A third scenario, Scenario 3, was performed to determine how much water can be extracted before this artificial aquifer or subsurface dam runs dry. The pumping rate was increased to 30 m^3/d (pumping every second day) at the same time interval as Scenario 1 and 2. Pumping for 71 days still showed sustainable results, the well only started to dry out with Scenario 4 after day 66, where pumping rates of 40 m^3/d were simulated. This resulted in the water table to drop 1.5 m. The initial saturated depth was 2.5 m for the subsurface dam scenario, thus a 1 m saturated depth remains after 66 days of pumping at these rates.

Constructing a subsurface dam would therefore allow the farmer to pump almost three times (2.67 times) the current pumping rate of 15 m^3/d (irrigating every second day), indicating the 0.175 ha of cro could expand to 0.467 ha. Pumping at a rate of 40 m^3/d could perhaps be more sustainable if rainfall patterns return to normal, as the Limpopo region is experiencing extreme drought conditions. The rainfall events of 2016/2017 used in the transient groundwater model was one of the driest years recorded in Limpopo. The maximum allowable abstraction rate of 40 m^3/d (pumping every second day) can therefore be used. This pumping rate is less than the initial calculated abstraction rate of 44.11 m^3/d (irrigating every day) in the Groundwater Reserve section, suggesting that the pumping rate of 44.11 m^3/d (irrigating every day) from the subsurface dam would not be sustainable and is somewhat overestimated.

Pumping 40 m^3/d for every second day would add up to 1400 m^3 per irrigation season of 71 days (20 September to 30 November), which is by no means large. Again, recharge or rainfall was not simulated for which should increase the extractable yield substantially. As observed in the field the water level in the riverbed recovers after a day through baseflow, however, it is slowly declining and would only

be fully replenished during rainfall which is predominantly during December to February (see Figure 4-16 for rainfall seasons).

The drawdown shown in Figure 4-20 clearly affects the water levels with a distinctive cone of depression around the well, which is expected on such an excellent aquifer. Abstraction affected a river reach of 300 m in Scenario 3. Scenario 4 shown below extended to a 400 m radius. Below the wall (black feature) the shallow groundwater flow is normal and undisturbed.

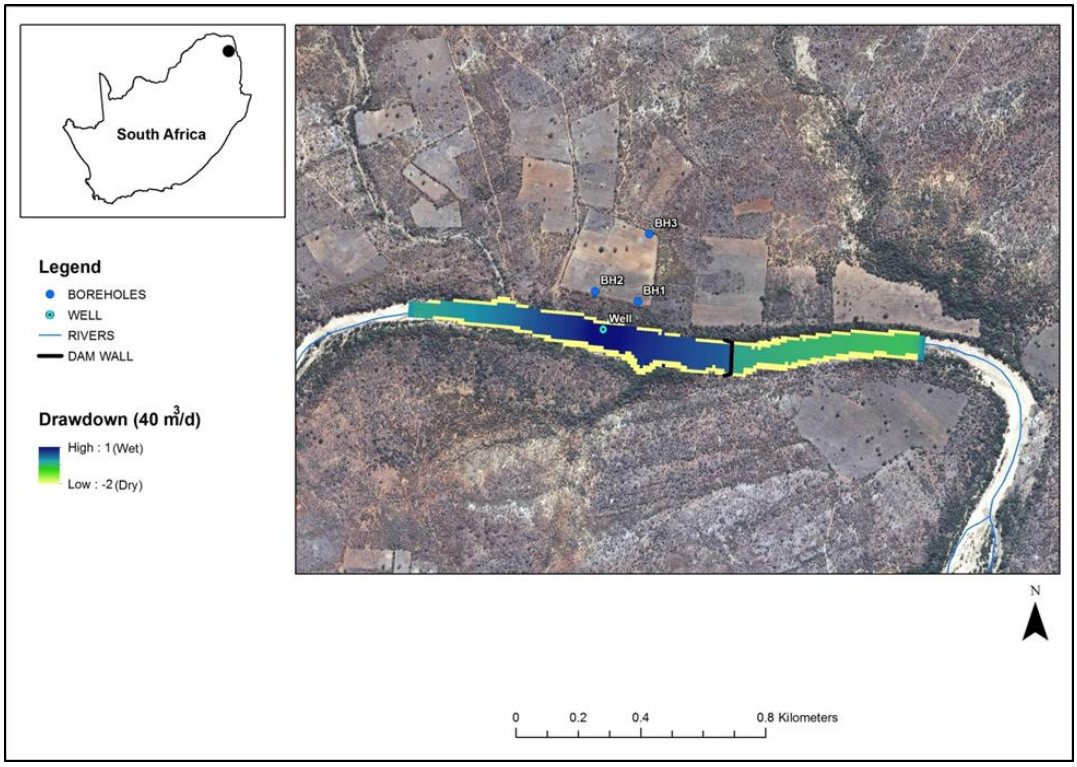

Figure 4-20: Draw down map of the artificial aquifer showing a distinctive cone of depression in dark blue around the well, pumping at 40 m^3/d for every second day over a 71 day period. Coordinates of the well: latitude -23.568148°, Longitude 30.819999°.

The artificial aquifer was also simulated to determine what would happen if pumping would occur continuously for 71 days (seen in Figure 4-21 below). Scenario 5 shows that after implementing the subsurface dam, continuous pumping of 15 m^3/d is sustainable. The water table only dropped 0.5 m from the initial depth of 2.5 m. For Scenario 6 and 7, it is a different case. Pumping continuously with a pumping rate of 30 m^3/d (pumping every day) was, however, not sustainable. It ran dry after 34 days, therefore supplying shallow groundwater only halfway through the season. Scenario 7 runs dry after 16 days of continuous pumping at a rate of 40 m^3/d. Scenario 6 and 7 shows that pumping at these higher rates, time for recovery of the riverbed sand aquifer is essential and irrigating every second day is more sustainable.

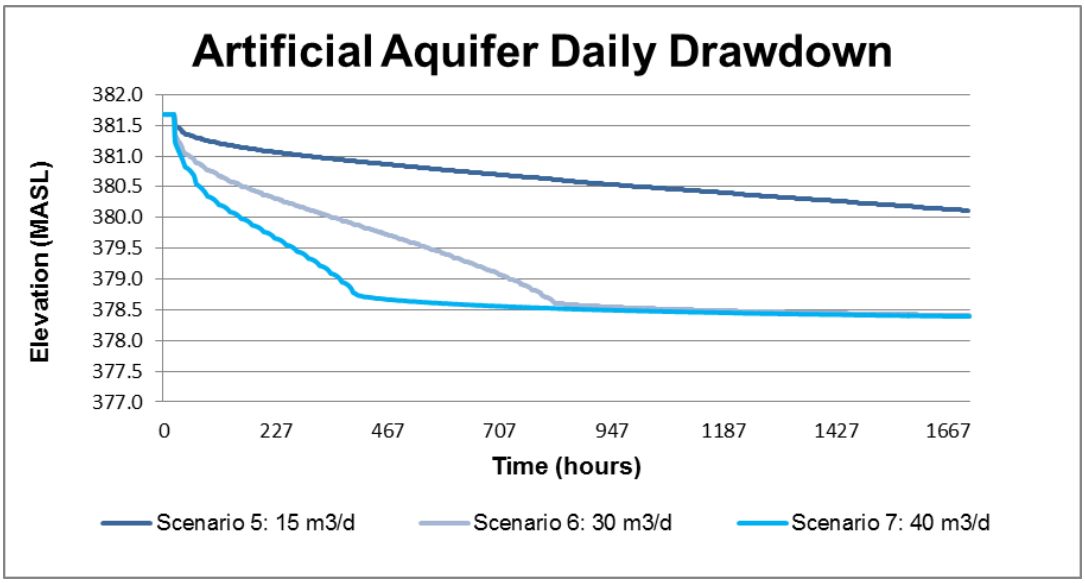

Figure 4-21: Drawdown at the well point of the artificial aquifer after implementing the subsurface dam structure by pumping continuously.

In reality, to prevent the wells from running dry, multiple well points that are connected with pipes to a main abstraction well could be installed. The well points should be designed and constructed to reach about 6 m below riverbed level and slotted with perforated casing to potentially tap shallow groundwater not only from the alluvial aquifer but also from the under laying weathered and fractured rock. This would increase the groundwater yield significantly and would allow for potentially higher pumping rates.

It can be concluded that numerical groundwater models are very useful tools for assisting in the simulation and prediction of groundwater movement under proposed scenarios. They are however always theoretical, and are only based on available data collected in the field. Careful interpretation of the results and regular updates of the model is required in order to draw the most informative conclusions.

4.4 Hydrological Study

The Molototsi catchment is known for occasional high flows during the summer months and very low to absent flows for most of the year particularly during the dry winter months. Most of these ephemeral streams generally become dry within one to two weeks after the rainy season. Only two flow gauge stations exist in the upper reaches of the Molototsi River (B81G) at the Modjadji Dam outlet. However, in B81H quaternary catchment there are limited climatic data available to determine accurate runoff, peak flows, floodlines and the potential surface water needed to recharge the subsurface dam reservoir. The nearby South African Weather Services (SAWS) rainfall station data of the surroundings will be used. This section includes a hydrological study and floodline investigation to recognize the potential extent of the various return period peak flows of the Molototsi River. The results of the return peak flows will therefore contribute to the structural design of the subsurface dam.

4.4.1 Topography and Drainage

The rainfall in the two quaternary catchments B81G and B81H of the Molototsi River catchment is strongly influenced by the topography, with the mean annual precipitation varying from less than 400 mm in the Lowveld plains of B81H (the study area) to more than 1,000 mm in mountainous areas of B81G. About 11 % of quaternary catchment B81G lie on the escarpment, 26 % consists of foothills and steep valleys and 63 % of Lowveld plains. Quaternary catchment B81H consists of 5 % of the Giyani outcrop and 95 % of Lowveld plains.

The project area is characterised by a defined watercourse with large trees and thick bush cover on the banks and grasslands on plains. The surroundings are mostly rural, undeveloped farm and grazing land. The riverbed itself was found to have a slope below 1% and is composed partially of bedrock and sand. It has very steep banks at some locations with high banks of up to 10 m. The banks are also significantly eroded in some areas, especially where water pathways or tributaries enter the river. River controls in the area include the Modjadji Dam (see location in Figure 4-22 below) upstream of the site with little data available on the river flow. The highest spillway overflow rate recorded at this gauge was 2.1 m^3/d (the gauge only show records of 5 years with some readings taken during the September months which is the dry season and can therefore not be used as a reliable flow rate) which would greatly increase in the summer months depending on the water level of the dam and the amount of rainfall received. Approximately 20 km downstream of the dam, is a large bridge which is well clear of the river and won't have any effect on the flow at the site. Another bridge is situated approximately 15 km upstream of the project site which would also have little to zero effect on the flow when running the hydrological model.

4.4.2 Catchment Yield

The amount of surface water which a catchment will yield greatly depends on the rainfall, hydrogeological setting and nature of the catchment area. The Molototsi catchment was delineated in order to identify the area which contributes to surface flow events during rainfall. The following table (Table 4-14) shows a summary of the catchment details.

Table 4-14: Details listing the area, hydraulic length, the slope of the entire Molototsi River and quaternary catchments. The site catchment details are the portion of the Molototsi catchment contributing to the subsurface dam site. The hydraulic length of the site is taken from below the Modjadji Dam in B81G to the subsurface dam site in B81H.

Molototsi Catchment Details			
Catchment	Area (km^2)	Hydraulic length (km)	Slope (m/m)
Molototsi	1180.17	106.61	0.0034
B81G	512.48	44.58	0.0043
B81H	667.69	62.03	0.0028
Site	855.02	72.64	0.0022

In order to establish the peak flows and floodline extent of the site, it was required to further delineate the main catchment into a more accurate area as the lower portion of the B81H catchment downstream of the subsurface dam would not contribute to flow. The peak flow generated during a rainfall event would also be smaller in the upper reaches of B81G compared to the lower reaches in B81H, near the Molototsi confluence, due to smaller contributing areas.

According to the Resources Quality Objectives (DWA , 2014), the natural Mean Annual Runoff (nMAR) for quaternary catchments B81G and B81H is 16.72 Mm^3/a and 25.84 Mm^3/a respectively. The records of the two runoff gauge stations in the B81G quaternary catchment will give a limited estimation of expected flows in the Molototsi River catchment. Both stations are situated in the lower foothills of B81G quaternary catchment downstream of the Modjadji Dam. The one gauge station, B8H069 (obtained from the Department of Water Affairs website), only has 5 recorded yearly gauge readings from non-consecutive years with only one year's data being useful. The records of the second gauge station B8R011, was found in the Resource Quality Objectives (DWA , 2014), which show the natural mean annual runoff and total flows.

The project site being further downstream in the B81H quaternary catchment, would possibly experience lower flow velocities due to a smaller slope. Examining the data from gauge stations B8H069, will not be relevant due to the little data recorded. Although gauge station B8R011 can be considered for spills and releases (DWA , 2014), it was not used for the flood peak calculations. The following is a summary of runoff observed at both gauge station in catchment B81G.

Table 4-15: Discharge for gauge station B8H069 in cubic meters per second (m^3/s) for every 10 cm rise in water level. The date recorded was 05-09-1997 which was during the dry season of the Molototsi catchment (Data was obtained from the Department of Water and Sanitation).

Gauge Station B8H069 (05-09-1997)		Gauge Station B8R011	
Depth (m)	Flow rate (Q) (m3/s)	nMAR (Mm^3/a)	Total Flows (Mm3/a)
0.10	0.0494	0.64	0.063
0.20	0.2810		
0.30	0.7360		
0.40	1.3520		
0.50	2.1040		

It is clear when examining the different catchment data that there are considerable differences in average annual runoff estimations based on the specific characteristics and rainfall of the catchment. Floods of high intensity have been recorded in numerous arid catchments and not necessarily in the

higher rainfall areas. Estimations from only one parameter such as the available 5 year flow records alone could be very misleading. Therefore, the peak flows were calculated based on the Standard Design Flood Method (SDFM) which is discussed in the sections below.

4.4.3 Rainfall

The design rainfall depths obtained from a grid estimate based on nearby rainfall stations was too conservative as it was much higher compared to the nearest rainfall station, thus a representative station was adopted. The selected station for the investigated site is the Eiland station (as seen in Figure 4-22 and Table 4-16) which is located approximately 18 km South West of the Duvadzi farm and project site. The station shares a similar altitude and is located in similar topography. Both locations also have similar vegetation and geology therefore using the rainfall data from this station would be the closest to the true rainfall.

Table 4-16: Mean annual rainfall data of the six rainfall stations nearest to the subsurface dam site (data was obtained from the Daily Rainfall Extraction Utility programme by Lynch (2003)).

Station Name	Station Number	Distance from site of interest (km)	Record Available (years)	Mean Annual Precipitation (mm)
Eiland	0680280_W	18.5	71	477
Konowi	0680494_W	18.8	26	459
Mahale	0680821_W	19.5	44	456
Letaba Ranch	0681069_W	26.8	40	501
Platveld	0680439_W	27.9	43	490
Black Hills	0680225_W	28.1	66	536

Figure 4-22: A Google Earth map showing all the rainfall stations surrounding the site. The site is shown as a red square (and red dot is the proposed subsurface dam location). The rainfall stations ae shown in dark blue and the Molototsi River and Modjadji Dam in light blue.

The average annual rainfall used for the project site is 477 mm. The various storm return periods for the station are shown in Table 4-17 below.

Table 4-17: Various storm rainfall depths for the subsurface dam site using the rainfall station, Eiland 0680280_W (data was obtained from the Design Rainfall programme by Smithers and Schulze (2002)).

Station Name	Station #	Record Length (years)	MAP (mm)	Duration (min/h/d)	Return Period (1:x) (years)						
					2	5	10	20	50	100	200
Eiland	Gridded value	71	477	5 min	8.3	12.1	14.9	17.8	21.8	25.2	28.8
				10 min	13.2	19.2	23.6	28.2	34.7	40	45.7
				15 min	17.4	25.2	31	37	45.4	52.4	59.9
				30 min	23.7	34.5	42.4	50.5	62.2	71.7	81.9
				45 min	28.5	41.4	50.9	60.7	74.7	86.1	98.4
				1 h	32.5	47.2	57.9	69.1	85	98	112
				1.5 h	39	56.6	69.6	83	102.1	117.7	134.5
				2 h	44.4	64.5	79.2	94.6	116.3	134.1	153.2
				4 h	51.6	75	92.1	109.9	135.1	155.8	178
				6 h	56.4	81.8	100.5	119.9	147.5	170.1	194.4
				8 h	60	87.1	107	127.7	157	181	206.9
				10 h	62.9	91.4	112.3	134	164.8	190	217.1
				12 h	65.5	95.1	116.8	139.4	171.4	197.6	225.8
				16 h	69.7	101.2	124.3	148.3	182.4	210.3	240.3
				20 h	73.1	106.2	130.5	155.7	191.4	220.7	252.2
				24 h	76.1	110.5	135.7	161.9	199.1	229.6	262.4
				1 d	63.1	91.7	112.6	134.3	165.2	190.5	217.7
				2 d	78.8	114.4	140.5	167.6	206.1	237.7	271.6
				3 d	89.6	130.2	159.9	190.8	234.6	270.5	309.1
				4 d	97.9	142.2	174.6	208.4	256.2	295.5	337.6
				5 d	104.8	152.2	187	223.1	274.4	316.4	361.5
				6 d	110.8	161	197.7	235.9	290.1	334.5	382.3
				7 d	116.2	168.7	207.3	247.3	304.1	350.7	400.8

The result indicates that T_c = 19.08 hours (t = 60T_c = 1144.85 minutes), therefore, the storm rainfall depth for a 16 h return period will be suitable for calculating the flow rate. However, all the above design rainfall estimations shown are determined according to the Rational Method which is mostly used for small catchments < 15 km^2.

Table 4-18: Time of concentration (T_c) results.

Time of concentration		
Method	Equation	T_c (hours)
US Soil Conservation Service	$T_c = (0.87L^2 / 1000S_{av})^{0.385}$	19.08

The portion of the Molototsi catchment contributing to the subsurface dam site is 855.02 km^2, thus the Standard Design Flood Method (SDFM) is used. The Rational method does however form the basis of this method. The rainfall obtained from the design rainfall data will be used to compare with the representative rainfall basin used in the SDFM (van Vuuren, van Dijk, and Smithers, 2013).

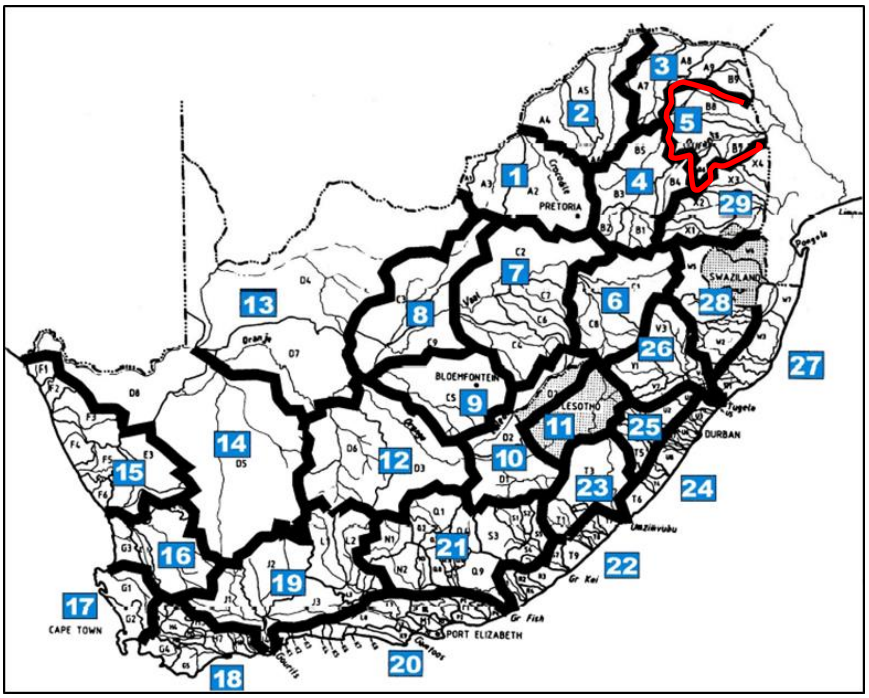

Figure 4-23: Standard Design Flood Basins obtained from the Drainage Manual (van Vuuren, van Dijk, and Smithers, 2013). Drainage basin 5 indicated with a red boundary is representative of the project site.

The SDFM requires to identify the drainage basin in which the site is located, from Figure 4-23 above. The site catchment is situated within drainage basin 5 of which Leydsdorp station is representative of the catchment (see the daily rainfall in Figure 7-4 of Appendix C). Leydsdorp has the following storm rainfall return periods.

Table 4-19: Details and return periods of Leydsdorp taken from TR102 (Adamson, P.T, 1981).

Water service station	Leydsdorp		Mean Annual Precipitation (MAP)		620		mm
Weather Service Station no.	680059		Coordinates		Lat: 23°59' & Lon: 30°22'		
Duration (days)	Return period (1:x) (years)						
	2	**5**	**10**	**20**	**50**	**100**	**200**
1 day	78	116	146	181	233	279	331
2 day	99	156	203	257	241	416	503
3 day	105	165	215	271	358	434	524
7 day	135	225	301	389	528	653	798

After extracting the return periods (T) from the Drainage Manual (van Vuuren, van Dijk, and Smithers, 2013) the point precipitation depth ($P_{t,T}$) was calculated for the basin.

Table 4-20: Modified Hershfield equation for calculating point precipitation using the 1 day return period values of Leydsdorp.

Point Precipitation							
Method	Equation				T = Return Period, t = 1144.85 min, M = 78 mm, R = 10 days		
Modified Hershfield equation	$P_{t,T} = 1.13(0.41 + 0.64 \ln T)(-0.11 + 0.27 \ln t)(0.79 M^{0.69} R^{0.20})$						
Return Period (1:x) (T) (years)	**2**	**5**	**10**	**20**	**50**	**100**	**200**
$P_{t,T}$ (mm)	43.73	73.77	96.49	119.22	149.26	171.98	194.71

The results of the Rational method indicate that if the time of concentration (T_c) is between 6 and 24 hours, a linear interpolation of the values from the 1 day point rainfall (calculated in Figure 7-3 of Appendix C) and the point precipitation depth ($P_{t,T}$) should be used. The results are shown in Table 4-21 below.

Table 4-21: Linear interpolation of the modified Hershfield point precipitation were then calculated due to T_c = 18.34 hours.

Leydsdorp Rainfall							
Return Period (1:x) (years)	**2**	**5**	**10**	**20**	**50**	**100**	**200**
1-day return period (mm)	78	116	146	181	233	279	331
Point Precipitation ($P_{t,T}$) (mm)	43.73	73.77	96.49	119.22	149.26	171.98	194.71
Linear Interpolation ($L_{Pt,T}$)	68.89	98.93	121.65	144.38	174.42	197.14	219.87

When comparing the linear interpolated rainfall data of Leydsdorp with the 16 hour storm duration (T_c = 19.08, therefore use a duration ≤ 19.08 hours) of the Eiland station as shown in Table 4-17, they show very similar results. For this reason, using the linear interpolated values for further calculations would be more realistic (the linear interpolated results are shown in Table 4-21 above and with a dashed line in Figure 4-24 below).

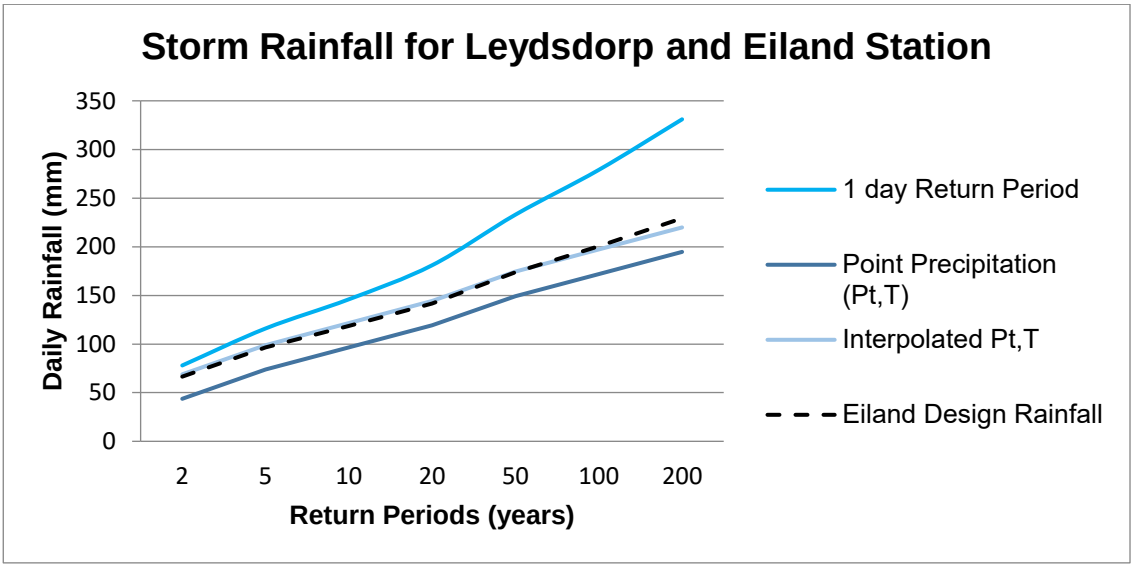

Figure 4-24: Comparison of storm rainfall for the Leydsdorp and Eiland stations.

In order to determine the average rainfall of the catchment for the various return periods (T), the point precipitation depth ($P_{t,T}$) was multiplied by the area reduction factor (ARF). Firstly, the ARF was calculated, where A = 855.02 km^2 and t = 1144.85 minutes.

Table 4-22: Results of the area reduction factor.

Area Reduction Factor		
Method	Equation	ARF (%)
UK Flood Studies Report	ARF = (9000 – 12800 ln A + 9830 ln t)$^{0.4}$	88.08

The corresponding rainfall intensity (I_T) is then obtained by dividing the average rainfall of the catchment by the time of concentration (T_c = 19.08) which is shown below.

Table 4-23: Rainfall intensity calculation results.

Average Intensity							
Method	Equation			$P_{t,T}$ = mm, ARF = 0.8808, T_c = 19.08 hours			
Rational Method	$I_T = (P_{t,T} \times ARF)/T_c$						
Return Period (1:x) (T) (years)	**2**	**5**	**10**	**20**	**50**	**100**	**200**
Linear Interpolated $P_{t,T}$ (mm)	68.89	98.93	121.65	144.38	174.42	197.14	219.87
I_T (mm/hour)	3.18	4.57	5.62	6.67	8.05	9.10	10.15

The calibrated runoff coefficients C_2 (2-years return periods) and C_{100} (100-year return period) used in the SDFM, including the return period factor (Y_T), were obtained from the Drainage Manual, which is based on statistical analysis of recorded data within the corresponding drainage region (see Figure **7-5** of Appendix C). The runoff coefficient (C_T) is therefore, designed as a regional parameter and not as a site-specific value. See the following calculated relationship in the equation below.

Table 4-24: Calibrated Runoff coefficient calculation used in the Standard Design Flood Method.

Runoff Coefficients							
Method	Equation						
DWAF	$C_T = (C_2/100) + (Y_T/2.33)((C_{100}/100)-(C_2/100))$						
Calibration factors	C_2 (2-year return period) (%)		15	C_{100} (100-year return period) (%)			70
Return period (years)	**2**	**5**	**10**	**20**	**50**	**100**	**200**
Return period factors (Y_T)	0	0.84	1.28	1.64	2.05	2.33	2.58
Runoff coefficient (C_T)	0.15	0.348	0.452	0.537	0.634	0.7	0.759

4.4.4 Flood Peak

Finally the flood peaks for the various return periods were determined for the site using an empirical regionally calibrated version of the Rational Method (van Vuuren, van Dijk, and Smithers, 2013). The results show extreme flows with steep increases in flow magnitude with the increase in return years.

Table 4-25: Adopted flood peaks (Q) for various return periods of the project site with a contributing catchment area (A) of 855.02 km^2.

Flood Peak							
Method	Equation						
Rational Method	$Q_T = (C_T \times I_T \times A)/3.6$						
Return period (1:x) (years)	**2**	**5**	**10**	**20**	**50**	**100**	**200**
Q_T (m^3/s)	113.30	377.47	602.87	850.07	1212.44	1513.03	1829.71

The 1 in 50 year return period having a flow rate above 1000 m^3/s indicate very high flows which could result in severe damage on structures and river banks within the Molototsi River system. Therefore, the subsurface dam structure will be designed using engineering factors of safety to withstand the uncertainty of the flood estimates. Using these peak flows for flood modelling will provide for better understanding on how severe these flood magnitudes potentially could be.

4.4.5 Flood Model

The flow peaks indicate that under both the 1 in 2 and 1 in 100 year return period events seen in Figure 4-25, the flood is largely confined to the defined watercourse boundary. There are two instances where 1 in 100 year overflow would possibly occur, causing the channel to flow into the tributary outlet. Damaged banks are highly likely in these areas. Similar results were observed for scenario two even

though it had a 1.0 m high wall. For the most part of the project area, damage by floodwaters can be minimized through watercourse training, as required, to alleviate water erosion potential on the banks.

The mentioned flood events generally bring the catchment close to saturation during the first part of the heavy storm rainfall, followed by continues rainfall that allows the Molototsi to flow strong. The Molototsi being a dry non-perennial river throughout most of the year, greatly relies on these flood events to recharge the riverbed. Therefore, it is also important to look at the 1 in 2 year return period peak flow for this project as the 2-year flow rate would be the most frequent flood event. Knowing the potential peak flow of this 1 in 2 year storm event, one could design an adequate subsurface structure to withstand the severe forces and retain sustainable volumes of shallow groundwater.

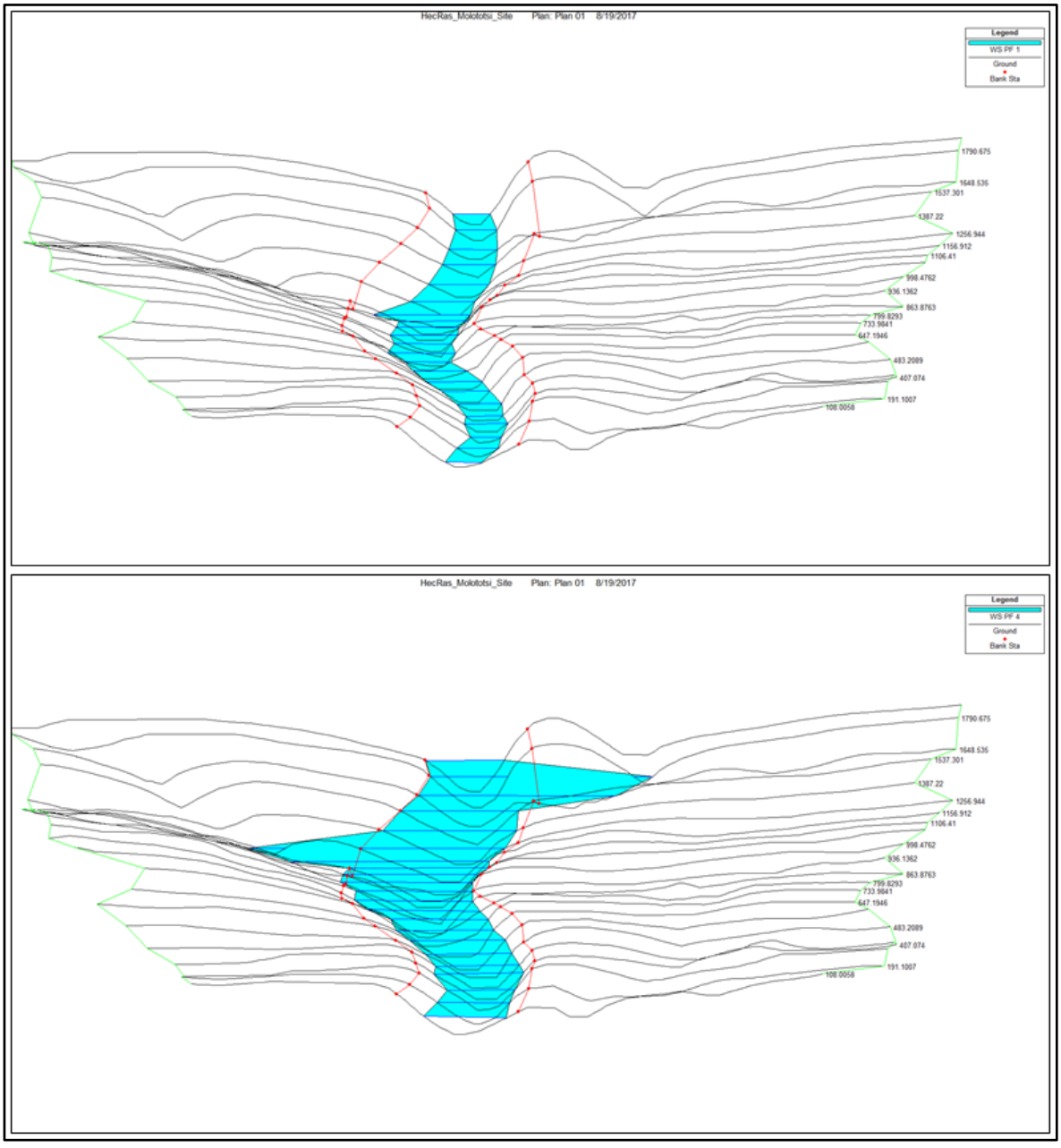

Figure 4-25: Flood modelling were done using ArcGIS and HecRAS where A) shows the 1:2 year return period peak flows and B) the 1:100 year peak flows . The results in B) clearly show bank overflows at the two tributary outlets.

4.4.6 Floodlines

The 1 in 2 and 1 in 100 year floodlines for the existing situations are given (see Figure 4-26), which allows for the future development of pump stations or any structure along the river. At the location of the subsurface dam, one would expect the floodline to widen but this would only be the case at a surface dam. When looking at the exposed wall model (scenario two), floodlines are not widened with a 0.5 meter wall, it only happens with a wall above 2 meters, therefore having little to no effect on the floodwaters at the site. This is to be expected since the floodwaters are in the order of 6 meters above the riverbed for the 1 in 50 and 1 in 100 year flood. The floodlines do however widen in the areas where tributaries or water pathways enter the Molototsi River.

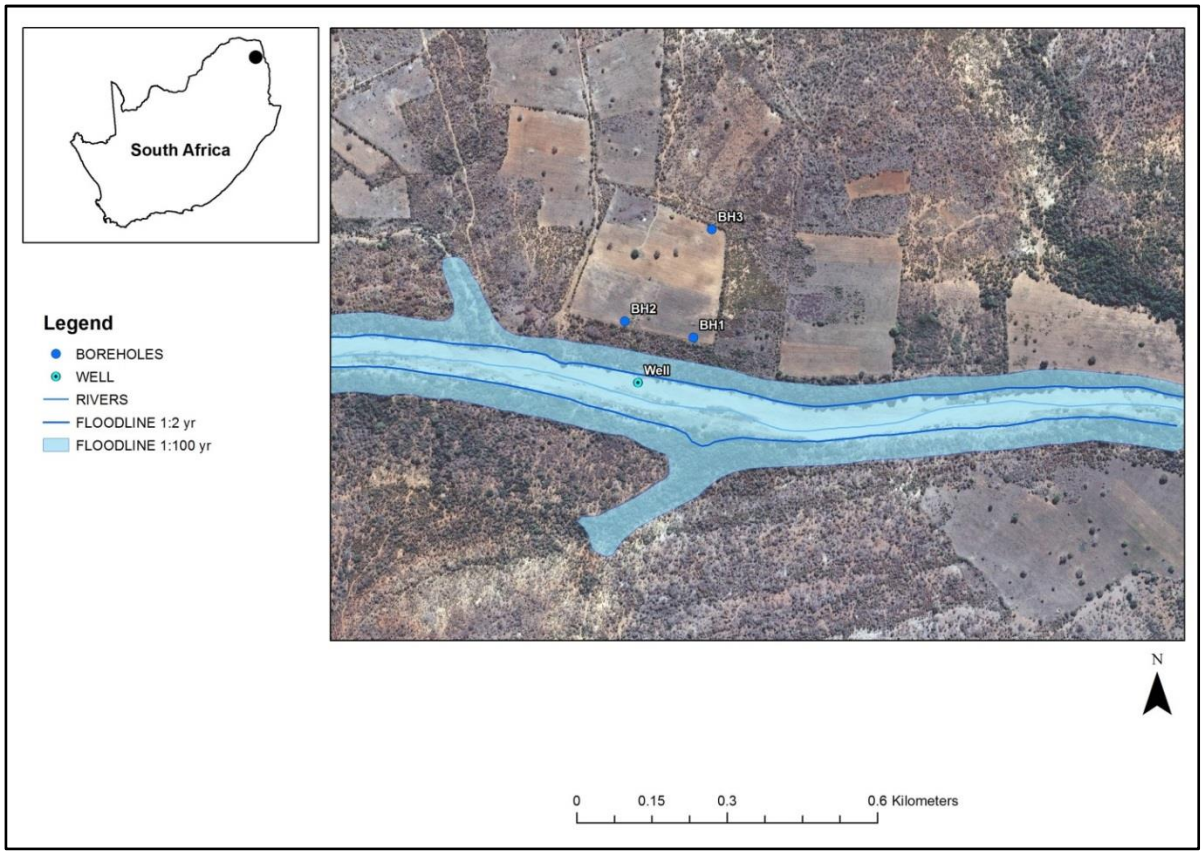

Figure 4-26: The extent of the 1 in 100 and 1 in 2 year peak flow events for this reach of the Molototsi River. Coordinates of the wall structure: latitude -23.568542°, Longitude 30.823947°.

4.4.7 Sediment Transportation

Floods with various peak intensities will have different transportation capacities, thus the transported grain size is greatly dependent on the slope and the flow velocity. The Molototsi predominantly consists of medium to coarse sands, which needs high flow velocities to be transported. Therefore, the subsurface dam structure will reduce the flow velocity of the river in the case of the exposed 0.5 m wall scenario, resulting in deposition of the sands upstream of the wall structure. The Molototsi River also transports finer materials, like silt and clay. Since most of the land in the catchment is bare and over grazed during the dry winter months, soils are poorly protected against erosion and end up in the river during rainy seasons. However, these finer sediments have lower deposition velocities compared to sand, thus staying in suspension and would be transported over the dam structure. Sedimentation will continue until it reaches the height of the subsurface dam structure. This may take one or several rainy seasons depending on the availability of coarse material and the river discharge.

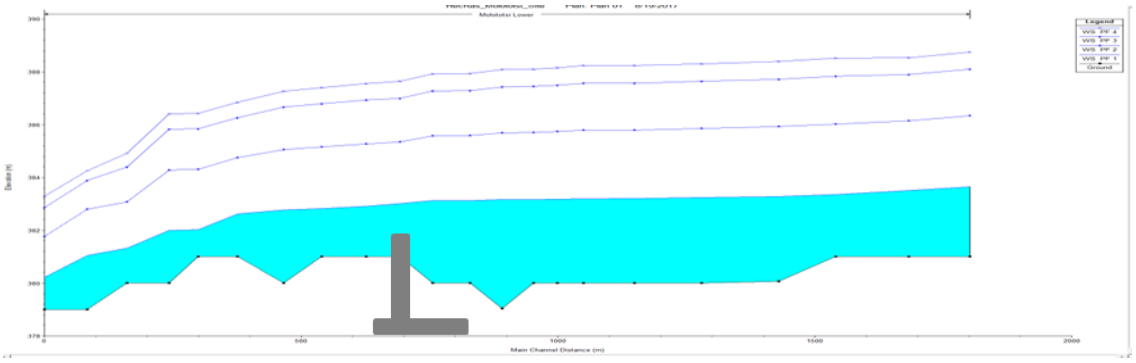

Figure 4-27: Cross section of the riverbed from the upper reaches (right) to the lower reaches (left). From the top is the 1:100 year peak flow line, second is the 1:50 peak flow, third is the 1:10 year and blue fill is the 1:2 year return period peak flow. The grey structure is the location of the subsurface dam wall; here sedimentation will occur behind the 1 m exposed wall.

4.5 Geotechnical Investigation

The geotechnical investigation conducted includes a general site survey and digging of test pits to determine the geotechnical characteristics and suitability of the selected subsurface dam site.

4.5.1 Soil Profiles

The knowledge of the soil profile is very important when establishing a subsurface dam site within a riverbed. It reveals the properties of the soil which are not visible at the surface. The soil in the study area have developed on the crystalline bedrock which consists of reddish-brown to light brown silty loam soils and yellowish-brown coarse grained sands. Table 4-26 below, shows a summary of each soil profile and its coordinates. The following soil profiles were conducted on the Molototsi River catchment (see Figure 4-28,

Figure 4-29, and Figure 4-30 below).

Table 4-26: Soil profile summary

Soil Profile	Description	Coordinates	SP depth (m)	Water level (m)
SP1	Molototsi riverbed	23.56729 S 30.82098 E	2.5	1.5
SP2	Molototsi River bank	23.56712 S 30.81966 E	9	-
SP3	Failed sand dam bank	23.56536 S 30.82118 E	3.8	-

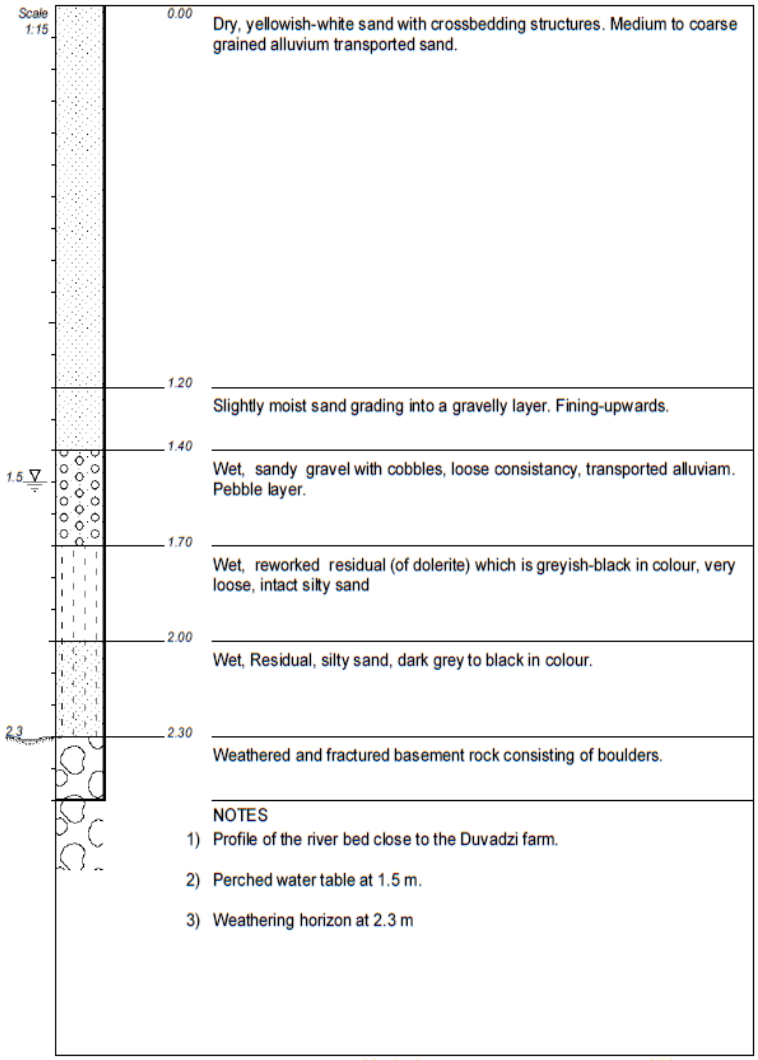

SP1: Soil profile of the Molototsi riverbed near the sand mining operation at the Duvadzi farm.

SP1: Molototsi Riverbed

The first 1.20 m was dry, yellowish-white sand with visible crossbedding structures. The particle sizes were medium to coarse grained alluvium sand which is typical of crystalline complexes. Due to small percentages of silt and/or clay this layer has good drainage. The second layer was slightly moist gravelly sand grading into a gravel layer. Layer 3 (at 1.40 m) was a distinct gravel layer containing minor cobbles. Layers 4 and 5 was classified as the wet residual where layer 4 seemed to be the reworked residual due to some disturbance and its greyish-black colour compared to layer 5 which had a darker grey to black colour. Layer 6 which is at 2.30 m consisted of weathered and highly fractured basement rock with boulders. This layer was very difficult to excavate thus the true depth of fresh hard rock is unknown. A perched water table was encountered at 1.50 m during the driest month of the year (October 2017), indicating high potential groundwater within the primary sand aquifer.

In A) one can see the gravel layer along with cobbles and boulders and in B) the distinct greyish-black residual (regolith) layer. Excavator were used to dig tests pits for soil profiling at a sand mining area.

Figure 4-28: Soil Profile 1 description.

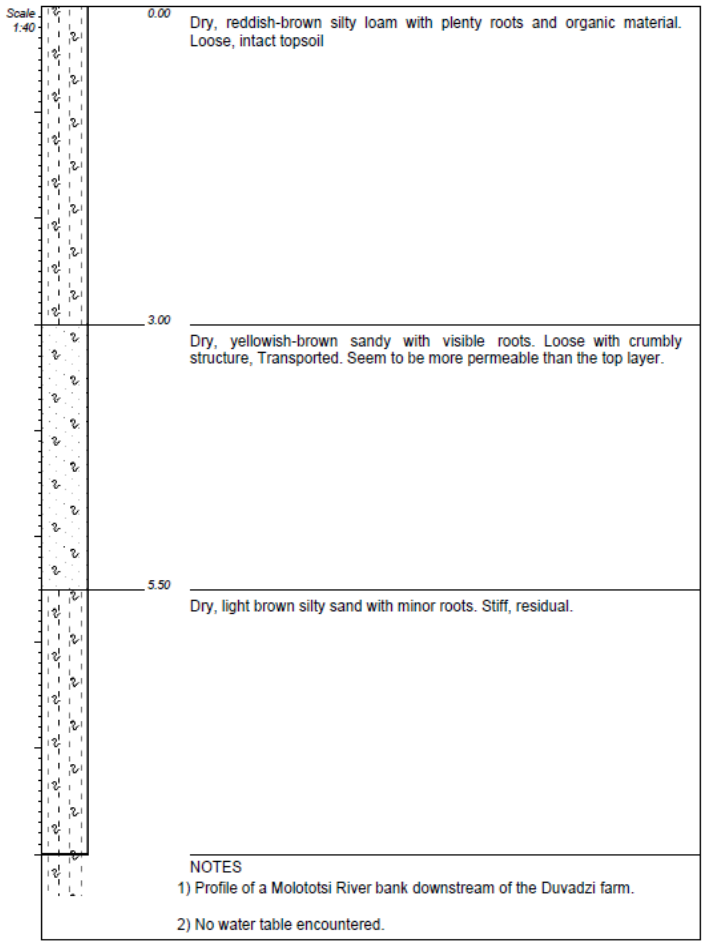

SP2: Soil profile of the Molototsi river bank which is about 500 m downstream of the Duvadzi farm.

SP2: Molototsi River bank

An eroded slope downstream of the Duvadzi farm constitute to a well exposed soil profile of the Molototsi River banks. It is important to remember that although the banks seem to consist solely of soil at some locations with heights ranging up to 10 m, the soil depth further away from the crest of the river bank decreases drastically to about 1 to 3 m. The first three meters of topsoil from the profile to the left is a reddish-brown silty loam with plenty of roots and decomposing organic material. The second layer (at 3 m) is a more yellowish-brown sandy soil with a crumbly structure and visible roots. This layer also seems to have better drainage characteristics than the top layer. Layer three is light brown silty sand which is possible granite residual. The presence of root is minor. Hard rock could be expected to be 2 to 3 m down where this layer reaches the riverbed.

In A) one could see the three different layers present with the top layer being more reddish, middle layer yellowish-brown and the bottom layer light brown. In B) which is a zoomed-in image, one could see distinct structure in the river bank sediments (regolith). The roots present on the same layer possibly represent an old water table, while the black dash-line is the bottom of an ant nest. This supports the assumption of an old water table as ants would not dig their tunnels deeper than the general water table.

Figure 4-29: Soil Profile 2 description.

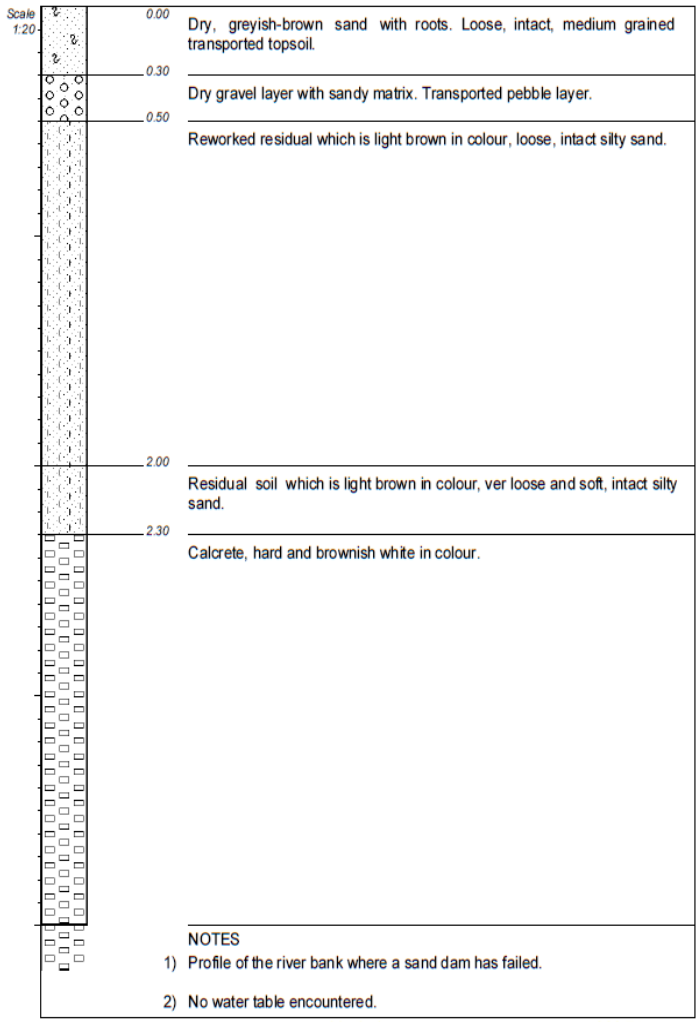

SP3: Soil profile of a bank at a failed sand dam in one of the tributaries of the Molototsi River which is some distance from the Duvadzi farm. The river bypassed the sand dam wall because it was built into the soft soil on top of the Calcrete with no flank.

SP3: Failed sand dam bank

A bank was profiled at a failed sand dam some distance away from the Duvadzi farm where a river bypassed the dam wall because it was not built onto hard rock. The first 0.30 m was dry, greyish-brown sand with visible roots and organic matter. The topsoil consisted of loose transported silty sand. The second layer was a distinct gravel layer known as the pebble marker. Layers 3 and 4 are dry residual silty sand layers with both being light brown in colour. However, layer 4 appeared to be looser and soft thus deeper eroded than the top layer. The bottom layer consists of a brownish-white hard rock called calcrete which is cemented calcareous material. This impermeable crust is formed when calcite is dissolved in groundwater and, as water evaporates under drying conditions the remaining water becomes more and more concentrated, resulting calcium-carbonate to precipitate. This is a typical phenomenon in semi-arid regions with fluctuating climate conditions.

In A) the distinct pebble layer near the top can be seen and B) shows a clearer image of the whitish calcrete layer at the bottom.

Figure 4-30: Soil Profile 3 description

4.5.2 DCP

Dynamic cone penetrometer tests (DCP's) were conducted on the proposed site where the subsurface dam embankment would be constructed (see red dots in the riverbed of Figure 3-3 in the Methodology section). DCP 1 is located close to the edge of the northern river bank, and DCP 2 towards the middle of the riverbed. Both DCP's indicate somewhat loose material down to a depth of about 0,6 m but below this depth the sands have been slightly compacted over time by the weight of the above sediments. It is also possible that the layer 0.6 to 0.9 m consists of silty sands.

Moving more towards the middle of the riverbed, DCP 3 indicate a dense layer within the upper 0,6 m with medium dense material up to 0.9 m. Below this level, looser material exists showing DCP penetration rates of more than 30 mm per blow. The material close to the southern edge of the river bank located at DCP 4 consists of loose material down to 0.6 m with somewhat medium dense silty sand layer below 0.6 m.

From the geotechnical investigation undertaken it is observed that sand mining had taken place near the site to a level of 1.2 m. DCP tests 5 and 6 were conducted here to penetrate below the one meter reach with DCP 6 done within the test pit of the excavated sand mining area (see the images of the SP1, section 4.5.1). DCP 5 showing loose material up to 1.5 m below riverbed level with more medium dense sand down to 1.7 m and loose sand layer again down to 1.8 m. DCP 6 indicate that more medium dense material occurs below 1.9 m with gravelly material at 2.1 m and large broken boulders from the slightly weathered dolerite found below 2.3 m.

DCP 1 and 2 is inferred to be representative of the consistency of the natural material generally observed in top meter of the riverbed, therefore, summarizing the material in the loose to medium dense consistency range. The results of the DCP test can be seen in Figure 4-31 with tables showing mm/blow in Appendix B.

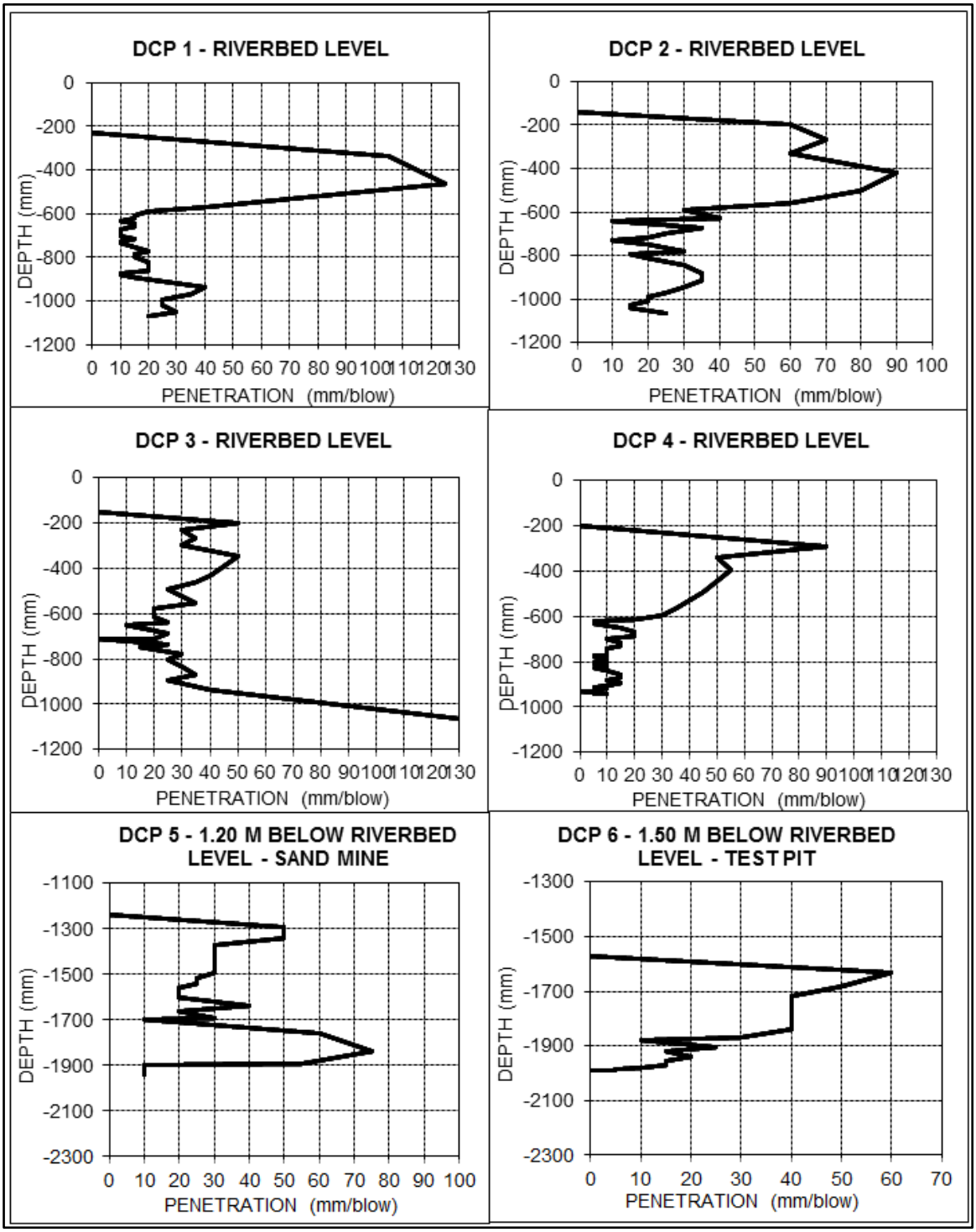

Figure 4-31: DCP's done in the Molototsi River close to the Duvadzi Farm. DCP's 1 to 4 was done at riverbed level. DCP 5 was done at 1.20 m depth on the sand mining pit level. DCP 6 was done at 1.50 m depth within the test pit that was excavated.

Founding on the site is expected to be good as the foundation will be on solid granitic bedrock; however, it is likely that in some places the bedrock will be slightly weathered for several meters. The overlying riverbed sand will need to be excavated. The excavated sand could then be used for backfill and concrete mixing in the case of constructing a concrete retaining structure. The most economical and destructive founding system for a reinforced concrete retaining structure on the hard rock would be to use strip footing. When cutting into the riverbank, it is recommended to create platforms in cut rather than deep foundations as this will be far costlier due to more extensive earth works. The banks

consist predominantly of hard crystalline bedrock at the base with highly weathered granite and in-situ topsoil towards the surface. Therefore, proper measures should be taken to not introduce articulation joints between the founded areas on bedrock and those on soil.

4.5.3 Excavatability

Excavation of the riverbed will yield approximately 2 to 3 meters of alluvial sands and minor silty sand lenses which have loose to medium dense stiffness down towards the hard rock. At this depth the water table will be reached thus influencing the excavation during construction. In these non-cohesive sands, it is vital to control the groundwater flow as it will result in erratic settlement caused by the loss of sand into the excavated area. Therefore, the shallow groundwater will need to be diverted downstream or pumped to a temporary pond for irrigation and construction purposes. The water table is at its lowest at about 1.5 meters below the riverbed level during the dry winter months in June to October. It is suggested that construction should be undertaken during these months. Below the sand, slightly weathered granite and dolerite, consisting of large boulders and gravels, will be encountered. Therefore, relatively rapid refusal of excavation will occur in places underlain by slightly weathered to unweathered granite or dolerite. Excavating and sorting these hard rocks on site could reduce the costs of aggregates significantly as it is suitable for concrete, gabions and stone pitching. Excavation into the slopes will tend to yield similar granitic rock and broken bedrock, however, it consists of a sandy loam soil with increased stiffness and plant material. Trenching of the sand, boulder-breaking and flattening of the granitic surface where possible is likely to be difficult therefore a digger-loader is required rather than an excavator.

4.5.4 Construction Material Investigation

During the site visits, numerous dolerite intrusions were observed within the riverbed. At some localities the dykes and sills were very hard and unweathered, which could be used for concrete aggregates as dolerite is a sought after material in its unweathered state. Naturally occurring alluvial sand sources are in immediate supply along the Molototsi River. The sands are medium to coarse grained which is perfect for building supply (see the particle analysis section below for more detail on riverbed sand as building material). Few clayey silty sand sources were seen along the riverbed, which are in short supply. Also, the river banks consist of reddish brown, slightly clayey or silty sands with sandy loam soils in the upper reaches further away from the river, suggesting the construction of a clay embankment would not be viable. The diverted water or water from the riverbed can be used for concrete mixing (as water constitutes 14 to 18 % of the concrete ingredients) and other construction purposes as the water quality with specific emphasis on the iron (Fe) content of the deep crystalline aquifer and shallow sand aquifer are non-corrosive and suitable for drinking, therefore, complies to the minimum requirements for construction reference.

Particle Analysis

The riverbed sand was analysed according to the ASTM (American Society for Testing and Materials) method to determine whether it could be used for as concrete aggregate. Below are the results of particle size analysis (seen in

Figure 4-32 and Table 7-2 of Appendix D) of five sand samples taken from the Molototsi River. The sand samples all show similar results, being coarse grained (more than 50 % > 0.063 mm) material predominantly consisting of sand (more than 50 % of coarse fraction < 2mm) with minor fines (0 to 5 %), therefore classified as SP: poorly graded sands, gravelly sands, with minor fines. These sands also have little iron-oxide coating, minor organic or vegetation material and little salt content, indicating that these angular and clean riverbed sands are suitable for concrete aggregate.

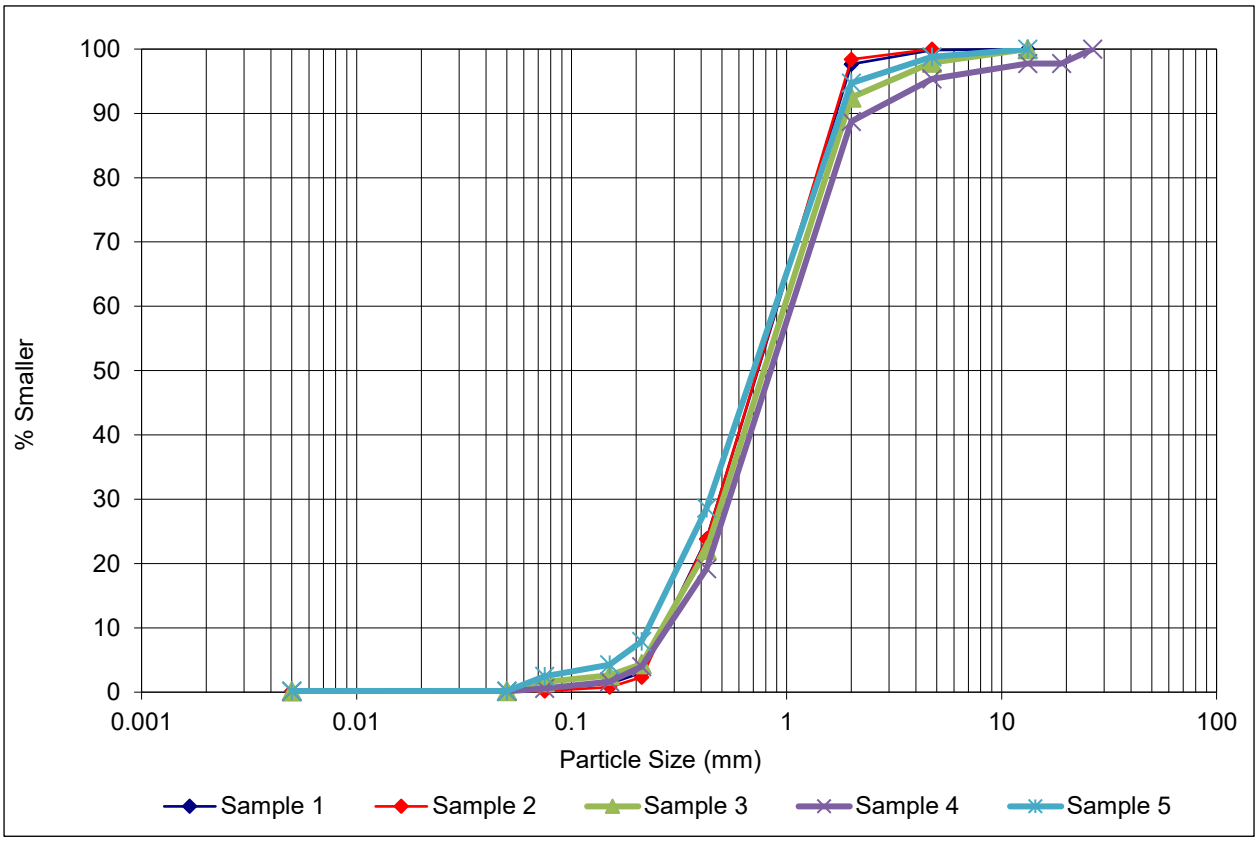

Figure 4-32: Particle analysis of five samples which were all collected within the Molototsi River and plotted on a particle size distribution curve on a semi-logarithmic plot, the ordinate being the percentage by mass of particles smaller than the size given by the abscissa. The above distribution curves are steep, therefore, indicating smaller particle size ranges which corresponds with the Unified Classification System workings.

4.5.5 Soil Erosion

The loose and relatively non-cohesive sandy loam of the river bank slopes is highly erodible if cleared of vegetation from its uppermost horizon. The clearing of areas along the Molototsi River for agricultural use is rapidly increasing erosion of the slopes which will soon reduce the thin soil layer down to bedrock unless adequate preventive measures are implemented. The large thorn and mopani trees have been noticeably contributing to arrest the flow of surface water and damage to the slopes by stabilizing the banks with their trunk and root systems. It is therefore, strongly recommended that at least 20 meter vegetation buffer is considered along the Molototsi River and subsurface dam site. Also, a major contributor to slope failure of the Molototsi River banks is the continuous sand harvesting for construction material. The mining of sand is not only decreasing the shallow groundwater level which conserve water for plant growth on the river banks but also increases lateral erosion which results in undercutting of the slopes. Consideration should be given to stop or minimize the mining of sand in the Molototsi riverbed as it has negative effects on a rivers system that could possibly hold promising water yields for human consumption and irrigation. Assuming that sand mining would go ahead, constructing the subsurface dam structure could be a possible solution for this as the structure can be designed to withhold and increase sediment loads behind the wall, thus implying that sand harvesting can continue at the rate of sedimentation.

4.5.6 Soil Parameters

The geotechnical characteristic of the sand needs to be determined for design purposes. The sand samples collected from the Molototsi River consists of the following properties.

Water Content

The water content determined for the sand was 23%. This value was also determined for the specific storage in the Aquifer Parameter section and was used throughout the thesis.

Table 4-27: Water Content

Water Content		
Equation	$W = (M_w - M_d)/M_d$	
Description	Water Content (W)	W (%)
Original sand sample (not sieved)	0.23	23

Specific Gravity

The specific gravity of the soil particles was calculated to be 2.73.

Table 4-28: Specific gravity

Specific Gravity	
Equation	$G_s = M_d/(V_v - M_w)$
Description	Specific Gravity (G_s)
Original sand sample (not sieved)	2.73

Dry Density

For a completely dry sand, the dry density was calculated to be 1675 kg/m^3 which corresponds to a bulk unit weight weight (Y) of 16.75 kN/m^3.

Table 4-29: Dry Density

Dry Density	
Equation	$P_d = 1/(1 + W)$
Description	Dry Density (P_d) (kg/m^3)
Original sand sample (not sieved)	1675

Void Ratio

Void density was determined to be 0.63.

Table 4-30: Void Ratio

Void Ratio	
Equation	$P_d = (G_s \times P_w)/(1 + e)$
Description	Void Ratio (e)
Original sand sample (not sieved)	0.63

Degree of Saturation

The degree of saturation in this case was 0.997, therefore it can be taken as fully saturated.

Table 4-31: Degree of saturation

Degree of Saturation	
Equation	$S_r = (W \times G_s)/e$
Description	Degree of Daturation (S_r)
Original sand sample (not sieved)	0.997

Porosity

As calculated previously in Aquifer Parameter the porosity of the Molototsi River sand is generally high, suggesting it is an excellent shallow groundwater aquifer. The value determined is within the recommended range for coarse sand compared to other literature.

Table 4-32: Porosity

Porosity		
Equation	n = e/(1+e)	
Description	Porosity (n)	n (%)
Original sand sample (not sieved)	0.39	39

Air Content

Air content of the saturated sand was minor, suggesting that the sand saturated successfully overnight.

Table 4-33: Air content

Air Content	
Equation	$A = n(1 - S_r)$
Description	Air Content (A)
Original sand sample (not sieved)	0.00117

Saturated Density

For a fully saturated sand, where $S_r = 1$, were calculated to be 2062 kg/m^3 which corresponds to a saturated unit weight (Y_{sat}) of 20.67 kN/m^3. The value of 20.67 kN/m^3 was rounded to the nearest digit which is equal to 21 kN/m^3. This value was used for the design calculations.

Table 4-34: Saturated density

Saturated Density	
Equation	$P_{sat} = (G_s + (S_r \times e))/(1 + e)$
Description	Saturated Density (P_{sat}) (kg/m^3)
Original sand sample (not sieved)	2062

Buoyant Unit Weight

The buoyant unit weight of the sand is expressed as the saturated unit weight minus the unit weight of water.

Table 4-35: Buoyant unit weight

Buoyant Unit Weight	
Equation	$Y_{sub} = Y' = Y_{sat} - Y_w = (P_{sat} \times g) - (P_w \times g)$
Description	Buoyant Unit Weight (Y_{sub}) (kN/m^3)
Original sand sample (not sieved)	10.62

Shear Strength

As seen in the results below (Figure 4-33), the characteristics of dry and saturated sands are the same. The cohesion (c') of sand is zero. In the case for design purposes the cohesion (c') is generally taken as zero. This is to allow for a factor of safety. The density of the saturated sand was 1942 kg/m^3. The angles of shear resistance (Ø') for both tests were particularly very high, showing angles of 51.7 - 53°, compared to literature ranges of 27 to 48°.

Note: Obtaining undisturbed samples of sand for laboratory testing was not possible; however, these loose unconsolidated sands were reconstituted in the apparatus at realistic and appropriate densities to coincide with the in-situ structure of the riverbed.

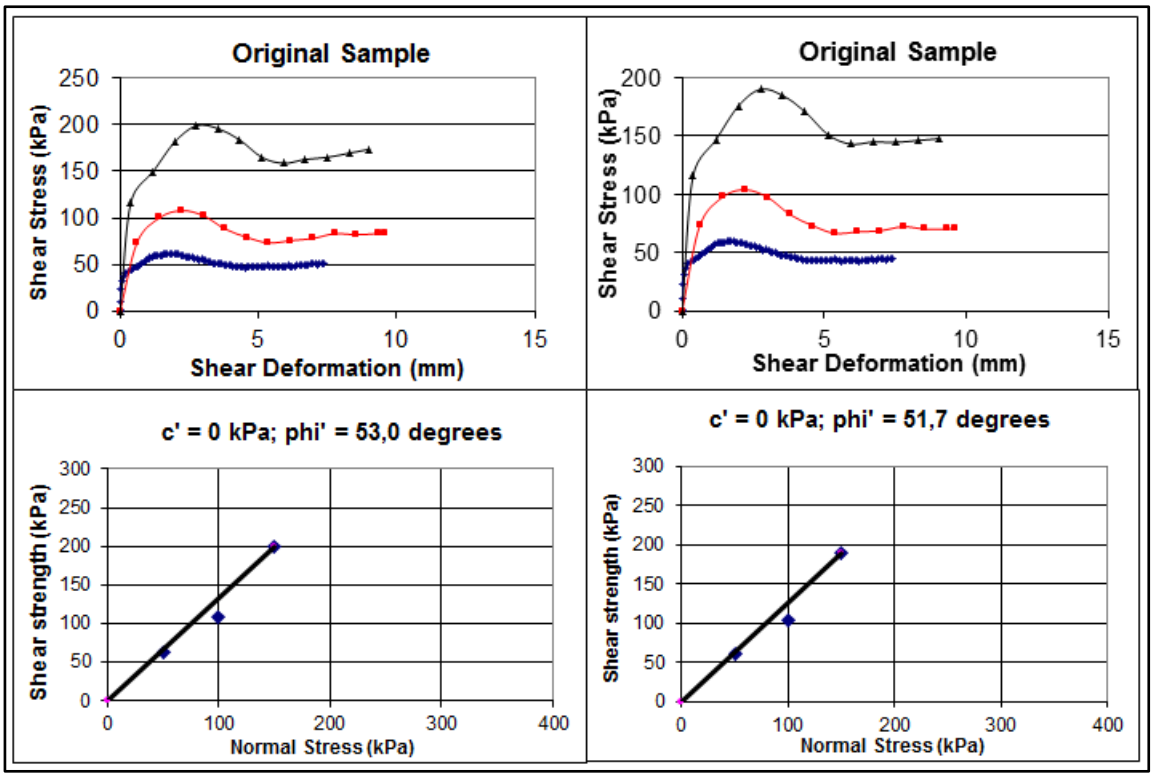

Figure 4-33: Shear box test results conducted to determine the cohesion and shear resistance.

4.6 Subsurface Dam Design

In order to design a subsurface dam, all the measures from the previous sections will be taken into consideration. The first step in design is to determine what type of embankment is the most suitable. For this project a gravity wall would be a robust structure given the severe peak flow events in the Molototsi River. The most economic gravity walls are reinforced concrete cantilevers because the backfill itself, acts on the base, and is designed to provide most of the required dead weight. The second step is to determine if the design is satisfactory. The following sections cover the design of the subsurface dam wall.

4.6.1 Geotechnical Design

To determine the dam height, it is important to consider the peak floods as the water level after construction should remain within the banks. The proposed wall of 3 m for the subsurface dam would predominantly be below surface at a depth of 2 m; only extending the riverbed by 1 m. The 1 m cantilever was therefore modelled in Hec-Ras, simulating the various peak floods. The results show that the wall has little to no effect on the flow as the peak water levels (determined in the Flood Model) extended well above the wall. The idea behind the exposed wall is to increase the sand bed height which would greatly increase the extractable groundwater reserve volume by 6 440 m^3. Although the water level can reach heights of 6 m during flooding which could allow for designing a wall of 2 m or higher, it is recommended by the author to systematically extend the wall after a couple of seasons to minimize the risk of damage to the structure. Nilsson (1988) also suggests constructing these dams in stages. A rapid extent would result in less water to reach the lower Molototsi and cause environmental problems. Thus, the height of 1 m was deemed adequate.

The design of the concrete cantilever wall is combined with counterforts to make the design more suitable for withstanding flow forces. The proposed design is shown in Figure 4-34 below. Generally, for a subsurface dam the sand depth on both the active and passive sides of the wall is at the same height. To design for the worst case scenario, the sand level in front of the wall was made 0 m, therefore making allowance for the possibility of future riverbed erosion. Although it is evident that the water table on the active side would fluctuate from season to season as discussed in the Hydrological section, the sand and water levels behind the wall should represent the most unfavourable conditions in practice, therefore, a fully saturated sand of 3 m is used. The unit weight of the medium to coarse sand backfill is 21 kN/m^3 and is inclined at <1 ° angle. A minimum surcharge pressure of 10 kN/m^2 is assumed to act on the riverbed sand behind the wall. The characteristic values of the shear strength parameters for the backfill are c' = 0 and Ø = 53 ° as determined in the Geotechnical section. The angle of friction between the base and the foundation rock mass is 35 ° which is used for granite bases. The unit weight of the concrete is taken as 23.5 kN/m^3. Given all the above parameters, the satisfactory of the wall design will be determined according to a) the traditional approach and b) the limit state (EC7) approach.

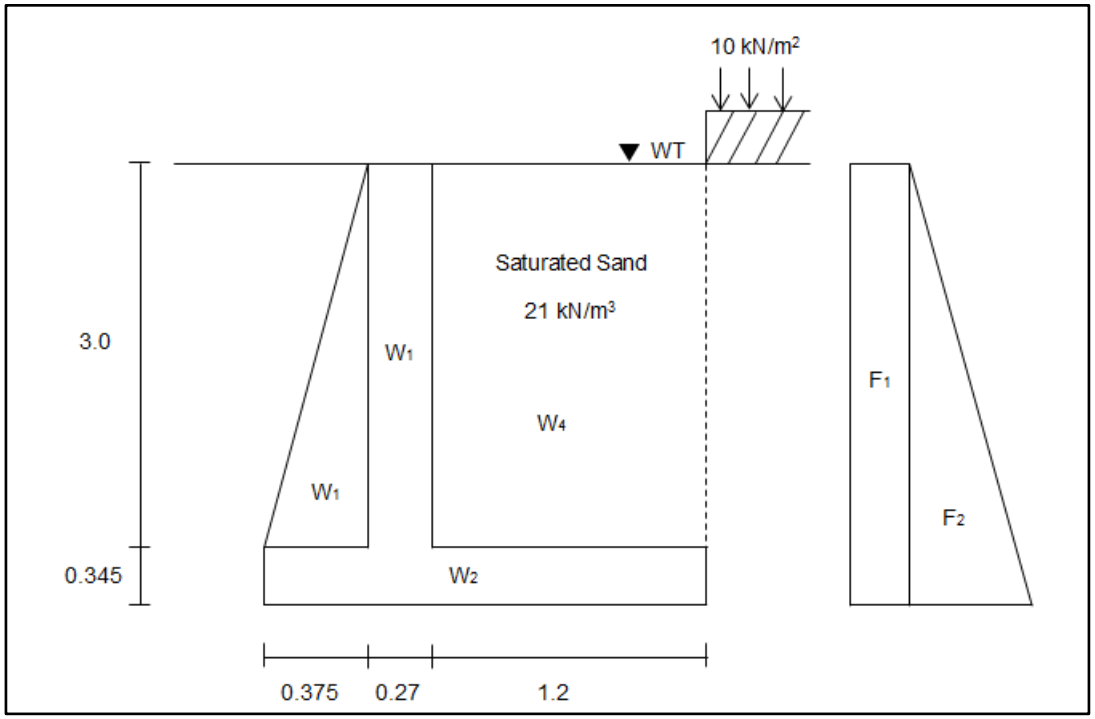

Figure 4-34: A cross sectional side view of the subsurface dam wall. All measurements are in meters (m) with a surcharge pressure of 10 kN/m^2 acting on the backfill behind the wall. F1-2 represents the horizontal overturning force and W1-4 are the vertical resisting force acting on the base. The saturated sand has a saturated unit weight of 21 kN/m^3 which was estimated in the Soil Parameters section above.

Traditional Approach

Firstly, all the forces on the wall are determined, from which the horizontal and vertical components of the resultant force (R) acting on the wall are obtained which can be seen in Table 4-36 below.

Table 4-36: Resulting forces that act on the retaining wall according to the traditional approach.

Overturning (Horizontal)					
Description	Force (kN)		Arm (m)	Moment (kN m)	
F_1 (surcharge)	0.11 x 10 x 3.345	= 3.3795	1.6725	5.6500	
F_2 (saturated sand backfill)	0.5 x 0.11 x 21 x (3.3795)^2	= 12.9233	1.1150	14.410	
	Total H	= 16.30		Total M_H	20.06
Resisting (Vertical)					
W_1 (stem)	3 x 0.27 x 23.5	= 19.0350	0.5100	9.7100	
W_2 (base)	0.345 x 1.845 x 23.5	= 14.9583	0.9225	13.799	
W_3 (counterfort)	0.5 x 0.375 x 3 x 23.5	= 13.2188	0.2500	3.3050	
W_4 (saturated sand backfill)	3 x 1.2 x 21	= 75.6000	1.2450	94.122	
	Total V	= 122.81		Total M_V	120.94
				∑ M	100.88

Thereafter, Rankine's K_a value needs to be calculated as no shear stresses (δ) act on the virtual wall surface, where Ø' = 53 ° and δ = 0, K_a = 0.11.

$$K_a = \frac{1 - sin\emptyset}{1 + sin\emptyset} = 0.11$$

Referring to the calculations shown in Table 4-36. The lever arm of base resultant is given by

$$\frac{\sum \mathrm{M}}{V} = \frac{100.88}{122.81} = 0.82$$

The eccentricity of the base reaction is,

$$e = Arm_{base} - \frac{\sum M}{V} = 0.9225 - 0.82 = 0.102 \quad < 0.31$$

The eccentricity do not exceed $\frac{1}{6}B$, where B is the base width, therefore the resultant acts within the middle third rule.

5) The factor of safety against overturning of the wall is,

$$\text{Overturning FOS} = \frac{M_V}{M_H} = \frac{120.94}{20.06} = 6.03 \quad > 1.5 \;\; OK$$

6) The factor of safety against sliding is given by

$$\text{Sliding FOS} = \frac{V\ tan\ \delta}{H} = \frac{122.81\ tan\ 35\ °}{16.30} = 5.28 \quad > 1.5 \;\; OK$$

Where, the friction angle between the base and foundation is δ = 35 °.

7) The maximum and minimum base pressures are given by

$$\mathrm{p} = \frac{V}{B}\left(1 \pm \frac{6\ e}{B}\right)$$

$$= \frac{122.81}{1.845}\left(1 \pm \frac{6\ (0.11)}{1.845}\right)$$

$$= 88.64 \quad or \quad 44.48$$

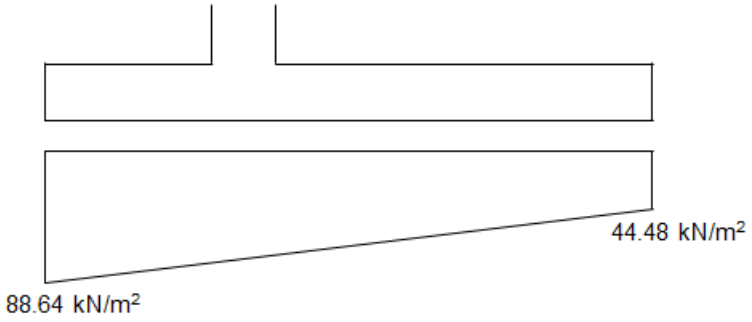

Figure 4-35: Minimum and maximum base pressure of the traditional approach calculation.

The Pmax = 88.64 kN/m^2 at the toe of the wall, which is < 120 kN/m^2, therefore OK and

Pmin = 44.48 kN/m^2 at the heel.

The design of the wall is satisfactory.

Ultimate Limit State Approach

The limit state approach is based on Eurocode 7 (EC7) where partial factors are applied to actions and soil properties to ensure that all requirements are satisfied under conceivable circumstances. For the geotechnical design of retaining structures, Case C in the EC7 is primarily concerned with

uncertainties in soil properties. The partial factor recommend for cantilevers is 1.30 due to the variable unfavourable actions of surface surcharge loading. For favourable actions the partial factor is 1.00. The design value of Ø' = tan-1 (tan 53 °/1.25) = 46.7 ° from which K_a is calculated,

$$K_a = \frac{1 - sin\emptyset}{1 + sin\emptyset} = 0.16$$

As mentioned, Case C is relevant to this structure, therefore a partial factor of 1.30 is applied to force one (F1), as the surcharge pressure being a variable unfavourable action. The rest of the forces are favourable. The total V and Total Mv remains the same.

Table 4-37: Resulting forces that act on the retaining wall according to the limit state approach.

Overturning (Horizontal)					
Description	Force (kN)		Arm (m)	Moment (kN m)	
F_1 (surcharge)	0.16 x 10 x 3.345 x 1.30	= 6.9576	1.6725	11.637	
F_2 (saturated sand backfill)	0.5 x 0.16 x 21 x $(3.3795)^2$	= 19.187	1.1150	21.394	
	Total H	= 26.14		Total M_H	33.03
Resisting (Vertical)					
	Total V	= 122.81		Total M_V	120.94
				∑ M	87.91

Referring to the calculations shown in Table 4-37 above. The lever arm of base resultant is given by

$$\frac{\sum \mathrm{M}}{V} = \frac{87.91}{122.81} = 0.72$$

The eccentricity of the base reaction is,

$$e = Arm_{base} - \frac{\sum M}{V} = 0.9225 - 0.72 = 0.20 \quad < 0.31$$

The eccentricity do not exceed $\frac{1}{6}B$, where B is the base width, therefore the resultant acts within the middle third rule.

1) The factor of safety against overturning of the wall is,

$$\text{Overturning FOS} = \frac{M_V}{M_H} = \frac{120.94}{33.03} = 3.66 \quad > 1.5 \;\; OK$$

2) The design value of δ is factored, 0.75 x 46.7 ° = 35 °. The factor of safety against sliding can now be calculated,

$$\text{Sliding FOS} = \frac{V\ tan\ \delta}{H} = \frac{122.81\ tan\ 35\ °}{26.14} = 3.28 \quad > 1.5 \;\; OK$$

3) The maximum and minimum base pressures are given by

$$\mathrm{p} = \frac{V}{B}\left(1 \pm \frac{6\,e}{B}\right)$$

$$= \frac{122.81}{1.845}\left(1 \pm \frac{6\,(0.2)}{1.845}\right)$$

$$= 109.86 \quad or \quad 23.27$$

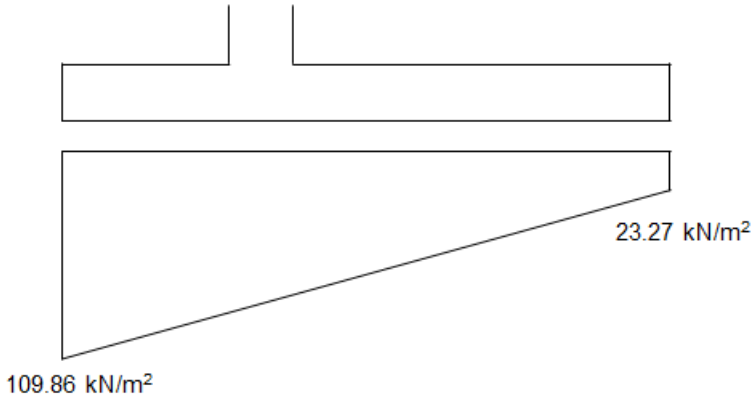

Figure 4-36: Minimum and maximum base pressure of the limit state approach.

The Pmax = 109.86 kN/m² at the toe of the wall, which is < 120 kN/m², therefore OK and

Pmin = 23.27 kN/m² at the heel.

The design of the wall is satisfactory.

Bearing capacity

The subsurface retaining structure will presumably be founded on an irregular hard rock surface consisting of granite and dolerite with possible founding through in-situ soils on the banks. As the foundation of the cantilever wall would predominantly be on hard rock the bearing capacity would be in the recommended MPa range. The applied bearing capacity of the structure acting on the rock would thus apply a much smaller bearing capacity. The hard rock is more than sufficient to withstand the load of the structure, therefore the assumption can be made that the subsurface dam would be stable and anchored to the ground.

Seepage

The natural flow in the riverbed channel would represent a uniform water table level which is roughly parallel to the surface, and constructing a subsurface wall in the riverbed will create a groundwater divide of the flow in the channel. The shallow groundwater level will rise on the upstream side of the wall, thereby increasing the pressure, until it reaches the crest where it is released as overflow. The shallow groundwater would most definitely seep through the fractured rock below the sand layer and within the banks, ending up on the downstream side of the wall. The probable effect on the groundwater divide on the shallow groundwater flow is shown below.

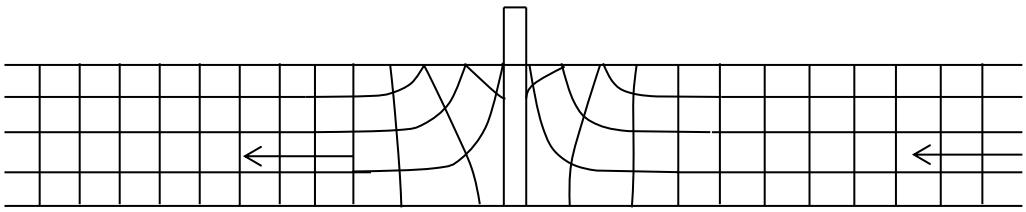

Figure 4-37: Effect of the groundwater divide on the flow.

4.6.2 Design Plans

The following design plans are included, namely a Cross sectional view, plan view, and a visual layout. The wall is 70 m in length across the riverbed with flanks of 7 m entering the banks. The plan view also shows the area reno-mattresses are advised to protect the bank from future erosion.

Cross Sectional View

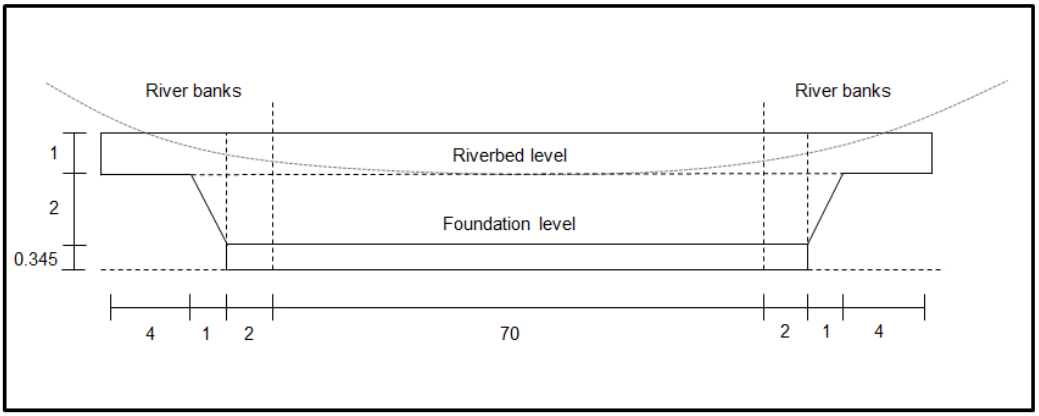

Figure 4-38: Cross sectional view looking downstream.

Plan View

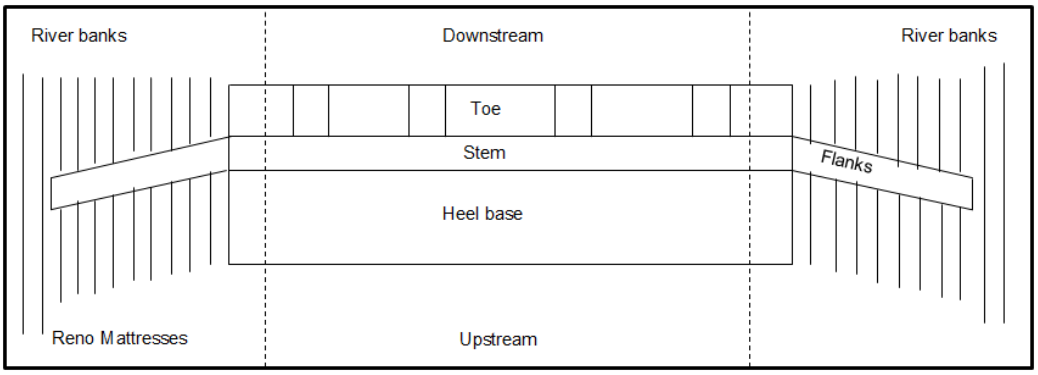

Figure 4-39: Plan view of the cantilever wall with counterforts or buttresses on the toe side. The downstream side is at the top of the illustration. Reno-mattresses are presented on the banks.

Visual Layout

Figure 4-40: Visual layout of how the surface water (shown in blue) would dam up behind the 1 m exposed wall. Reno-mattress are shown in orange around the flanks. Coordinates: latitude -23.568542°, Longitude 30.823947°.

5 Discussion

A summary of the results is discussed in this section with specific focus on the feasibility of subsurface dams.

5.1 Sustainability of Subsurface Dams

The Molototsi catchment as mentioned before is a semi-arid region, which experiences short and intense rainfall events, often resulting in flash floods. The Molototosi River generally flows for only 1 to 2 days a year. The estimated rainfall of 477 mm/a would provide recharge of 35 mm/a for the targeted sand aquifer. The boreholes on the Duvadzi research farm did, however, not react to rainfall, only showing recharge of 1.40 mm/a at the site. The percentage that the MAP contributes to the shallow sand aquifer is approximately 7.5 % and only 0.29 % for the deep crystalline aquifer. This indicates little groundwater interflow between the shallow alluvial and the deep crystalline aquifers. While recharge by surface runoff is the dominant process of replenishing the sand aquifer in the summer, the riverbed baseflow of 10 000m^3/a is the only contributor from the upper reaches during the dry winter months.

The estimated average extractable reserves for the natural sand aquifer is approximately 9 660 m^3 with a 26.47 m^3/d abstraction rate for a river reach of 400 m; however, for the lowest sand aquifer level at 1 m, the extractable reserve is approximately 6490 m^3. These volumes and abstraction rates are in conjunction with what was experienced in the field, the shallow groundwater levels decreased significantly to depths of 1.5 m below the riverbed level after 2 to 3 months of pumping. This was only after abstracting 507 m^3 from the riverbed well within 71 days of pumping 15 m^3/d (every second day) which is not near the estimated average extractable reserve. Calculations were therefore made to establish the extent to which a subsurface dam would increase the shallow groundwater volumes for abstraction purposes. A subsurface dam of 3 m was proposed which showed a large increase in capacity, storing 27 300 m^3 of shallow groundwater for a 2.5 m saturated sand with a river reach of 400 m. The determined extractable reserve was 16 100 m^3, which is substantially larger than the natural aquifer. This extractable amount corresponds to a pumping rate of 44.11 m^3/d, which is almost three times the current pumping rate of 15 m^3/d.

In order to test the above mentioned estimates, the abstraction rates were simulated with a groundwater model. The natural aquifer, Scenario 1, was successfully simulated to represent the actual situation of the well running dry on day 72 by pumping for 71 days. The artificial aquifer, Scenario 2 to 7, was therefore compared to Scenario 1. The main outcome obtained from the model was that subsurface dams increases the extractable reserve significantly. The maximum pumping rate of 40 m^3/d (pumping every second day) was deemed sufficient for a time period of 71 days where the well runs dry for the first time on day 66 (1589 hours). The pumping rate of 44.11 m^3/d (irrigating every day) was therefore not sustainable. Pumping 40 m^3/d for every second day would add up to 1400 m^3 per irrigation season of 71 days (20 September to 30 November). Comparing the results of the Molototsi River to literature by De Hamera, D., Owend, Booija, and Hoekstra (2008) shows contradicting storage volumes. The Mnyabezi River in Zimbabwe was also simulated in MODFLOW with an average width of 10 m and a depth 0.9 m. The hydraulic conductivity used for the alluvial aquifer was 69 m/d which is more than double the hydraulic conductivity of 34 m/d estimated for the alluvial aquifer of the Molototsi. The potential water supply ranged from 2,107 m^3 (5.7 months) in a dry year to 3,162 m^3 (8.7 months) in a wet year. This is more than double the extractable volume of 1400 m^3 determined for the Molototsi groundwater model which were performed using a hydraulic conductivity of 14 m/d, a river width of 70 m and a saturated depth of 2.5 m. However, it is not exactly clear for what length the authors modelled the Mnyabezi River. Nevertheless, the direct recharge or rainfall used in the Molototsi River model represents one of the driest years, only receiving 100 mm of rain during 2016/2017. This shows that even during the driest year the sand aquifer could still provide

sustainable volumes. The low rainfall used in the transient Molototsi Model could be the controlling factor responsible for the lower water supply compared to the Mnyabezi Model. The rainfall-runoff model performed by De Hamera, D., Owend, Booija, and Hoekstra (2008) was only calibrated on one rainfall event which could causes large uncertainties in the amount of inflow of the sand storage dam which could explain the higher storage volumes. The water storage capacities from both models are by no means large and is recommended by literature that it should only be used as an additional water resource.

As observed in the field the water level in the riverbed after pumping, recovers after a day through baseflow, however, it is slowly declining. The Molototsi River model supports this which shows that water levels drop from a saturation depth of 2.5 m to 1.0 m after 66 days and remain at that level. However, without pumping the water levels was observed during the driest recorded year, not to exceed 1.0 to 1.2 m in depth. This corresponds closely to the 1 m evaporation line mentioned in the literature by Love, de Hamer, Owen, Booij, & Uhlenbrook (2007). Results from a campaign on the hydrological processes of sand storage dams in Kenya indicated that groundwater levels during the dry season declined slow and more gradual after constructing the dam (Quilis, Hoogmoed, Ertsen, & Foppen, 2009). The literature also showed that groundwater levels increase quickly after precipitation (de Hamera, D., Owend, Booija, & Hoekstra, 2008). This was also observed during the field visits, suggesting that the subsurface dam would fully recover during the wet season after excessive pumping.

Pumping at rate of 40 m^3/d (every second day) showed a cone depression for a river reach of 400 m, indicating that if a second well was built within this distance their depression would overlap and as a result, decrease the extractable amount which is supported by Quilis, Hoogmoed, Ertsen, and Foppen (2009). For this season, no wall structure or abstraction well should be built 400 m up and downstream of the well. To make allowance for interference between two abstraction wells, it is recommend constructing the wells 1 km apart.

Adequate abstraction wells could also be installed to increase the groundwater supply. For example, a caisson well sunk onto the hard rock in the middle of the river with radiating perforated pipes or a system with a pump shaft on the river bank, joined to a central feeding line with cross members and well points. The latter being the most effective and economical. The shallow groundwater can then be pumped to a central abstraction station and diverted to small reservoirs on the surrounding farms, subsequently expanding small holder farming.

5.2 Feasibility of Subsurface Dams

In terms of the pre-feasibility stage the proposed subsurface dam is recognized as an artificial recharge scheme. The Hydrogeological section discusses the ability of the aquifer to infiltrate and retain water which was deemed an excellent aquifer. The extractable reserves and the advised abstraction rates were quantified in this study along with the methods of abstraction. Monitoring of the water levels and water quality test were also conducted and considered fit for irrigation and possibly for human consumption. The potential environmental impacts of the subsurface dam were not addressed in this study and would require further research. However, from a scientific and engineering point of view, constructing the subsurface dam would have minor impacts on the environment. The Molototsi River is recharged by large volumes of natural runoff every rainy season; therefore, the dam structure would not affect the lower reaches of the Molototsi. The main purpose of the subsurface dam is to retard water flow to accumulate sand until it reaches the crest of the wall structure, and as a result increasing the storage capacity of shallow groundwater. This artificial water scheme would decrease evaporation losses due to the thicker aquifer and also store water for longer periods without flowing downstream as baseflow. For these reason subsurface dams are considered viable.

The main reason of the feasibility study is to determine whether the subsurface dam is cost effective and sustainable prior to the implementation or construction phase. The proposed design and the necessary engineering issues were discussed in the Geotechnical Investigation and Subsurface Dam Design sections. Although constructing a concrete retaining wall is the most robust over the long run, cheaper methods are available as the natural riverbed already provides sufficient amounts of water. Other methods to use for increasing the extractable reserve are the implementation of geosynthetic sheets, stacked sandbags or bentonite injection. Numerous other methods exist but were not included in this study and further research is needed on the robustness of these methods. The concrete retaining structure is therefore deemed the most suitable structure to withstand the destructible flash floods of the Molototsi River. Below the costs of constructing a subsurface dam is considered.

5.2.1 Cost

The cost of the subsurface sand dam greatly depends on the structure type, which in this case is a reinforced concrete cantilever. Reinforced concrete cantilevers are seen as the most economical gravity wall to construct compared to other gravity walls as the backfill acts directly onto base, and as a result provides most of the required dead weight, stabilizing the structure. The factors that influence the costs are the remoteness and accessibility of the subsurface dam site and the availability of the material in the area. Sand and water is readily available on site, therefore commissioning of a screening plant may be feasible. Hard rock outcrops exist in the area as discussed in the Geotechnical Investigation section. Hard rock can also be excavated for the base and blinding preparation. For this reason, a crusher plant should be considered, as aggregate transport could be costly. The bill of quantities does not make allowance for labour or professional fees, however if the community and/or farm workers along the Molototsi River assist and contribute to the project labour cost could reduce drastically. The following costs involved (in Table 5-1) are determined for the Limpopo area which includes: preparation of the site, materials to construct the wall, and materials needed to strengthen and protect the banks against erosion.

Table 5-1: Bill of quantities for constructing a subsurface dam wall.

Bill of Quantity						
No	**Pay Reference**	**Description**	**Unit**	**Quantity**	**Rate**	**Amount**
	SANS 1200 C	**Site Clearance**				
	8.2.1	Clear and Grub:				
1	8.2.1	Clear site and remove debris and shrubs which will prohibit works, with the strict exclusion of trees larger than 200 mm, which will require to remain in position.	ha	0.06	R 45 000	R 2 700
	SANS 1200 D	**Earth Works**				
	8.3.2	Bulk Earthworks:				
2	8.3.2	Excavate top 2 m thick sand material for retaining wall structure and deposit sand on upstream side of wall	m^3	700	R 80	R 56 000
	8.3.2b	Extra over for:				
3	8.3.2b1	Intermediate Excavation	m^3	7	R 130	R 910
4	8.3.2b2	Hard Rock Excavation	m^3	50	R 520	R 26 000
	SABS 1200 GA	**Concrete**				
	8.2	Formwork:				
5	8.2.1	Formwork to the side of the concrete stem/base	m^2	470	R150	R 70 500
	8.3	Reinforcement:				
6	8.3.1	Mild steel bars 10 mm diameter	t		R 12 000	sum
7	8.3.1	High tensile 12 mm diameter	t		R 12 000	sum
	8.4	Concrete:				
8	8.4.1	15MPa/ 19mm Stone in mass concrete in-situ edge beams to Reno mattress dissipater	m^3	40	R1 250	R 50 000
9	8.41	20 MPa in blinding layer minimum 75mm thick	m^2	140	R 160	R 22 400
10	8.4.1	30 Mpa Reinforced concrete in shaft cap slabs	m^3	75	R1 450	R 108 750
	SANS 1200 DK	**Gabions**				
	8.2.2	Reno Mattress:				
11	8.2.2	Reno mattress on banks with basket size 6000mm long x 2000mm wide x 300mm high to base of channel at the cantilever and banks contact	m^3	30	R 4000	R 120 000
					Total	**R 457 260**

6 Conclusions and Recommendations

Based on the results of this study, the Molototsi catchment is clearly not a water rich area. However sufficient groundwater resources are available and underutilized with specific focus on shallow groundwater. The sand of the Molototsi riverbed is a near ideal aquifer; unfortunately, it is relatively shallow with an average depth of 2 m. According to the geophysics, shallow groundwater depths of approximately 10 m below the riverbed level exists, taking the weathered and fractured rock layer beneath the sand into account. The groundwater flow model determined that a river reach of 400 m contains an annual extractable reserve of approximately 507 m^3 for the natural river. The volume extractable from the sand is by no means large but is sufficient to supply groundwater for irrigating 0.175 ha of crop per season. An alternative to increase the extractable reserve is to construct subsurface dams.

From the foregoing study on subsurface dams, the following conclusions were made:

- The geological investigation and GIS applications proved effective for finding the most favourable subsurface dam sites. The selected site is located 350 m downstream of the Duvadzi farm and is the best possible location to construct the subsurface dam. It consists of all the needed characteristics of a subsurface dam site with hard rock on both sides of the banks.
- Geologically the site has a semi-impermeable layer below the coarse riverbed sands with impermeable crystalline rock at the base, forming this natural river channel. Numerous weathered and fractured dolerite dykes and lineaments are found cross cutting the riverbed which are possible shallow groundwater feeders. These dykes should be targeted for shallow wells.
- The sand aquifer is the main target for this project. However, it is important to remember that the weathered and fractured rock below the sand riverbed was not accounted for. According to the geophysics the riverbed aquifer extends down to 9 m, therefore indicating a weathered and fractured rock aquifer of 6 m below the riverbed. This could contribute significantly to the extractable reserve; however, further studies need to be conducted to support this assumption.
- The hydrological conditions at the site show suitable formations to retain shallow groundwater. The sand aquifer has a high hydraulic conductivity of 34 m/d, porosity of 39 % and an extractability of 23 %, indicating that satisfying yield can be expected. The dominant recharge process of the Molototsi riverbed is the natural runoff during the rainy seasons where baseflow is main contributor during the dry season.
- Constructing a subsurface dam will increase the extractable reserve by 893 m^3 per season as the flow model showed an extractable reserve of 1400 m^3 compared to the extractable reserve of 507 m^3 per season for the natural aquifer. The hydrological model therefore confirms that subsurface dams will significantly increase water availability throughout the dry season.
- Groundwater abstraction could increase 2.67 times more at the Duvadzi farm to irrigate a 0.467 ha crop per season pumping at a rate of 40 m^3/d (irrigating every second day). The extractable reserve could also be subdivided with a quota system to supply groundwater to various farmers in the vicinity. Consequently, growing and improving small holder farming in the Molototsi catchment.
- The main abstraction well should be vertical and at least 2 to 3 m in depth, onto the underlying hard rock. The main well should be connected to horizontal feeder pipes up and down stream of the main abstraction well with cross members in a backbone structure (multiple well point

or wellfield type). This system should be placed at least 1 to 1.5 m below the riverbed. All well points must have perforated sidewalls and at least 8 m deep, penetrating the underlying dykes and fractured rock. The pipe feeders should also be perforated but only on the topside. This method could possibly increase the extractable reserve substantially.

- The minimum distance between abstraction well points is determined to be 800 m as drawdown was effecting the shallow groundwater level in the model by a distance of 400 m up and down stream of the abstraction point. To avoid interference between two adjoining abstraction wells during pumping it is concluded that abstraction well points should be constructed 1 km apart. This also suggests that the main abstraction well should be constructed 400 m from the subsurface dam wall. All pump stations should be constructed outside of the 1 in 100 floodline.
- From a geotechnical point of view, the proposed 3 m high concrete cantilever wall is designed to withstand the forces of the Molototsi River during peak floods and should not be destructed by the 1 in 100 year flood, therefore considered satisfied and stable. The surface water model show that the Molototsi River experience peak floods above 1000 m^3 for both the 1 in 50 and 1 in 100 year return periods. These flood events will flow well above the exposed 1 m subsurface dam wall. In terms visual impact and practicality, it is recommended that the wall flanks extent 7 m into banks with a stepped structure if not in contact with hard rock. The banks should also be completely covered with reno-matrasses for 10 m up and downstream of the wall. This will protect the banks from future erosion and prolong the life of the structure.
- From the feasibility study the storage capacity and function of the subsurface dam is considered viable and sustainable.
- Although the cost of the cantilever wall structure is approximately R 457 260 (only for material and construction), the economic and social benefits it would have on the surrounding community along with the profits that could be gained from farming crops, possibly justifies the cost. This is supported by a study conducted in Kenya, which indicated that the average income increased by as much as 60 percent for farmers living near these dams (Lasage R., 2008)).
- Constructing a subsurface dam is therefore deemed feasibility and a viable option.

The increasing population and severe droughts of the Limpopo region will trigger water shortages in the near future. Water shortages are not only a reality in the Limpopo region but in the Western Cape as well. For this reason, subsurface dams can be an attractive solution to increase water availability for both human consumption and agricultural purposes. This study along with methodologies proved effective and should guide stakeholders in search of favourable site with the necessary characteristics for preliminary design and commissioning.

The following are recommendations for legal requirements:

- Subsurface dams involve artificial storage and abstraction of water, which forms part of an artificial recharge scheme, therefore requires licensing.
- A valid water use license needs to be obtained for an artificial recharge scheme according to the National Water Act 36 of 1998 (Gazette No. 19182, Notice No. 1091).
- While The National Water Act does not specifically mention that storing water in a sand aquifer requires licensing, this can by assumed as the main function of a subsurface dam is to store water.

- A Basic Assessment (BA) is required for testing the scheme according to the National Environmental Management Act, 1998 (Act No. 107 of 1998), Amendment of the Environmental Impact Assessment Regulations Listing Notice 1 of 2014, however it is advised to consult with an Environmental Assessment Professional first to assure that a BA is triggered.
- An Environmental Impact Assessment (EIA) should be conducted prior to implementing or constructing the subsurface dam according to National Environmental Management Act, 1998 (Act No. 107 of 1998), Amendment of the Environmental Impact Assessment Regulations Listing Notice 2 of 2014.
- The determination if it has an effect on the environment according to the Environmental Conservation Act (No. 73 of 1989).
- Compliance to the National Heritage Resources Act (No.25 of 1999) preserves the heritage of resources for future generations.

Although South Africa's water use licensing and environmental legislation have not been tested with the processing of applications for artificial recharge schemes, both the National Water Act and the National Environmental Management Act provide framework for artificial recharge applications. The necessary applications and authorization steps can be obtained from the Department of Water Affairs.

The following are recommendations for future studies:

- Subsurface dams along with other types of sand storage dams could be researched much further. The findings of this research should be compared with measurements, models and data of other catchments to determine whether these methods are generally applicable.
- Ongoing research for this thesis would involve more accurate and long term data capturing of water levels within the riverbed and banks. This could be done by installing and monitoring numerous piezometers within shallow boreholes along the riverbed and banks. The mentioned method was not conducted due to limited funding.
- Future studies could also include the effect subsurface dams have on groundwater recharge as rivers with primary sand aquifers could be directly connected, interconnected, or completely disconnected to the secondary aquifers below.
- Given the lack of data with regards to shallow groundwater levels of ephemeral rivers across South Africa, provides researchers the opportunity to captured this information. The data should include porosity, specific yield, runoff, and recharge of ephemeral river basins. Having this data available would allow researchers to determine the potential sand storage dam locations, the potential reservoir yield, and abstraction estimates for river basins across South Africa. This will allow stakeholders to accommodate high priority areas with numerous small but dependable water supplies.
- With groundwater modelling and local data captured on potential subsurface or sand storage dam locations could guarantee a successful determination of sustainable water storage dams. When these storage volumes are estimated from the scenarios, the number of water users per dam and the number of dams per community can be determined.
- Maps should be made instantly available that show the 'Potential Sand Storage River Basins' similar to Figure 6-1 below. Figure 6-1 shows the Potential Artificial Recharge Areas' which is also a good indicator map for locating potential sand storage river basins. These zones on the map show susceptible rock formations and sediments for water storage. However, this

assumption made by the author requires further investigation as favourable sediment size may not be available at other locations. The type of sediment strongly determines the hydrological effectiveness of a subsurface or sand storage dam.

- The thesis provides information and clarity to decision-makers for constructing subsurface dams, however, a complete desktop feasibility study could contribute to the investment decision-making phase. This future study could include methodologies such as social-economics, domestic and agricultural demand, priority zones, quick hydrogeological assessment of these zones, reliability of riverbed yields, and costs involved. The results would contribute in planning and implementing of the technology in other regions

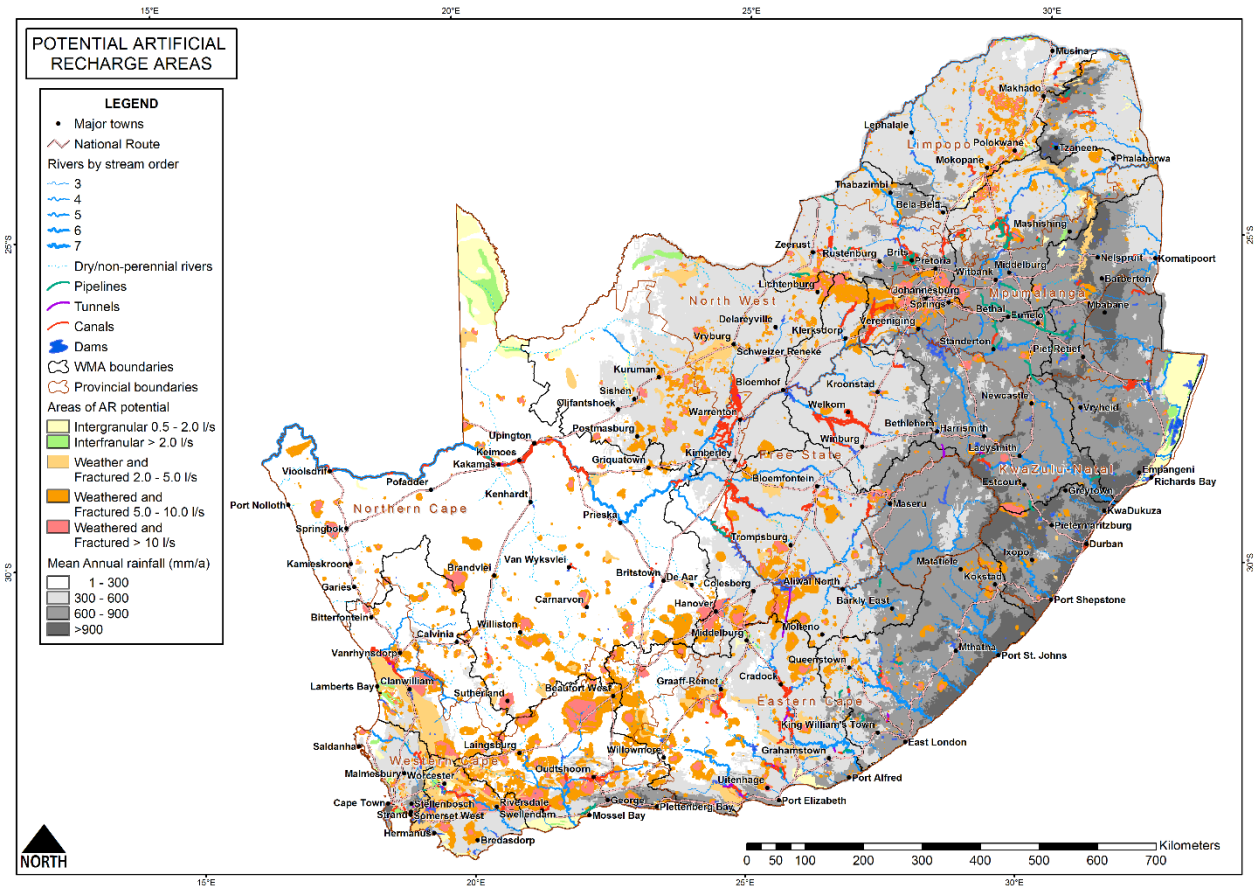

Figure 6-1: The potential artificial recharge areas of South Africa. The map was obtained from the artificial recharge website (Department of Water and Sanitation).

Acknowledgements

The author wishes to express his sincere gratitude to his supervisor Leon Croukamp (Stellenbosch University) and his co-supervisor Dr Nebo Jovanovic (CSIR) for their support and guidance. The author would also like to convey thanks to the CSIR, the Water Research Commission, the Department of Water and Sanitation (Polokwane Office), and the Department of Agriculture and Rural Development for providing the necessary support and data. The Water Research Commission and National Research Foundation are acknowledged for funding the field campaigns. A special thanks to the Duvadzi farmers for making their land available for research purposes. The author would like to acknowledge SRK Consulting (Cape Town Office) for providing me with software and hours of training to model and simulate the data collected in the field. Last but not least I would like to thank my parents and friends for their support and patience throughout the completion of this thesis.

7 References

Adams, S., & Titus, R. a. (2004). Groundwater recharge assessment of basement aquifers of Central Namaqualand. *WRC Report no 1093/1/04. Water Research Commision* .

Adamson, P.T. (1981). *Southern African Storm Rainfall.* Pretoria: Department of Water Affairs and Forestry.

Aerts, J. L. (2007). *Robustness of Sand Storage Dams under Climate Change.* Vadose Zone J., 6, 572–580.

Anhaeusser, C. (1992). *Structures in granitoid gneisses and associated migmatites close to the boundary of the Limpopo Belt, South Africa.* Precambrian Res., 55: 81-92.

Bear, J. (1979). Hydraulics of Groundwater. *McGraw-Hill, New York*, 569p.

Bird, P. B.-A. (2006). *Patterns of Stress and Strain Rate in Southern Africa. .* K.Geophys. Res., 111(B8). B08402.

Borst, L., & de Haas, S. (2006). Hydrology of Sand Storage Dams. A case study in the Kiindu catchment, Kitui District, Kenya. *Master thesis Hydrogeology.*

Brandl, G. a. (1993). *Preliminary results of single zircon studies from various Archaean rocks of the north-eastern Transvaal.* Abstr. 16th Coll. African Geology, Mbabane, Swaziland, (1): 54-56.

Brandl, G. C. (2006). *Archaean Greenstone Belts.* The geology of South Africa. Geological society of South Africa, Johannesburg/Council for Geoscience, Pretoria.

Craig, S. (2004). *Craigs Soil Mechanics 7th Edition.* Department of Civil Engineering, University of Dundee, UK.

de Hamera, W., D., L., Owend, R., Booija, M., & Hoekstra, A. (2008). Potential Water Supply of a Small Rervoir and Alluvial Aquifer System in Southern Zimbabwe. *Department of Water Engineering and Management, University of Twente. Mineral Resources Centre, University of Zimbabwe*.

Du Toit, M. V. (1983). *Some aspects of the geology, structure and metamorphism of the Southern Marginal Zone of the Limpopo metamorphic complex.* Spec. Publ. Geol. Soc. S. Afr., 8, 121-142.

DWA . (2013). *Classification of Water Resources and Determination of the Resource Quality Objectives in the Letaba Catchment. Status Quo Assessment, IUA and Biophysical Node Delineation and Identification.* Prepared by: Rivers for Africa eFlows Consulting.

DWA . (2014). *Classification of Water Resources and Determination of the Resource Quality Objectives in the Letaba Catchment. Resource Quality Objectives.* Prepared by: Rivers for Africa eFlows Consulting.

DWAF. (1996). *South African Water Quality Guidelines.* Pretoria, South Africa: Volumes 1 to 4. Department of Water Affairs and Forestry.

DWAF. (2004). *Luvuvhu/Letaba Water Management Area: Internal Strategic Perspective.* Pretoria, South Africa: Department of Water Affairs and Forestry.

Ertsen, M., & Hut, R. (2009). Two waterfalls do not hear each other. Sand Storage Dams, Science and sustainable development in Kenya. *Physics and Chemistry of the Earth 34 (1-2)*, 14-22.

Gbetibouo, G. ,. (2010). *Vulnerability of the South African farming sector to climate change and variability: an indicator approach.* Natural Resources Forum 34, 175-187.

Gezahenge, W. (1986). *Subsurface dams for rural water supply in arid and semi-arid regions of developing countries.* Department of Civil Engineering, Tampere University of Technology.

Holland, M. (2011). *Hydrological characterization of crystalline basement aquifers within the Limpopo Province, South Africa.* South Africa: PhD thesis, University of Pretoria.

Ishida S, T. T. (2011). *Sustainable use of groundwater with underground dams.* ARQ 45(1), 51–61.

Jamali, I. A. (2016). *Subsurface Dams in Water Resource Management - Methods for Assessment and Location.* PhD thesis, Engineering Geology and Geophysics, Royal Institute of Technology.

Jones, C. (2004). *Dynamic Cone Penetrometer tests and analysis.* Department of International Development.

Jones, M. (1985). The weathering zone aquifers of the basement complex area of Africa. *Journal of Engineering Geology, 18*, 35-46.

Kinzelbach, W., Aeschbach, W., Alberich, C., Goni, I., Beyerle, U., Brunner, P., . . . and Zoellmann, K. (2002). A survey of methods for groundwater recharge in arid and semi-arid regions. *Early warning and Assessment Report Series. UNEP/DEWA/RS. United Nations Environment Programme, Nairobe, Kenya*.

Kramers, J. K. (2001). *Crustal heat production and style of metamorphism: a comparison between two Archaean high-grade provinces in the Limpopo Belt, southern Africa.* Precambrian Res., 112,149-163.

Kramers, J. M. (2006). *The geology of South Africa.* Geological Society of South Africa, Johannesburg/Council for Geoscience, Pretoria, 209-236.

Kroner, A. J. (2000). *Single zircon ages for felsic to intermediate rocks from the Pietersburg and Giyani greenstone belts and bordering granitoid orthogneisses, northern Kaapvaal Craton, South Africa.* J. Afr. Earth Sci., 30, 773-793.

Lasage R., A. J. (2008). *Potential for community based adaptation to droughts: Sand Dams in Kitui, Kenya.* Phys Chem Earth 33(1–2), 67–73.

Lasage, R. a. (2011). *Impact of sand dams and climate change on modelled discharge. Dawa river basin, Ethiopia.* IVM Institute for Environmental Studies, VU University, Amsterdam, The Netherlands.

Lasage, R. A. (2013). *The role of small scale sand dams in securing water supply.* Mitig Adapt Strateg Glob Change.

Love, D., de Hamer, W., Owen, R., Booij, M., & Uhlenbrook, S. (2007). Case Studies of Groundwater – Surface Water Interactions and Scale Relationships in Small Alluvial Aquifers. *Department of Water Engineering and Management, University of Twente. Mineral Resources Centre, University of Zimbabwe. Delft University of Technology, Department of Water Resources*.

Lynch, S. (2003). *The Development of Raster Database of Annual, Monthly, and Daily Rainfall for Southern Africa.* Water Research Commission.

Masvopo, T. (2008). Evaluation of the Groundwater Potential of the Malala Alluvial Aquifer, Lower Mzingwane River, Zimbabwe. *Masters Degree. Department of Civil Engineering. University of Zimbabwe*.

McCourt, S. a. (1992). *Structural geology and tectonic setting of the Sutherland greenstone belt, kaapvaal Craton, South Africa .* Precambrian Res., 55, 93-110.

Neal, I. (2012). *The potential of sand dam road crossing.* Dams and Reservoirs, 22 (3 and 4), 129-143.

Nilsson, A. (1988). *Groundwater dams for small-scale water supply.* Intermediate Technology Publications Limited, London 69.

Petzer, K. (2009). *Structural geological controls on the flow and occurrence of groundwater in the basement lithologies of the Limpopo Province, South Africa .* Unpublished M.Sc Dissertation, University of Pretoria, South Africa.

PSD. (2005). *Partners for Sustainable Development.* Rainwater Partnership.

Quilis, R., Hoogmoed, M., Ertsen, M., & Foppen, J. (2009). Measuring and Modeling Hydrological Processes of Sand Storage Dams on Different Spatial Scales. *Physics and Chemistry of the Earth 34*, 289–298.

RAIN. (2007). *A practical guide to sand dam implementation.* Amsterdam, The Netherlands: RAIN.

Robb, L. J. (2006). *Archaean Granitoid Intrusions.* The geology of South AfricaGeological Society of South Africa, Johannesburg.

SACS. (1980). *Statigraphy of South Africa.* South African Committee for Stratigraphy. Lithostratigraphy of the Republic of South Africa.

Stettler, E., & de Beer, J. a. (1989). Crustal domains in the northern Kaapvaal as defined by magnetic lineaments. *Precambrian Res, 45*, 263-276.

Uken, R. a. (1997). *An interpretation of mafic dyke swarms and their relationship with major mafic magmatic events on the Kaapvaal Craton and Limpopo Belt. .* S. Afr. J. Geol., 100(4): 341-348.

Van Heerden, P. C. (2009). *Integrating and updating of SAPWAT and PLANWAT to create a powerful and user-friendly irrigation planning tool .* WRC.

Van Reenen, D. R. (1990). *The granulite facies rocks of the Limpopo Belt southern Africa.* Granulite and Crustal Evolution. Kluwer, Dordrecht, 257-289.

van Vuuren, van Dijk, and Smithers. (2013). *SANRAL Drainage Manual 6th Edition.* The South African National.

Vorster, C. (1979). *Die geologie van Klein-Letaba gebied, noordoos-Transvaal met spesiale verwysing na die granitiese gesteentes .* M.Sc. thesis (unpubl.), Rand Afrikaans Univ., Johannesburg, 138 pp.

Wipplinger, O. (1953). *Storage of Water in Sand. An Investigation of the Properties of Natural and Artificial Sand Reservoirs and of methods of developing asuch Reservior.* Stellenbosch University.

Wood, W. (1999). Use and misuse of chloride mass balance method in estimating groundwater recharge. *Groundwater, 37*, 2-3.

Xu, Y. a. (2003). Groundwater recharge estimation in South Africa. *UNESCO*.

Appendices

Appendix A: Geophysical survey of targeted boreholes on the Duvadzi farm.

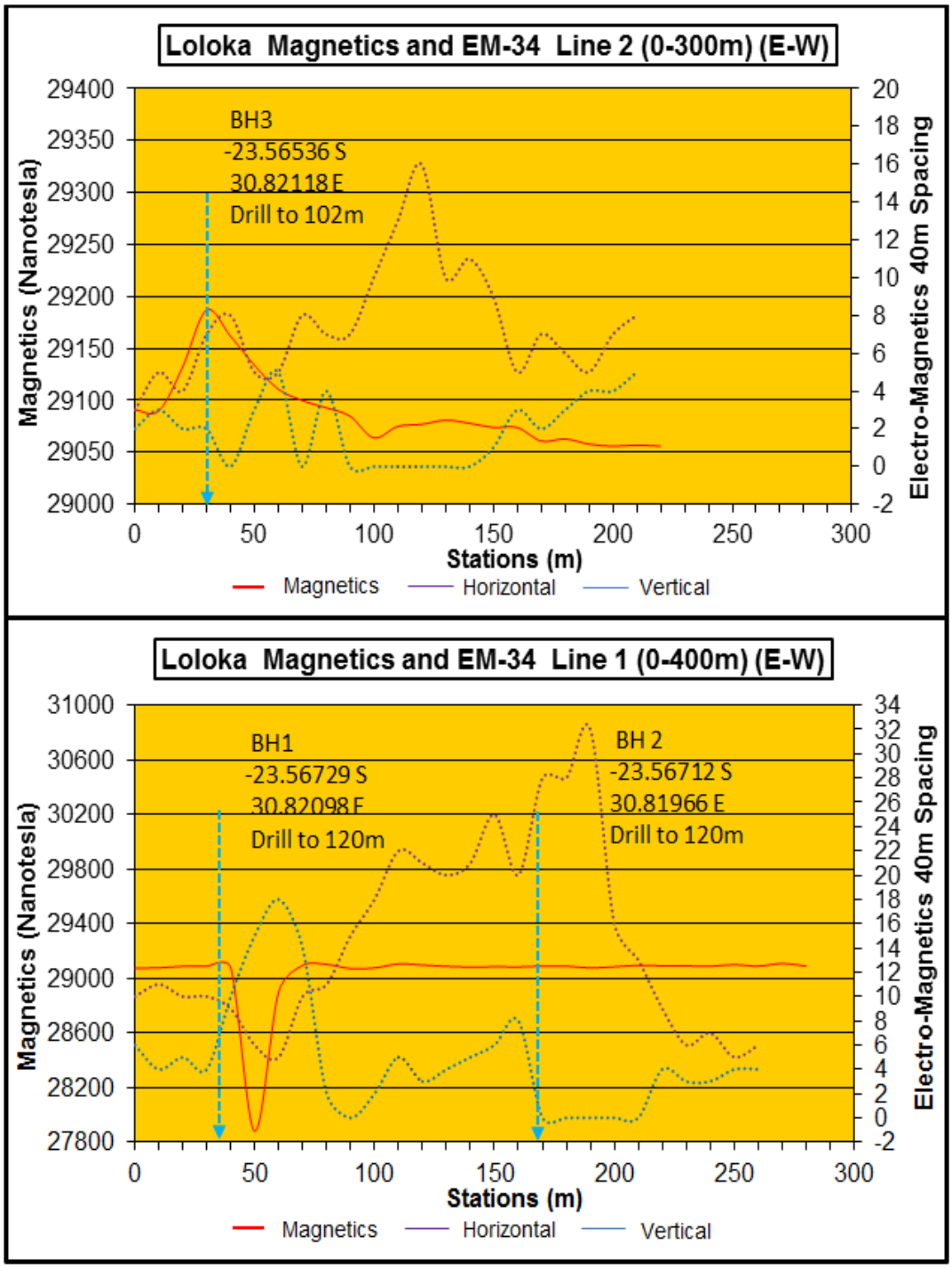

Figure 7-1: Results of the magnetic and electro-magnetic measurements for Duvadzi farm. The recommended drill positions for targeting groundwater are shown on the graphs as blue vertical dash lines.

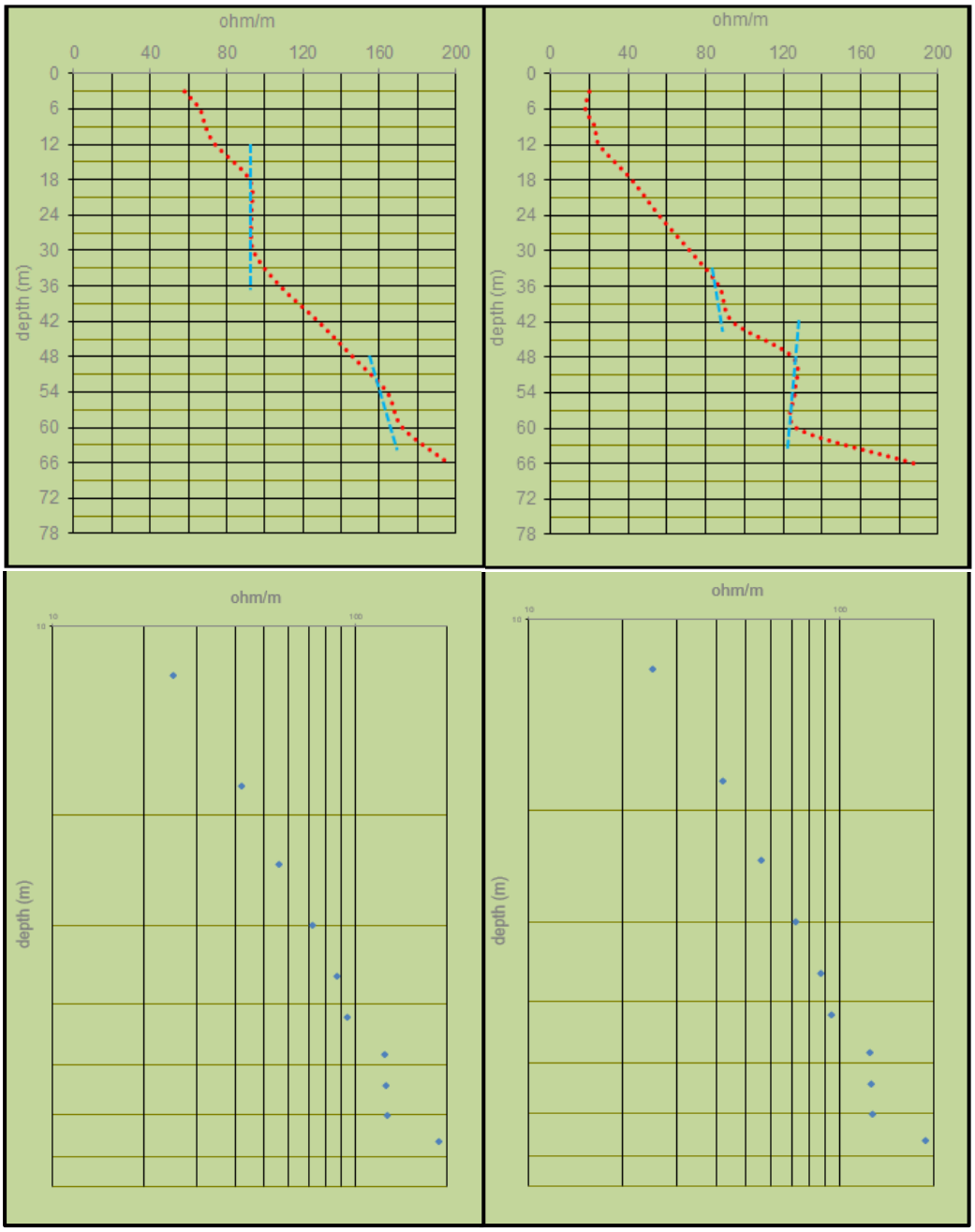

Figure 7-2: Results of the resistivity measurements for Duvadzi farm are shown here. The top two are showing weathered and fractured zones (major anomalies) which were used as the recommended drilling positions. The bottom two graphs are representative of the top two plotted on a log-log graph. The left graphs represent the results of BH1 (H14-1701). The right graphs represent the results of BH2 (H14-1702) and BH3 (H14-1703) as it was drilled on the same profile.

Appendix B: DCP Results

Table 7-1: DCP results showing the consistency in mm/blow.

Blows	Penetration Depth in [mm]					
	Test 1	Test 2	Test 3	Test 4	Test 5	Test 6
0	230	140	150	200	1240	1570
1	335	200	200	290	1290	1630
2	460	270	230	340	1340	1680
3	530	330	265	395	1370	1720
4	570	420	295	445	1400	1760
5	590	500	345	490	1430	1800
6	605	560	390	530	1460	1840
7	620	590	430	565	1490	1870
8	630	630	465	595	1515	1880
9	645	640	490	615	1540	1905
10	660	675	520	620	1560	1920
11	670	700	555	630	1580	1940
12	680	720	575	635	1600	1955
13	690	730	595	650	1640	1970
14	700	750	615	670	1660	1980
15	715	780	640	690	1690	1985
16	725	795	650	700	1700	1990
17	735	815	665	715	1760	1990
18	750	845	690	730	1835	
19	770	880	710	740	1890	
20	785	915	710	750	1900	
21	800	945	735	760	1910	
22	820	970	750	770	1920	
23	840	990	780	775	1930	
24	860	1010	805	780	1940	
25	870	1025	835	790		
26	880	1040	870	800		
27	895	1065	895	805		
28	935		935	810		
29	970		1070	820		
30	995			825		
31	1020			830		
32	1050			840		
33	1070			855		
34				870		
35				880		
36				895		
37				905		
38				910		
39				920		
40				925		
41				930		
42				930		
43				940		
44				945		

Appendix C: Hydrological Determinations

Standard Design Flood Method							
Description of catchment							
River detail							
Calculated by					Date		
Physical characteristics							
Size of catchment (A)	855.02	km2					
Longest watercourse (L)	72.64	km	Time of concentration (Tc)			19.08	hours
Average slope (Sav)	0.0022	m/m					
SDF basin	5		Time of concentration, t			1144.85	min
2-year return period rainfall (M)	78	mm	Days of thunder per year (R)			10	days/years
TR 102 n-day rainfall data							
Water service station	Leydsdorp		Mean Annual Precipitation (MAP)			620	mm
Weather Service Station no.	680059		Coordinates	Lat: 23°59' & Lon: 30°22'			
Duration (days)	**Return period (years)**						
	2	**5**	**10**	**20**	**50**	**100**	**200**
1 day	78	116	146	181	233	279	331
2 day	99	156	203	257	241	416	503
3 day	105	165	215	271	358	434	524
7 day	135	225	301	389	528	653	798
Rainfall							
Return period (years), T	**2**	**5**	**10**	**20**	**50**	**100**	**200**
Point precipitation depth (mm), Pt,T	43.73	73.77	96.49	119.22	149.26	171.98	194.71
Linear Interpolation (LI) of Pt,T	68.89	98.93	121.65	144.38	174.42	197.14	219.87
Area reduction factor (%), ARF	88.08	88.08	88.08	88.08	88.08	88.08	88.08
Average intensity (mm/hour), IT	2.02	3.41	4.45	5.50	6.89	7.94	8.99
Average intensity (mm/hour), IT using LI	3.18	4.57	5.62	6.67	8.05	9.10	10.15
Runoff Coefficients							
Calibration factors	C2 (2 year return period) (%)		15	C100 (100 year return period) (%)			70
Return period (years)	**2**	**5**	**10**	**20**	**50**	**100**	**200**
Return period factors (YT)	0	0.84	1.28	1.64	2.05	2.33	2.58
Runoff coefficient (CT)	0.15	0.348	0.452	0.537	0.634	0.7	0.759
Peak flow (Q) (m3/s)	71.92	281.46	478.20	701.92	1037.54	1319.95	1620.32
Peak flow (Q) (m3/s) using LI	113.30	377.47	602.87	850.07	1212.44	1513.03	1829.71

Figure 7-3: Flood peak calculations done in excel using the Standard design Flood Method (van Vuuren, van Dijk, and Smithers, 2013).

Basin number	Station number	Name	Latitude	Longitude	Years of record	Mean annual rainfall (mm)	Duration (days)	Minimum annual recorded	Maximum annual recorded	Maxima for return periods (years for the duration) (mm)					
										2	5	10	20	50	100	200
1	546204	STRUAN	25°24'	26°07'	48	549	1	23	111	56	80	99	119	150	177	206
							2	32	155	71	105	132	161	205	243	286
							3	42	216	80	117	146	177	224	263	308
							7	42	284	102	154	196	242	310	369	435
2	675125	AUTORITEIT	23°35'	28°05'	45	452	1	24	178	62	93	117	145	187	223	264
							2	32	216	74	111	140	173	222	265	313
							3	32	254	80	122	156	193	250	300	355
							7	37	254	94	144	183	225	289	344	405
3	766324	SILOAM	22°54'	30°11'	46	472	1	25	188	64	95	119	146	187	222	262
							2	32	268	76	112	142	174	221	263	309
							3	33	329	84	129	165	205	266	319	378
							7	36	381	103	165	215	271	356	432	517
4	553351	WATERVAL	25°21'	29°42'	51	627	1	36	100	58	76	89	102	122	138	155
							2	40	140	69	90	106	123	146	165	185
							3	45	140	76	99	115	132	156	175	195
							7	53	184	98	131	154	178	211	238	266
5	680059	LEYDSDORP	23°59'	30°22'	45	625	1	23	195	78	116	146	181	233	279	331
							2	23	330	99	156	203	257	341	416	503
							3	27	357	105	165	215	271	358	435	524
							7	27	377	135	225	301	389	528	653	798
6	369030	SYLVAN	28°08'	29°01'	44	668	1	37	92	51	65	74	84	97	108	120
							2	42	115	64	85	99	113	133	149	166
							3	42	134	74	98	116	134	160	181	204
							7	50	145	92	121	142	164	193	217	242
7	328726	OLIVINE	28°06'	26°55'	45	507	1	22	103	49	68	82	96	118	137	157
							2	25	110	62	87	107	128	158	184	213
							3	34	119	68	94	115	136	167	193	221
							7	39	150	84	118	144	172	211	243	279
8	322071	DANIELSKUIL	28°11'	23°33'	61	377	1	11	116	47	69	86	104	132	156	183
							2	21	156	60	91	116	144	187	224	267
							3	21	186	65	100	128	160	208	250	297
							7	22	245	79	126	164	207	272	329	393
9	258458	JACOBSDAL	29°08'	24°46'	86	376	1	16	99	43	61	75	91	114	133	155
							2	20	141	54	78	98	119	151	179	210
							3	20	181	59	87	109	134	171	203	238
							7	27	239	70	104	131	160	203	240	280

Figure 7-4: Daily rainfall from TR102 obtained from the SANRAL Drainage manual **(van Vuuren, van Dijk, and Smithers, 2013)**.

Basin	SAWS station number	SAWS site	M (mm)	R (days)	C_2 (%)	C_{100} (%)	MAP (mm)	MAE (mm)
1	546 204	Struan	56	30	10	40	550	1800
2	675 125	Autoriteit	62	44	5	30	450	1900
3	760 324	Siloam	64	28	5	40	470	1700
4	553 351	Waterval	58	20	10	50	630	1600
5	680 059	Leydsdorp	78	10	15	70	620	1700
6	369 030	Siloam	51	54	15	60	670	1500
7	328 726	Olivine	49	39	15	60	510	1700
8	322 071	Danielskuil	47	39	5	20	380	2100
9	258 452	Jacobsdal	43	47	15	60	380	1800
10	233 049	Wonderboom	54	55	10	50	560	1600
11	236 521	Mashai	39	66	40	80	430	1400
12	143 258	Scheurfontein	39	52	5	30	290	2100
13	284 361	Wilgenhoutsdrif	40	55	5	15	70	2600
14	110 385	Middelpos	25	13	10	30	140	2400
15	157 874	Garies	22	11	5	20	130	2100
16	160 807	Loeriesfontein	28	11	10	40	210	1900
17	84 558	Elandspoort	45	1	40	80	500	1500
18	22 113	La Motte	59	4	30	60	810	1400
19	69 483	Letjiesbos	34	16	10	35	160	2200
20	34 762	Uitenhage	53	12	15	60	480	1600
21	76 884	Albertvale	45	23	10	35	460	1700
22	80 569	Umzoniana	84	26	15	60	820	1200
23	180 439	Insizwa	60	45	10	80	890	1200
24	240 269	Newlands	76	15	15	80	910	1200
25	239 138	Whitson	55	9	10	80	830	1200
26	336 283	Nqutu	61	17	15	50	760	1500
27	339 415	Hill Farm	85	17	30	80	890	1400
28	483 193	Maliba Ranch	75	54	15	60	740	1400
29	556 088	Mayfern	66	11	15	50	740	1600

Figure 7-5: Regional catchment values obtained from the SANRAL Drainage Manual **(van Vuuren, van Dijk, and Smithers, 2013)**.

Appendix D: Sieve analysis

Table 7-2: Summary of the sieve analysis

SOIL TYPE	GRAIN SIZE (mm)	% SMALLER				
		Sample 1	Sample 2	Sample 3	Sample 4	Sample 5
COBBLE	75					
GRAVEL	53					
	37.5					
	26.5				100.00	
	19				97.74	
	13.2	100.00		100.00	97.74	100.00
	4.75	99.82	100.00	97.90	95.34	98.80
SAND	2	97.68	98.40	92.48	88.72	94.72
	0.425	23.82	23.80	22.14	19.20	28.62
	0.212	3.04	2.33	4.38	3.97	7.92
	0.15	1.32	0.79	2.62	1.63	4.26
	0.075	0.45	0.20	1.55	0.57	2.46
FINES	0.05	0.17	0.17	0.18	0.13	0.20
	0.005	0.14	0.14	0.13	0.12	0.17